Generalized Gaussian Covariance Analysis in Multi-Market Risk Assessment

by

Kenneth Chiu

Submitted to the Department of Electrical Engineering and Computer Science
in partial fulfillment of the requirements for the degree of

Master in Operations Research

at the

MASSACHUSETTS INSTITUTE OF TECHNOLOGY

February 1995

Author .....
Department of Electrical Engineering and Computer Science
January 20, 1995

Certified by .....
Prof. Roy Welsch
Leaders for Manufacturing Professor of Management Science and Statistics
Thesis Supervisor

Certified by .....
Dr. Peter Kempthorne
Principal Research Scientist
Thesis Supervisor

Accepted by .....
Prof. Thomas Magnanti
George Eastman Professor of Management Science;
Codirector, Operations Research Center;
Director, Decision Sciences Program

Generalized Gaussian Covariance Analysis in Multi-Market Risk Assessment

by

Kenneth Chiu

Submitted to the Department of Electrical Engineering and Computer Science
on January 20, 1995, in partial fulfillment of the
requirements for the degree of
Master in Operations Research

Abstract

In this thesis, I propose and implement a generalized Gaussian methodology to accomodate the asymmetry and kurtosis of financial returns data, features not captured by standard Gaussian methods. The methodology extends from Gaussian methods with one variance-covariance matrix by estimating different variance-covariance matrices to characterize the differential risk exposures in long and short positions across portfolios of multiple assets. Estimation of the different variance-covariance matrices involves non-linear optimization in the variable space of positive definite matrices. Separate portfolio risk assessments are proposed for "normal" and "stressful" market conditions. An individual portfolio's conditional expected return under "stressful" market conditions is estimated using best linear unbiased estimators for the location and scale parameters of a univariate Gaussian distribution with censored data. Applications to market risk measurement in multinational currency and equity markets are provided.

Thesis Supervisor: Prof. Roy Welsch
Title: Leaders for Manufacturing Professor of Management Science and Statistics

Thesis Supervisor: Dr. Peter Kempthorne
Title: Principal Research Scientist

Acknowledgments

I would like to extend my special thanks to Professor Roy Welsch and Dr. Peter Kempthorne (Massachusetts Institute of Technology) for their encouragement and sound advice in helping me finish this thesis.

Thanks are offered to Bankers Trust for the supply of data, to the International Financial Services Research Center (IFSRC), the Center for Computational Research in Economics and Management Science (CCREMS) at Massachusetts Institute of Technology and the National Science Foundation (Grant Number DMS-93-06245) for providing my financial support during the master degree course.

Contents

List of Figures

List of Tables

Chapter 1

Introduction and Notations

Market risk has become a major consideration in the financial world. Different investors want to have a better understanding of what risk is, how to quantify it and what impact its measurement would have on their investment strategies. There are no real rules of thumb in the methodology or the kind of sophisticated analytics that should be used in quantifying risk. People may choose to rely on their own experiences and professional judgements. In this thesis, we choose to predict the risk exposure of a portfolio based on a projection from historical performance of the portfolio given the empirical returns data of the assets in the portfolio. The notations of a portfolio with n risky assets and the one-period portfolio return are given at the end of this chapter. The empirical asset return datasets are introduced in Section 2.2 in Chapter 2.

The first benchmark for market risk measurement was only recently publicized by J.P Morgan in October, 1994, $RiskMetrics^{TM}$. The model predicts future risk of a portfolio based on historical data, too. It estimates market risks under the Gaussian distribution assumption. The estimation depends on the volatility estimates of individual assets and the correlation estimates between pairs of assets. The $RiskMetrics^{TM}$ tool provides daily updates of any portfolio's risk exposure.

The Gaussian distribution has generally been accepted by most financial practitioners as the benchmark model to use to predict future returns. People have devised different ways to assess if Gaussian normality is the right hypothesis to assume. Over the past few years, tests of Gaussian normality have been performed on various sets

of financial instruments from equities to bonds. Most of them conclude that the return distributions are *leptokurtic* and *negatively skewed.* (Interested readers can refer to $RiskMetrics^{TM}$ or Kempthorne *et al* (1992) for a more detailed description). Chapter 2 illustrates bivariate Gaussianity assessment methods applied to financial return samples. The two features, leptokurtosis and skewed asymmetry, are shown by assessing the correlation between two assets, and by density contours. While it is difficult to illustrate with correlation assessment how leptokurtic a bivariate sample is, the density contours are able to pinpoint where leptokurtosis occurs within a sample. One of the implications of non-uniform leptokurtosis in a sample is that correlation between two assets may be volatility dependent.

When predictions of future returns are frequently required, easy and interpretable calculation of risk is the essence for many risk takers' practice in the financial world. The reason why people still favourably use the Gaussian model even knowing that it fails in capturing asymmetry and leptokurtosis of much financial data is that the Gaussian model offers easily interpretable measurements for future return predictions. Another reason why the Gaussian model is favoured is that many people have already been familiarized with the model. They would feel reluctant to use another distribution model unless that is proved to be much better than the Gaussian model in most aspects.

While the Gaussian distribution is recognized as one of the best parametric models that fit most historical financial return data, the distribution, as shown in this thesis, does not provide a fine enough calibration of a portfolio's risk exposure at times. In specific words, for a portfolio with a leptokurtic return distribution, the Gaussian model underestimates the impact from a disastrous return realization, and overestimates the potential loss of the portfolio when typical returns are expected. The underestimation results in insufficient coverage of the portfolio's position and consequently may lead to damages of a portfolio's credit rating. The overestimation may lead to too conservative an amount of capital reserve kept in the portfolio.

In Chapter 3, a non-parametric methodology that measures risk or volatility implied by the historical data on the Gaussian scale is proposed. This methodology

is able to accomodate skewed asymmetric and leptokurtic portfolio return distributions. $RiskMetrics^{TM}$ quantifies risk by the Gaussian volatility which is given in Section 3.2.2. The non-parametric methodology provides two measures to quantify risk under two distinguishing market conditions which are mathematically defined and characterized in Section 3.1.1. One measure is for the market condition when a normal typical portfolio return is expected. This measure is called *percentile-matched volatility*, which is defined in Section 3.2.3. Computation of the empirical percentile-matched volatility is based on population quantile estimation. The estimation method used in this thesis is presented in Section 5.4. Empirical percentile-matched volatilities are compared to the Gaussian historical volatility in Section 3.2.5

Another measure is for the market condition when a disastrous portfolio return is anticipated. This measure is called *stress expected return* and is defined in Section 3.4.1. To obtain an empirical estimate of stress expected return of a portfolio, we apply the principle of best linear unbiased estimation (BLUE) of Gaussian parameters given a censored sample and the formula for the conditional expectation of a univariate Gaussian variable. These two technical ingredients are presented in Chapter 5. Stress expected return of a portfolio estimated under the Gaussian distribution and the empirical distribution of the portfolio return data are compared in Section 3.4.5.

The last few sections of Chapter 3 introduce the *generalized variance-covariance matrix* and the *stress variance-covariance matrix* which summarizes respectively the percentile-matched volatilities and the stress volatilities of different portfolios. The estimation of these matrices involves the use of non-linear programming algorithms to solve optimization problems constrained in the space of positive definite matrices. The theory behind this estimation process is presented in Chapter 6. Due to different limits in the speed and size of a computation, we solve the optimization problems in the space of 2×2 positive definite matrices. A separate algorithm to build an $n \times n$ (n larger than 2) generalized or stress variance-covariance matrix that summarizes the risk exposure of a portfolio given known long or short positions of the n assets is presented in Section 3.6. While these matrices on their own can measure the

risk exposures of particular portfolios, they also illustrate the skewed asymmetry and kurtosis features of the financial return datasets. Illustrations of the different methods throughout Chapter 3 are given using an example dataset. Results for other datasets are summarized in the tables in Chapter 4, in terms of different 2×2 generalized and stress variance-covariance matrices.

Appendix A presents the background for the best linear unbiased estimation theory in Section 5.2. Starting with a review of the order statistics theory, we gather together the necessary ingredients to understand the David and Johnson method which approximates the expectation and the variance-covariance matrix of order statistics from an arbitrary known continuous distribution. With new findings of some properties of the David and Johnson approximation method, we include a more practical way to compute the variance-covariance matrix for large samples of Gaussian order statistics. The results of this chapter will be used in Chapter 5 to generate subsequent results.

Appendix B displays the written functions and programs in different sections titled in relation to the corresponding functions. All the results in this thesis are generated by functions and programs written in the S-PLUS language .

1.1 Portfolio Formation

Consider n risky (i.e., positive variance) assets traded in the capital market. Let $P_j(t)$ denote the price (per unit or share) of the j^{th} asset, $j = 1, \ldots, n$ at time t. Due to limited liability of assets, $P_j(t) \geq 0$ for all t, $j = 1, \ldots, n$. If $P_j(t) = 0$, then $P_j(t + \tau) = 0$ for all $\tau > 0$. Otherwise, there is an arbitrage opportunity for asset j.

Consider a portfolio comprised of the n assets at a given time t. Let N_j denote the number of units/shares of asset j selected for the portfolio, $j = 1, \ldots, n$. This notation is not a function of time t because we are not considering the dynamics of updating portfolios in this thesis. We are only concerned about measuring the risk exposure of a portfolio over a fixed period. $N_j < 0$ implies a short-sale of $|N_j|$ units/shares. We assume that shortsales of all assets are allowed, and that all

shortsales are 100% margined. Let $a_j(t)$ denote the dollar amount invested in asset j at time t, $j = 1, \ldots, n$. $a_j(t) < 0$ implies a short-sale of $|a_j(t)|$ dollars in asset j. At any given time t, the choices of $\{N_j\}$ and $\{a_j(t)\}$ must satisfy:

$$a_j(t) = N_j P_j(t). \tag{1.1}$$

Let $W(t)$ be defined as the value of the portfolio at time t. At any given time t, the choices of $\{N_j\}$ and $\{a_j(t)\}$ must satisfy:

$$\begin{aligned} W(t) &= \sum_{j=1}^{n} N_j P_j(t) \\ &= \sum_{j=1}^{n} a_j(t). \end{aligned} \tag{1.2}$$

Let $w_j(t)$ denote the fraction of the portfolio allocated to asset j at time t, $j = 1, \ldots, n$. By definition,

$$\begin{aligned} w_j(t) &= \frac{N_j P_j(t)}{\sum_{j=1}^{n} |N_j| P_j(t)} \\ &= \frac{a_j(t)}{\sum_{j=1}^{n} |a_j(t)|}. \end{aligned} \tag{1.3}$$

$w_j(t) < 0$ implies a short-sale of that fraction which is $|N_j|$ share/units of asset j. From Equation 1.3,

$$\begin{aligned} \sum_{j=1}^{n} |w_j(t)| &= \sum_{j=1}^{n} \| \frac{a_j(t)}{\sum_{j=1}^{n} |a_j(t)|} \| \\ &= 1. \end{aligned} \tag{1.4}$$

This implies that the weighting magnitudes of assets in any portfolio always add up to unity.

1.2 Portfolio Returns in Discrete Time

Let h be the trading interval, the length of time between revisions of the portfolio. This time scale is determined by the individual investor. For this thesis' purpose, h is the time between successive market trading days. Due to holidays and weekends, h is not a constant. When m is the number of trading intervals between 0 and T($\equiv mh$), (k) is the shorthand notation for (kh), $k = 0, \ldots, m$. For example, $P_j(k) \equiv P_j(kh)$, $w_j(k) \equiv w_j(kh)$, ... Suppose at the "end" of period k, the portfolio had $\{N_1, \ldots, N_n\}$ units of assets which are held from the beginning of period k until the beginning of period $(k+1)$. At the beginning of period $(k+1)$ before revision of the portfolio, the portfolio value $W(k+1)$ is

$$W(k+1) = \sum_{j=1}^{n} N_j P_j(k+1). \tag{1.5}$$

The one-period portfolio return in period k is by definition $[W(k+1) - W(k)]$ divided by the initial cost invested at the beginning of the period.

If the portfolio buys N_j units of asset j at time t, it will earn the one-period rate of the asset return $[P_j(k+1) - P_j(k)]/P_j(k)$. (For the purpose of this thesis, we assume that there are no transaction costs and taxes.). The initial cost is $N_j P_j(k)$ dollars.

On the other hand, the portfolio with a short position of $|N_j|$ units of asset j in a 100% margined account at time t earns the one-period rate of return $[P_j(k) - P_j(k+1)]/P_j(k)$. The initial cost is $|N_j|P_j(k)$ dollars.

The total initial cost for holding the n different positions in period k is

$$\sum_{j=1}^{n} |N_j| P_j(k) = \sum_{j=1}^{n} |a_j(k)|. \tag{1.6}$$

The portfolio return over the k^{th} period, denoted $X(k)$, $k = 1, \ldots, m$, is

$$\begin{aligned} X(k) &= \frac{W(k+1) - W(k)}{\sum_{j=1}^{n} |a_j(k)|} \\ &= \frac{\sum_{j=1}^{n} N_j [P_j(k+1) - P_j(k)]}{\sum_{j=1}^{n} |a_j(k)|} \end{aligned}$$

$$
\begin{aligned}
&= \sum_{j=1}^{n} \frac{N_j P_j(k)}{\sum_{j=1}^{n} |a_j(k)|} \left[\frac{P_j(k+1) - P_j(k)}{P_j(k)} \right] \\
&= \sum_{j=1}^{n} \frac{a_j(k)}{\sum_{j=1}^{n} |a_j(k)|} \left[\frac{P_j(k+1) - P_j(k)}{P_j(k)} \right] \\
&= \sum_{j=1}^{n} w_j(k) \left[\frac{P_j(k+1) - P_j(k)}{P_j(k)} \right]. \qquad (1.7)
\end{aligned}
$$

Let $Z_j(k)$ denote the k^{th} period return of a long position of asset j, $j = 1, \ldots, n$. By definition,

$$
Z_j(k) = \frac{P_j(k+1) - P_j(k)}{P_j(k)}. \qquad (1.8)
$$

In vector forms, let $\mathbf{w}(k) = (w_1(k), \ldots, w_n(k))'$ and $\mathbf{Z}(k) = (Z_1(k), \ldots, Z_n(k))'$. Then the portfolio return over the k^{th} period, $k = 1, \ldots, m$, can also be expressed as

$$
\begin{aligned}
X(k) &= \sum_{j=1}^{n} w_j(k) [\frac{P_j(k+1) - P_j(k)}{P_j(k)}] \\
&= \sum_{j=1}^{n} w_j(k) Z_j(k) \\
&= \mathbf{w}(k)' \mathbf{Z}(k). \qquad (1.9)
\end{aligned}
$$

In this form, a one-period portfolio return is a linear combination of the one-period asset returns. The linear combination is given by the portfolio weighting allocated to the assets. This portfolio return depends only on the portfolio weighting allocated to assets given by $\mathbf{w}(k)$. Let $\mathbf{w} = (w_1, \ldots, w_n)'$ denote an arbitrary portfolio weighting. In the k^{th} period, for $\mathbf{w}(k) = \mathbf{w}$, let $X(\mathbf{w}, k)$ denote the one-period return of the portfolio with weighting $\mathbf{w}$. Then,

$$
X(\mathbf{w}, k) = \mathbf{w}' \mathbf{Z}(k). \qquad (1.10)
$$

We are interested in comparing the return distributions and risk exposures of portfolios with different weightings of the assets. This leads us to compare $X(\mathbf{w}, k)$ for different $\mathbf{w}$'s that are subjected to the constraint given by Equation 1.4. Let $\mathcal{W}$

Figure 1-1: $\mathcal{W}$

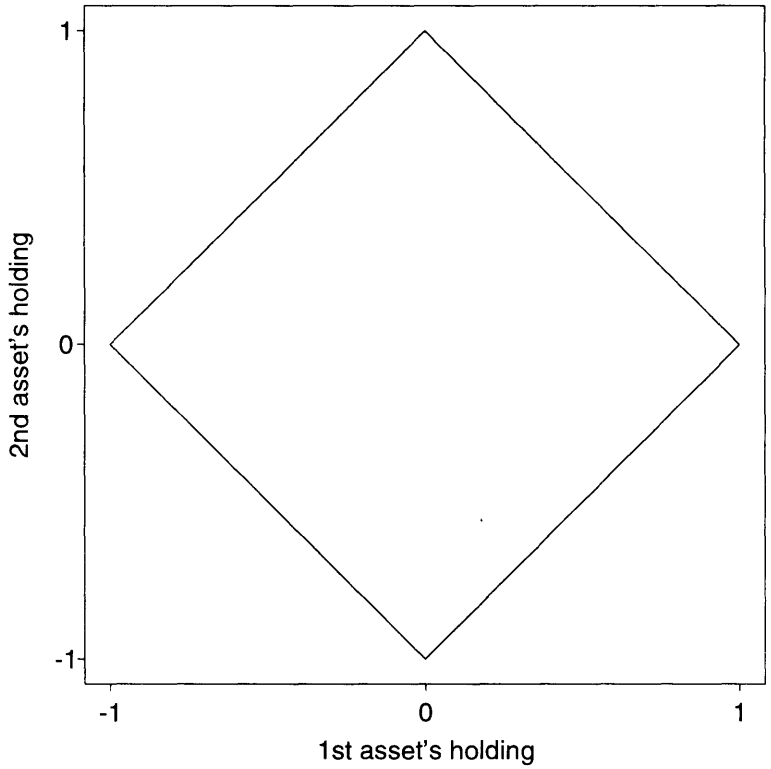

denote the set of all possible portfolio weightings. By definition,

$$\mathcal{W} = \{\mathbf{w} : \sum_{j=1}^{n} |w_j| = 1\}. \tag{1.11}$$

Figure 1-1 illustrates $\mathcal{W}$ for $n = 2$.

Chapter 2

Departure from Bivariate Gaussian Normality

2.1 Introduction

In this chapter, exploratory data analysis is performed on bivariate datasets. The bivariate sample that is used to illustrate the various data analysis tecnhiques consists of the US Dollar versus German Mark (USD/DEM) and the US Dollar versus Japanese Yen (USD/JPY) exchange rates from 1985 to July 1994. For a multivariate exploratory data analysis of these and other data, see Kempthorne *et al* (1992) .

Section 2.2 introduces the other currency exchange and equity index datasets used in this thesis, and provides notations for a sample of daily multi-asset returns, the historical portfolio return data based on this sample, and the mean and standard deviation of the portfolio return.

In Section 2.3, we start by comparing the price movements of two assets parallel in time. We then use a scatter diagram to illustrate the interdependence between the two asset simple daily return moves on the same day.

In Section 2.4, we assess the departure from Gaussian normality using the correlation between the two asset return moves. Interested readers can refer to $RiskMetrics^{TM}$ for a more detailed discussion of this assessment.

In Section 2.5, we try to illustrate asymmetry and leptokurtosis of the data using

density contours. In univariate analysis, one would use the Gaussian density function curve and empirical density histogram to illustrate asymmetry and leptokurtosis of return data. We could have done so in the bivariate scenario by constructing a density surface and a three-dimensional histogram. Practically, we are limited from doing this using two-dimensional graphics. Instead, we display the horizontal cross-sections of the density surface and the histogram at different densities. The cross-section of the normal density surface is an elliptical density contour. We generate the same density contour implied by the data under certain assumptions and compare this with the Gaussian density contour. Multivariate notations are used in this section although the graphs are limited to displaying results for bivariate samples.

2.2 The Dataset

Our currency data consist of daily nominal spot foreign exchange (FX) rates for eight currencies with the USD and six currencies with the DEM from January 1985 to July 1994[1]. The eight currencies with the USD are the Australian Dollar (AUD), Canadian Dollar (CAD), Swiss Franc (CHF), German Mark (DEM), French Franc (FRF), British Pound (GBP), Italian Lira (ITL) and the Japanese Yen (JPY). The six currencies with the DEM are the Swiss Franc, Spanish Peseta (ESP), French Franc, Italian Lira, Japanese Yen and the British Pound. The rates were recorded at the home market close.

Our equity market data consists of daily closing prices of four indexes from January 1986 through July 1990. They are the S&P 500 Index in New York (SP500), the Nikkei Index in Tokyo (Nikkei), the Frankfurt-Commerzbank Index in Frankfurt (Dax) and the CAC-40 Index in Paris (CAC-40).

The issues of missing or asynchronous data are ignored here. Interested readers can refer to Vyas (1992) and to Vyas and Kempthorne (1994).

[1]Bankers Trust provided this data for research at the MIT International Financial Services Research Center

2.2.1 Mean and Standard Deviation of Portfolio Returns

Let $\mathbf{z}(k)$, $(k = 1, \ldots, m)$ denote n series of m daily simple return data. The return data are computed using Equation 1.8. Given a multivariate dataset $\mathbf{z}(k)$ $(k = 1, \ldots, m)$ and a portfolio weighting $\mathbf{w}$, we define the linearly transformed univariate dataset $\mathbf{z}(\mathbf{w}, m)$ as

$$\mathbf{z}(\mathbf{w}, m) \equiv \{\mathbf{w}'\mathbf{z}(k) : k = 1, \ldots, m\}. \tag{2.1}$$

Let $\bar{\mathbf{z}}(\mathbf{w}, m)$ denote the sample average, and $s(\mathbf{w}, m)$ denote the sample standard deviation. Then,

$$\bar{\mathbf{z}}(\mathbf{w}, m) = \frac{1}{m}\sum_{k=1}^{m}\mathbf{w}'\mathbf{z}(k), \tag{2.2}$$

and

$$s(\mathbf{w}, m) = \sqrt{\frac{1}{m}\sum_{k=1}^{m}(\mathbf{w}'\mathbf{z}(k) - \bar{\mathbf{z}}(\mathbf{w}, m))^2}. \tag{2.3}$$

This sample standard deviation is commonly known as the portfolio volatility measure based on historical data.

2.2.2 Means, Variances and Covariance of Two Asset Returns

Given a bivariate daily return dataset (n=2) $\mathbf{z}(k)$ $(k = 1, \ldots, m)$, we estimate the Gaussian parameters (μ, Σ) with the *maximum likelihood estimators (MLE)* $(\hat{\mu}, \hat{\Sigma})$. Denote,

$$\begin{aligned} \hat{\mu} &= (\hat{\mu}_1, \hat{\mu}_2)', \\ \hat{\Sigma} &= \begin{pmatrix} \hat{\sigma}_1^2 & \hat{\sigma}_{12} \\ \hat{\sigma}_{12} & \hat{\sigma}_2^2 \end{pmatrix}. \end{aligned}$$

For $j = 1, 2$,

$$\hat{\mu}_j = \frac{1}{m}\sum_{k=1}^{m} z_j(k),$$

$$\hat{\sigma}_j^2 = \frac{1}{m}\sum_{k=1}^{m}(z_j(k) - \hat{\mu}_j)^2, \tag{2.4}$$

and

$$\hat{\sigma}_{12} = \frac{1}{m}\sum_{k=1}^{m}(z_1(k) - \hat{\mu}_1)(z_2(k) - \hat{\mu}_2). \tag{2.5}$$

$\hat{\mu}$ is the sample mean and $\hat{\Sigma}$ is the sample variance-covariance matrix of the bivariate dataset $\mathbf{z}(k)$ $(k = 1, \ldots, m)$.

2.3 Preliminary Assessment

Figure 2-1 compares the movement of the USD/DEM exchange rate with the movement of the USD/JPY exchange rate over the period January 1985 to July 1994. The chart shows some correlation: positive (negative) changes in USD/DEM are usually accompanied by the positive (negative) changes in USD/JPY.

The scatter diagram of the simple daily returns illustrates the correlation between the two asset return moves. (The definition of simple daily return is given by Equation 1.8 in Section 1.2). Figure 2-2 ("Original") is a scatter diagram of the USD/DEM and USD/JPY exchange rate return. Each point plots the USD/DEM simple daily return against the USD/JPY simple daily return for the same day. We see that the points are scattered within an elliptical region. If there were no correlation between the two exchange rate returns, the returns plotted in the scatter diagram would lie within a circular rather than an elliptical region. If there were perfect linear correlation between the two returns, plotting would be along a diagonal line.

2.4 Gaussian Normality Assessment

To check graphically whether the sample is consistent with a bivariate Gaussian distribution, we first transform the scatter diagram to the normalized scatter diagram which is a plot of the normalized daily returns. The transformation is in two steps:

Figure 2-1: USD/DEM and USD/JPY exchange rate history

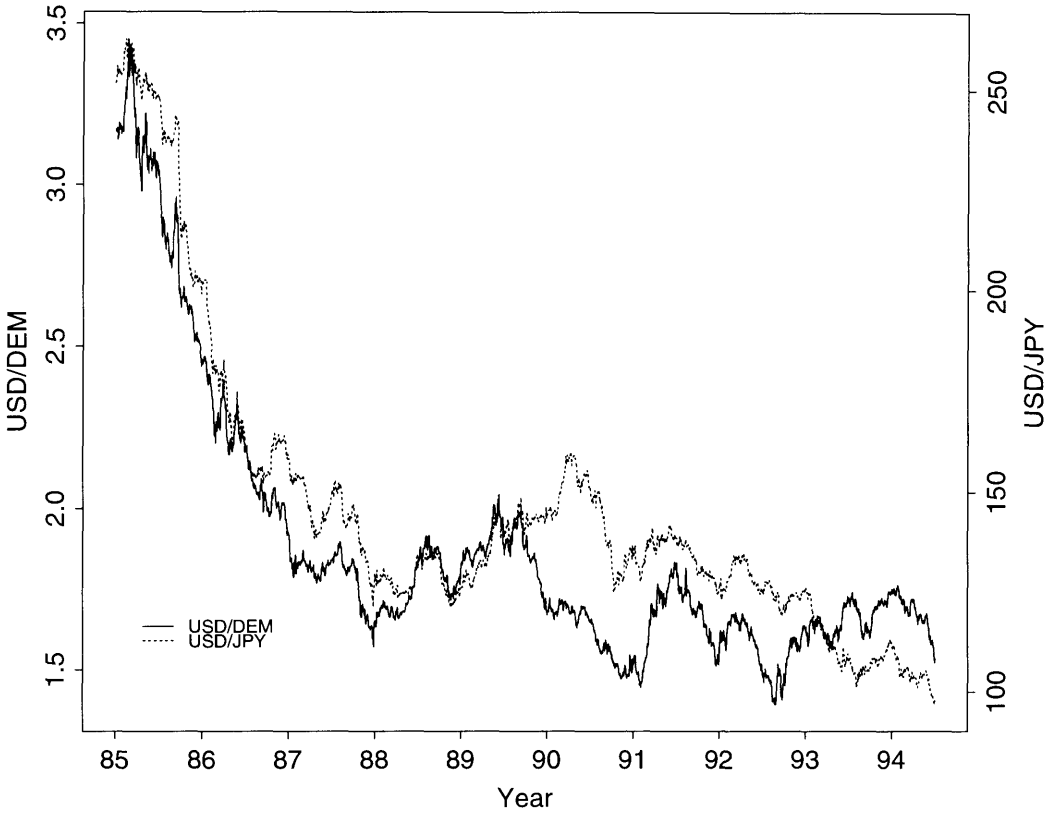

Figure 2-2: USD/DEM and USD/JPY daily changes

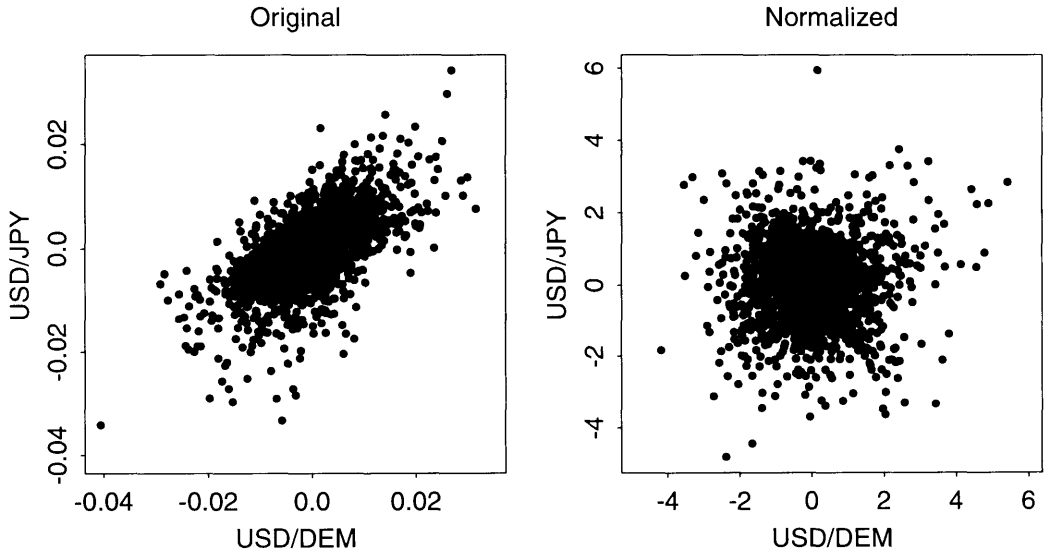

1. Under the assumption that the bivariate data are from a Gaussian distribution $N(\mu, \Sigma)$, we estimate the parameters with $(\hat{\mu}, \hat{\Sigma})$ as defined in Section 2.2.

2. Given the bivariate historical return data denoted as $\mathbf{z}(k)$ $(k = 1, \ldots, m)$ (Section 3.2), normalize the data to $\mathbf{x}(k)$ $(k = 1, \ldots, m)$ by the transformation (for $k = 1, \ldots, m$)

$$\mathbf{x}(k) = \hat{\Sigma}^{-\frac{1}{2}}(\mathbf{z}(k) - \hat{\mu}) \tag{2.6}$$

After the transformation, the points should be scattered within a circular region centered at the origin. Figure 2-2 ("Normalized") illustrates the transformed scatter diagram of the USD/DEM and USD/JPY exchange rate return.

We express all the transformed points $\mathbf{x}(k)$ in their polar coordinates $(R(k), \theta(k))$ instead of in the Cartesian coordinates. If the two asset returns are bivariate Gaussian, the transformed points should be well distributed in a circular region. More specifically the angles $\theta(k)$ $(k = 1, \ldots, m)$ should be uniformly distributed in $(0, 2\pi)$, and the radii $R(k)$ $(k = 1, \ldots, m)$ follow from

$$\begin{aligned} R(k)^2 &= (\mathbf{z}(k) - \hat{\mu})'\hat{\Sigma}^{-1}(\mathbf{z}(k) - \hat{\mu}) \\ &= (\mathbf{z}(k) - \hat{\mu})'\hat{\Sigma}^{-\frac{1}{2}'}\hat{\Sigma}^{-\frac{1}{2}}(\mathbf{z}(k) - \hat{\mu}) \\ &= \mathbf{x}(k)'\mathbf{x}(k) \end{aligned} \tag{2.7}$$

If each of the data $\mathbf{z}(k)$ $(k = 1, \ldots, m)$ were independent and identically distributed as $N(\hat{\mu}, \hat{\Sigma})$, then $\mathbf{x}(k)$ $(k = 1, \ldots, m)$ would be distributed as $N(0, I)$. The cross product or R^2 is distributed chi-square with 2 degrees of freedom. The radii, which are the square root of R^2, therefore, follow a chi distribution with 2 degrees of freedom.

The graphs in Figure 2-3 show the histograms for the angles and radii for the correlation of simple daily returns in USD/DEM and USD/JPY.

The left chart represents the distribution of angles of the normalized daily return pairs in USD/DEM and USD/JPY. The line is the plot of the cumulative frequency. The uniformity of the distribution is indicated by the straightness of this line. The

Figure 2-3: Correlation of daily returns in USD/DEM and USD/JPY

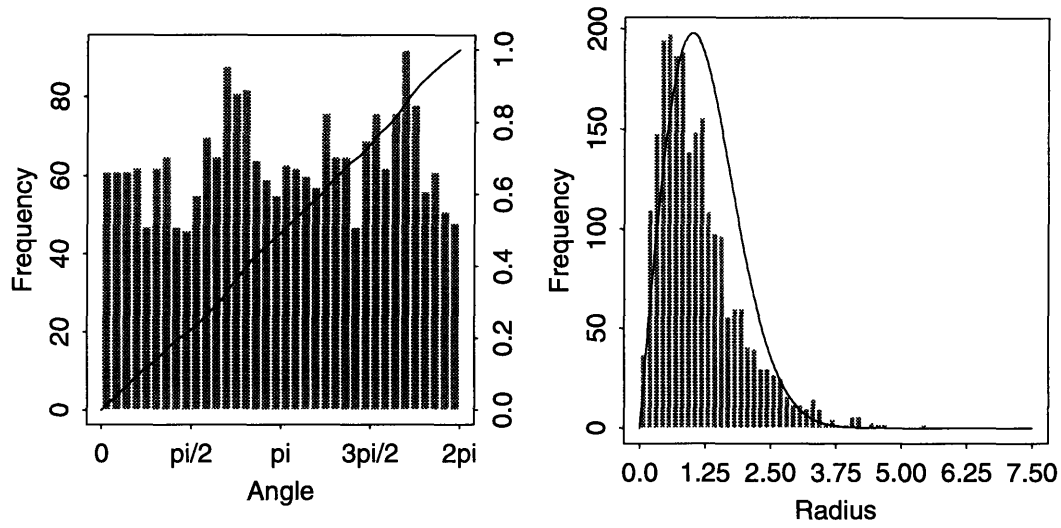

right chart displays the distribution of the radii compared to a standard χ distribution with 2 degrees of freedom. We could use formal chi-square goodness of fit tests here to check whether the sample is consistent with a bivariate Gaussian distribution or is leptokurtic. The frequencies of the return with very small radii and very large radii are higher than expected by the chi distribution. The frequency of return with medium radii is lower than expected by the chi distribution. This shows leptokurtosis of the data.

2.5 Gaussian Density Contour

Under the multivariate Gaussian normality assumption, the contours on which the Gaussian density is constant are concentric ellipsoids. To generate a density contour graphically, suppose $\mathbf{Z} \sim N(\mu, \Sigma)$ in n dimensions, then

$$(\mathbf{Z} - \mu)'\Sigma^{-1}(\mathbf{Z} - \mu) \sim \chi^2_n \tag{2.8}$$

That is, the Mahalanobis' distance between μ and $\mathbf{Z}$ (left hand side of Equation 2.8) has the χ^2 distribution of degree n. The exponent of the multivariate Gaussian density

of $\mathbf{Z}$ is

$$f(\mathbf{Z}/\mu,\Sigma) = \frac{1}{\sqrt{2\pi}^n|\Sigma|}\exp\{-(\mathbf{Z}-\mu)'\Sigma^{-1}(\mathbf{Z}-\mu)\} \tag{2.9}$$

Given μ and Σ, $\mathbf{Z}$ is the only variable in the density. We then see that the density is constant if and only if the exponent in the density function is constant. It follows that the density contour which contains $100(p)\%$ of the distribution is algebraically given as

$$(\mathbf{Z}-\mu)'\Sigma^{-1}(\mathbf{Z}-\mu) = c(p,n) \tag{2.10}$$

where $c(p,n)$ is a constant dependent on p and n. The region within the density contour has higher density than the density contour. Hence, if $\mathbf{x}$ is a point within the contour and $\mathbf{z}$ is a point on the contour, we have

$$\begin{aligned} & f(\mathbf{x}/\mu,\Sigma) \geq f(\mathbf{z}/\mu,\Sigma) \\ \Rightarrow \quad & \tfrac{1}{\sqrt{2\pi}^n|\Sigma|}\exp\{-(\mathbf{x}-\mu)'\Sigma^{-1}(\mathbf{x}-\mu)\} \geq \tfrac{1}{\sqrt{2\pi}^n|\Sigma|}\exp\{-(\mathbf{z}-\mu)'\Sigma^{-1}(\mathbf{z}-\mu)\} \\ \Rightarrow \quad & (\mathbf{x}-\mu)'\Sigma^{-1}(\mathbf{x}-\mu) \leq (\mathbf{z}-\mu)'\Sigma^{-1}(\mathbf{z}-\mu) \end{aligned}$$

That is, any point inside the density contour has a smaller Mahalanobis distance from the mean than any point on the contour. Given the constraint that the density contour should have $100(p)\%$ of the distribution within it, we have

$$Pr((\mathbf{Z}-\mu)'\Sigma^{-1}(\mathbf{Z}-\mu) \leq (\mathbf{z}-\mu)'\Sigma^{-1}(\mathbf{z}-\mu)) = p \tag{2.11}$$

By Equation 2.8, we have

$$\begin{aligned} & Pr(\chi_n^2 \leq (\mathbf{z}-\mu)'\Sigma^{-1}(\mathbf{z}-\mu)) = p \\ \Rightarrow \quad & (\mathbf{z}-\mu)'\Sigma^{-1}(\mathbf{z}-\mu) = F_{\chi_n^2}^{-1}(p), \end{aligned} \tag{2.12}$$

where $F_{\chi_n^2}(.)$ is the distribution function of the χ^2 distribution with n degrees of freedom.

Equation 2.12 holds for any point $\mathbf{z}$ lying on the contour. Hence, this contour,

which is also denoted as $E_p(\mu, \Sigma)$, is given as

$$\begin{aligned} E_p(\mu, \Sigma) &= \{\mathbf{z} \in \Re^n : (\mathbf{z} - \mu)'\Sigma^{-1}(\mathbf{z} - \mu) = F^{-1}_{\chi^2_n}(p)\} \\ &= \{\alpha r^*_p(\alpha/\Sigma) + \mu : \alpha'\alpha = 1, r^*_p(\alpha/\Sigma) = \sqrt{\frac{F^{-1}_{\chi^2_n}(p)}{\alpha'\Sigma^{-1}\alpha}}\}. \end{aligned} \tag{2.13}$$

2.5.1 Gaussian Case

Given a multivariate dataset $\mathbf{z}(k)$ $(k = 1, \ldots, m)$, suppose each $\mathbf{z}(k)$ is independent and identically distributed from the Gaussian distribution $N(\mu, \Sigma)$. We estimate the parameters the estimators denoted $(\hat{\mu}, \hat{\Sigma})$. As mentioned in Section 3.2, the estimates are respectively the sample mean and sample variance-covariance matrix by maximum likelihood theory. Let $\hat{E}_p$ denote the estimate of $E_p(\mu, \Sigma)$ using $(\hat{\mu}, \hat{\Sigma})$. Then,

$$\begin{aligned} \hat{E}_p &= \{\mathbf{z} \in \Re^n : (\mathbf{z} - \hat{\mu})'\hat{\Sigma}^{-1}(\mathbf{z} - \hat{\mu}) = F^{-1}_{\chi^2_n}(p)\} \\ &= \{\alpha r^*_p(\alpha/\hat{\Sigma}) + \hat{\mu} : \alpha'\alpha = 1, r^*_p(\alpha/\Sigma) = \sqrt{\frac{F^{-1}_{\chi^2_n}(p)}{\alpha'\hat{\Sigma}^{-1}\alpha}}\}. \end{aligned} \tag{2.14}$$

2.5.2 Nonparametric Case

For the empirical distribution of $\mathbf{z}(k)$ $(k = 1, \ldots, m)$, let $\tilde{E}_p$ be the empirical percentile-matched ellipse that is to be compared to $\hat{E}_p$. Given $\alpha \in \Re^2$ such that $\alpha'\alpha = 1$, i.e. α is a point on the unit circle centered at the origin, let $\tilde{F}_\alpha(.)$ be the empirical distribution function of the transformed dataset $\mathbf{z}(\alpha, m) = \{\alpha'\mathbf{z}(k) : k = 1, \ldots, m\}$.

Given (μ, Σ), each $\mathbf{z} \in E_p(\mu, \Sigma)$ has a dual relationship with the quantity

$$\begin{aligned} f_p(\alpha/\Sigma) &\equiv \Phi\left(\frac{r^*_p(\alpha/\Sigma)}{\sqrt{\alpha'\Sigma\alpha}}\right) \\ &= \Phi\left(\frac{F^{-1}_{\chi^2_n}(p)}{\sqrt{\alpha'\Sigma\alpha}\sqrt{\alpha'\Sigma^{-1}\alpha}}\right). \end{aligned} \tag{2.15}$$

For each $\mathbf{z} \in E_p(\mu, \Sigma)$, $f_p(\alpha/\Sigma)$ is the Gaussian cumulative distribution function value of $\mathbf{z}$ in the Gaussian distribution with parameters $(\alpha\mu, \alpha'\Sigma\alpha)$ where $\alpha = \mathbf{z}/|\mathbf{z}|$. From Equation 2.15, we see that $f_p(\alpha/\Sigma)$ only depends on Σ and not μ. The dual

relationship is one-to-one because the Gaussian distribution function $\Phi(.)$ is monotone and one-to-one.

A distribution is uniquely represented by its distribution function, e.g. the standard Gaussian distribution by $\Phi(.)$ and the empirical distribution of $\mathbf{z}(\alpha, m)$ by $\tilde{F}_\alpha(.)$. To check if, for example, a Gaussian distribution fits the empirical distribution of $\mathbf{z}(\alpha, m)$, we plot the empirical fractiles against the fractiles of the standard Gaussian distribution. This is generally known as a QQ-plot. A good fit is indicated by a straight line on the plot. This QQ-plot, however, only works for univariate samples.

Borrowing the idea of a QQ-plot in the bivariate scenario, the projected value of each point in the ellipse $\hat{E}_p$ on the axis with slope α and passing through $\hat{\mu}$ is $r_p^*(\alpha/\hat{\Sigma}) + \alpha'\hat{\mu}$. This value is the $\{f_p(\alpha/\hat{\Sigma})\}^{th}$ fractile of the Gaussian distrbution $N(\alpha'\hat{\mu}, \alpha'\hat{\Sigma}\alpha)$. If this value were to be plotted in a QQ-plot fitting the Gaussian distribution $N(\alpha'\hat{\mu}, \alpha'\hat{\Sigma}\alpha)$ to the empirical distribution of $\mathbf{z}(\alpha, m)$, it would be plotted against the corresponding empirical fractile given by $\tilde{F}_\alpha^{-1}(f_p(\alpha/\hat{\Sigma}))$. (Refer to Section 5.4 for the definition and estimation of a general quantile function $F^{-1}(.)$.) We use this idea to generate, for different α such that $\alpha'\alpha = 1$, different values of $\tilde{F}_\alpha^{-1}(f_p(\alpha/\hat{\Sigma}))$. To display these values in a shape comparable to a Gaussian ellipse, we need to do the following transformation which would generate $\tilde{E}_p$.

For each α such that $\alpha'\alpha = 1$, define $\tilde{r}_p^*(\alpha/\Sigma)$ such that

$$\tilde{r}_p^*(\alpha/\hat{\Sigma}) = \tilde{F}_\alpha^{-1}(f_p(\alpha/\hat{\Sigma})) - \bar{\mathbf{z}}(\alpha, m) \tag{2.16}$$

Note that the sample mean $\bar{\mathbf{z}}(\alpha, m)$ is the same as the MLE Gaussian mean $\alpha'\hat{\mu}$ for every α. The significance of this is that the centres of the two ellipses $\hat{E}_p$ and $\tilde{E}_p$ would be the same. Comparison of the two ellipses is illustrating the difference between the repective spread of the empirical and the Gaussian distribution.

When this value is plotted on a two-dimensional graph to construct $\tilde{E}_p$, the point $\alpha\tilde{r}_p^*(\alpha/\hat{\Sigma}) + \hat{\mu}$ is plotted. To summarize the construction of $\tilde{E}_p$ in a single mathematical

Figure 2-4: $\hat{E}_p$ and $\tilde{E}_p$ for USD/DEM and USD/JPY, $p = 5\%, 95\%$

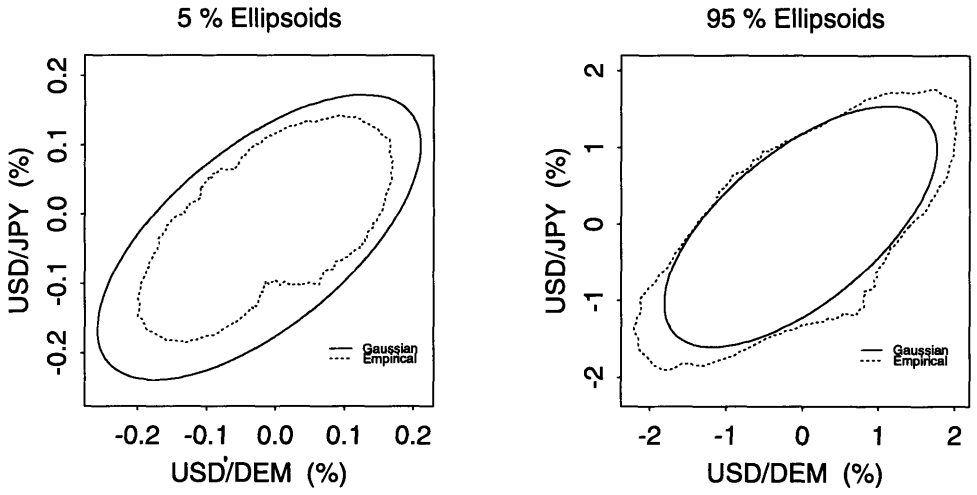

expression,

$$\tilde{E}_p = \{\alpha \tilde{r}_p^*(\alpha/\hat{\Sigma}) + \hat{\mu} : \alpha'\alpha = 1, \tilde{r}_p^*(\alpha/\hat{\Sigma}) = \tilde{F}_\alpha^{-1}(f_p(\alpha/\hat{\Sigma})) - \bar{\mathbf{z}}(\alpha, m)\} \qquad (2.17)$$

Section 5.4 discusses the estimation of empirical quantile.

Illustrations of $\hat{E}_p$ and $\tilde{E}_p$ for the returns of USD/DEM and USD/JPY $p = 5\%, 95\%$ are given in Figure 2-4. From the 5% graph, we see that $\tilde{E}_{5\%}$ is smaller than $\hat{E}_{5\%}$. This suggests that the empirical data has a peak around the mean higher than predicted by the Gaussian distrbution estimated by maximum likelihood. Further, from the 95% graph, we see that $\tilde{E}_{95\%}$ encapsulates $\hat{E}_{95\%}$. This shows a sign of kurtosis, especially with the distributions of positive or negative combinations of USD/DEM and USD/JPY returns. The two figures together give evidence of leptokurtosis of the data. When compared to Figure 2-3, these ellipses display leptokurtosis in a way that Figure 2-3 cannot. Leptokurtosis is shown in the χ distribution fit to the histogram of the "radii", but we do not know if leptokurtosis occurs around all "angles". The ellipses in Figure 2-4 show exactly this information. Leptokurtosis is only evident with the distribution of positive or negative combinations of USD/DEM

and USD/JPY returns.

Chapter 3

Portfolio Risk Measurement

3.1 Introduction and Definition of Stressful Market Condition

When a non-disastrous portfolio return is expected, we say that the portfolio is under non-stressful or normal market condition. Conversely, when a disastrous portfolio return is expected, we say that the portfolio is under stressful market conditions. This notion is mathematically defined and explained in Section 3.1.1.

This chapter provides two measures of the risk exposure of a portfolio. Section 3.2 presents the first measure, *return at risk*, which measures the loss tolerance level of a portfolio when a non-disastrous portfolio return is expected. The return at risk of portfolios with different weightings are estimated under two distribution assumptions - the Guassian distribution and the empirical distribution of the datasets as described in Section 2.2.

Under a portfolio return distribution other than the Gaussian distribution whose parameters are estimated by maximum likelihood theory, the measure of the uncertainty of portfolio return is given by a *percentile-matched volatility* which is defined in Section 3.2.3. This volatility measure is calibrated on a Gaussian scale. In Section 3.2.5, leptokurtosis and asymmetry of an empirical portfolio return distribution are shown by direct comparison between the empirical percentile-matched volatility

and the Gaussian standard deviation or the historical volatility of the portfolio return. Section 3.3 defines the empirical percentile-matched correlation. This is the correlation between two assets in a portfolio that matches the empirical percentile-matched volatilities of the portfolio and the two individual assets. Sampling fluctuation is illustrated by non-uniform estimates of this correlation using different portfolios. This correlation analysis tool is able to capture asymmetric correlations of upside and downside risk.

Section 3.4 presents the second measure of a portfolio's risk exposure. This measure is the *stress expected return*, which measures the expected return of a portfolio given that a disastrous portfolio return is anticipated. The stress expected return, when measured on the percentile-matched volatility scale, is given by the mean of return and the *stress volatility*, which is defined in Section 3.4.3. As in Section 3.2, estimates of measures under the Gaussian distribution and the empirical distribution are considered and compared. The empirical stress expected return is estimated using the best linear unbiased estimation theory for the Gaussian parameters and the formula for the conditional expectation of a Gaussian variable. These two technical ingredients are presented in Chapter 5.

Section 3.5 presents the *generalized variance-covariance matrix* which is the variance-covariance matrix that summarizes the percentile-matched volatilities of different portfolios with only two assets. Due to computational limits, only the 2×2 generalized variance-covariance matrices can be obtained by a method whose details are presented in Chapter 6.

Section 3.6 presents an algorithm to generate the generalized variance-covariance matrix that summarizes the percentile-matched volatilities of portfolios with n (more than 2) assets.

Section 3.7 presents the *stress variance-covariance matrix* which is the variance-covariance matrix that summarizes the stress volatilities of different portfolios.

3.1.1 Normal vs Stressful Market Conditions

If we assume that the asset returns over different periods are independent of one another, and that they are identically distributed as $\mathbf{Z}$, then given the same portfolio with weighting $\mathbf{w}$, the one-period portfolio returns $X(\mathbf{w}, k)$, $k = 1, \ldots, m$, are also independent and identically distributed. Let $X(\mathbf{w}, k)$, $k = 1, \ldots, m$, be distributed as $X(\mathbf{w}) \equiv \mathbf{w}'\mathbf{Z}$, the one-period return of a portfolio with weighting $\mathbf{w}$, whose distribution is independent of time.

Under the independent and identical distribution assumption, let $F_{\mathbf{w}}(.)$ be the distribution function of the one-period return distribution of a portfolio with weighting $\mathbf{w}$, i.e. the distribution of $X(\mathbf{w})$. For a given portfolio with weighting $\mathbf{w}$ and $p \in (0, 1)$, we say that the portfolio is *under* $100(p)\%$ *stressful conditions* if and only if it is expecting a realization $x(\mathbf{w})$ such that

$$F_{\mathbf{w}}(x(\mathbf{w})) < 1 - p. \tag{3.1}$$

Conversly, we say that the portfolio is not under 100(p)% stressful conditions if and only if it is expecting a return realization $x(\mathbf{w})$ such that

$$F_{\mathbf{w}}(x(\mathbf{w})) \geq 1 - p \tag{3.2}$$

With no knowledge of the true portfolio return distribution, we assume different distributions for it. For continuous distributions, the cumulative distribution function is continuous and usually differentiable. For discrete distributions, however, the probability distribution function is a step function. Different assumptions of the portfolio return distribution can lead to different interpretations of the same portfolio's stressful condition.

By Equation 3.1, we see that as p increases, the set of realizations $x(\mathbf{w})$ for the inequality to hold shrinks and only the lower (typically more negative) returns are included in the set. This implies that a portfolio with higher "stress" has on average lower returns. However, a portfolio with a lower return is not necessarily under more

stressful conditions.

3.2 Portfolio Risk Assessment under Normal Market Conditions

When analyzing investments, we define portfolio risk as variability or uncertainty of future returns of a portfolio resulting from price changes in the underlying assets. Its measurement depends on the distribution that charaterizes returns of the portfolio. The greater the variability in the probability distribution of returns, the riskier the investment.

Historical data provide an indication of the past relationship between return and risk. In this thesis, we base predictions of future portfolio risk on the empirical distribution of market movements.

An important step in quantifying daily risk exposure is the selection of a distribution that best charaterizes the historical daily returns. In this thesis, we consider and compare two distributions - the Gaussian distribution and the empirical distribution based on the data as described in Section 2.2. The Gaussian distribution has typically been used to characterize most historical financial return distributions. When the efficiency of the Gaussian model is assessed in the context of portfolio risk exposure, we may find that the model is not predicting the right exposure at times. The following section provides the definition of return at risk for a portfolio with a general return distribution.

3.2.1 Return at Risk

Given $0 < p < 1$, let the one-period *return at risk* (RaR) at the $100(p)\%$ tolerance level of a portfolio be defined as the worst portfolio return while the portfolio is *not* under $100(p)\%$ stressful conditions. The tolerance level indicates how much a portfolio can afford to lose over the one period. The higher the tolerance level, the more the portfolio can afford to lose. For a given portfolio with weighting $\mathbf{w}$, let

$S(\mathbf{w}/p)$ denote the one-period RaR at the $100(p)\%$ tolerance level. By definition,

$$\begin{aligned} S(\mathbf{w}/p) &= \inf\{x(\mathbf{w}) : F_{\mathbf{w}}(x(\mathbf{w})) \geq 1-p\} \\ &= \inf\{x(\mathbf{w}) : x(\mathbf{w}) \geq F_{\mathbf{w}}^{-1}(1-p)\}^1 \\ &= F_{\mathbf{w}}^{-1}(1-p) \end{aligned} \tag{3.3}$$

In developed and liquid markets, modest-sized positions can be unwound or hedged within a trading day. Risks of such positions can be measured using a 24-hour window. In such case, the daily RaR (DRaR) at the 95% tolerance level estimates the potential worst loss of a portfolio resulting from a move under non-stressful market conditions (i.e., 95% of the time) over a one-day period for unwinding.

Under the independent and identical distribution, a portfolio with a given weighting $\mathbf{w}$ on different trading days has the same portfolio return distribution. Moreover, for a given $p \in (0,1)$, the one-period RaR of the portfolio at the $100(p)\%$ tolerance level is also the same. With a larger portfolio size but the same weighting, the dollar amount at risk is proportionally larger.

3.2.2 Gaussian Case

If we assume further, that the n asset returns, $\mathbf{Z}$, are multivariate Gaussian with mean μ and variance-covariance matrix Σ, then the return of a portfolio with weighting $\mathbf{w}$, $X(\mathbf{w})$, is univariate Gaussian with mean $\mathbf{w}'\mu$ and variance $\mathbf{w}'\Sigma\mathbf{w}$. Let $\Phi(.)$ denote the distribution function of the standard Gaussian distribution. Under the Gaussian assumption, the one-period RaR of a portfolio with weighting $\mathbf{w}$ at the $100(p)\%$ tolerance level is

$$S(\mathbf{w}/p) = \mathbf{w}'\mu + \Phi^{-1}(1-p)\sqrt{\mathbf{w}'\Sigma\mathbf{w}}. \tag{3.4}$$

In this form, it is clear that RaR is determined by both the portfolio expected return, given by $\mathbf{w}'\mu$, and the degree of uncertainty of the portfolio return, given by $\sqrt{\mathbf{w}'\Sigma\mathbf{w}}$ which is its standard deviation. Let $\sigma(\mathbf{w})$ denote this standard deviation,

i.e.,

$$\sigma(\mathbf{w}) = \sqrt{\mathbf{w}'\Sigma\mathbf{w}}. \tag{3.5}$$

Given $(\hat{\mu}, \hat{\Sigma})$ as defined in Section 2.2, let $\hat{S}(\mathbf{w}/p)$ denote the estimated DRaR of the portfolio at the $100(p)\%$ tolerance level, and $\hat{\sigma}(\mathbf{w})$ denote the sample standard deviation of the portfolio return. In this thesis, we use the financial term, volatility, interchangeably with the statistical term, standard deviation.

$$\hat{S}(\mathbf{w}/p) = \mathbf{w}'\hat{\mu} + \Phi^{-1}(1-p)\sqrt{\mathbf{w}'\hat{\Sigma}\mathbf{w}}, \tag{3.6}$$

and

$$\hat{\sigma}(\mathbf{w}) = \sqrt{\mathbf{w}'\hat{\Sigma}\mathbf{w}}. \tag{3.7}$$

Calculating $\hat{\sigma}(\mathbf{w})$ does not necessarily invlove computing $\hat{\Sigma}$. Another way to obtain $\hat{\sigma}(\mathbf{w})$ is to compute the sample standard deviation of the sample $\mathbf{z}(\mathbf{w}, m)$ as given by Equation 2.3.

3.2.3 Percentile-Matched Volatilities

Under the Gaussian framework of analysing portfolio risk, risk is a measure of the spread of the return distribution. When we base the projection of future risk on historical performance of the portfolio, e.g. $\mathbf{z}(\mathbf{w}, m)$, portfolio risk can be measured by the historical *volatility* which is given by Equation 2.3, the standard deviation estimated by maximum likelihood. Analysing risk in this way, an identical historical volatility measure under two different portfolio return distributions would lead to the conclusion that the two portfolios are as risky as each other. This is precisely the implication behind fitting the maximum likelihood Gaussian model to empirical data. When the empirical return distribution is leptokurtic to the fitted Gaussian distribution, the conclusion is too general and may lead to mismatches of risk exposure measures. Specifically, the fitted Gaussian model underestimates the potential loss of a portfolio incurred by an extreme negative return, and overestimates the uncertainty of return when typical, normal reutrns are being realized.

We need to define a nonparametric volatility measure to overcome the risk mismatch problem which arises with leptokurtic samples. We choose to measure this nonparametric volatility on the Gaussian scale, the scale that is traditionally used to measure volatility. For $0 < p < 1$, we define the percentile-matched volatility (PMV) at the 100(p)% level of a portfolio with weighting $\mathbf{w}$ as the Gaussian volatility that matches the p^{th} percentile of the distribution of portfolio losses. Since a portfolio loss is the negative of a portfolio return, this PMV matches $(1-p)^{th}$ percentile of the portfolio return distribution. Let $\sigma(\mathbf{w}/p)$ denote this PMV. Mathematically, for the portfolio return distribution with distribution function $F_{\mathbf{w}}(.)$ and mean denoted by $m(\mathbf{w})$,

$$\sigma(\mathbf{w}/p) = \frac{F_{\mathbf{w}}^{-1}(1-p) - m(\mathbf{w})}{\Phi^{-1}(1-p)}. \tag{3.8}$$

Note that when the portfolio return distribution is the maximum likelihood Gaussian distribution, this percentile-matched volatility is the same as the historical volatility estimate which is given by Equation 3.7.

3.2.4 Empirical Case

If we assume that the distribution of $X(\mathbf{w})$ is an empirical distribution of $\mathbf{z}(\mathbf{w}, m)$ with distribution function $\tilde{F}_{\mathbf{w}}(.)$, then the estimated DRaR of a portfolio with weighting $\mathbf{w}$ at the $100(p)\%$ tolerance level under this assumption, denoted $\tilde{S}(\mathbf{w}/p)$ is

$$\tilde{S}(\mathbf{w}/p) = \tilde{F}_{\mathbf{w}}^{-1}(1-p). \tag{3.9}$$

Section 5.4 discusses the estimation of population quantiles.

Let $\bar{\mathbf{z}}(\mathbf{w}, m)$ denote the mean of the empirical distribution as defined in Section 2.2. Let $\tilde{\sigma}(\mathbf{w}/p)$ denote the empirical percentile-matched volatility (EPMV) of a portfolio with weighting $\mathbf{w}$ at the $100(p)\%$ tolerance level. By definition,

$$\tilde{\sigma}(\mathbf{w}/p) = \frac{\tilde{F}^{-1}(1-p) - \bar{\mathbf{z}}(\mathbf{w}, m)}{\Phi^{-1}(1-p)}. \tag{3.10}$$

Figure 3-1: Portfolio weighting plotted against the "position" axis, $\mathbf{w} \in \mathcal{W}$

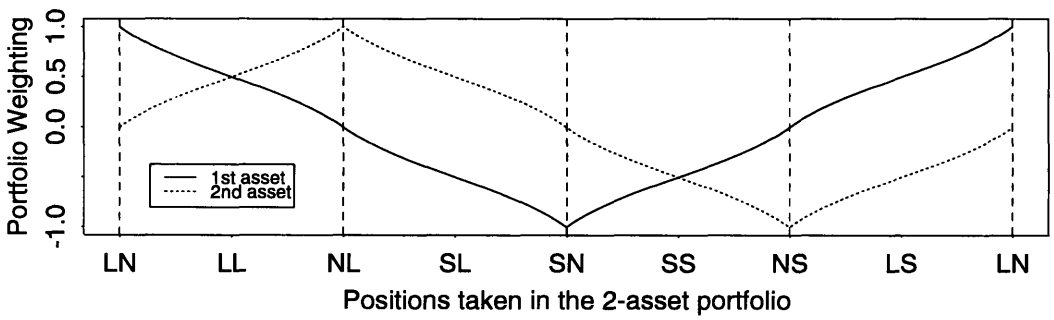

3.2.5 Gaussian vs Empirical

In this thesis, most risk-related measures, when displayed in graphs, are plotted against an x-axis that shows the holding positions in a 2-asset portfolio. Each portfolio weighting $\mathbf{w} \in \mathcal{W}$ is shown on the x-axis via its angle coordinate in the polar coordinate system. Let $\theta_{\mathbf{w}}$ denote the "angle" of $\mathbf{w}$. $\theta_{\mathbf{w}}$ traverses $\mathcal{W}$ in the anti-clockwise direction from 0, representing $\mathbf{w} = (1, 0)$, to 2π, representing the same portfolio weighting.

Figure 3-1 illustrates that when the values of w_1 and w_2 of a portfolio with weighting $\mathbf{w}$ are plotted against $\theta_{\mathbf{w}}$, the lines of w_1 and w_2 are not straight segments because w_1 and w_2 are trigonometric functions of $\theta_{\mathbf{w}}$.

The labels on the x-axis represent the different positions of the USD/DEM and USD/JPY taken in the portfolio. The two letters represent the positions in USD/DEM and USD/JPY respectively. L stands for "long", N stands for "neutral" and S stands for "short". For example, "LN" stands for a 100% long USD/DEM portfolio; "LL" stands for a portfolio which is half long USD/DEM and half long USD/JPY.

Figure 3-2 displays the estimated DRaR at the 95% tolerance level of a portfolio with weighting $\mathbf{w}$ under the Gaussian and the empirical distribution assumptions. $\mathbf{w} \in \mathcal{W}$ are weightings of portfolios that hold USD/DEM and USD/JPY.

We see that under both assumptions, the portfolio with a long position in one asset and short position in another at the same time is least exposed at the 95%

Figure 3-2: $\hat{S}(\mathbf{w}/95\%)$ and $\tilde{S}(\mathbf{w}/95\%)$ for USD/DEM & USD/JPY, $\mathbf{w} \in \mathcal{W}$

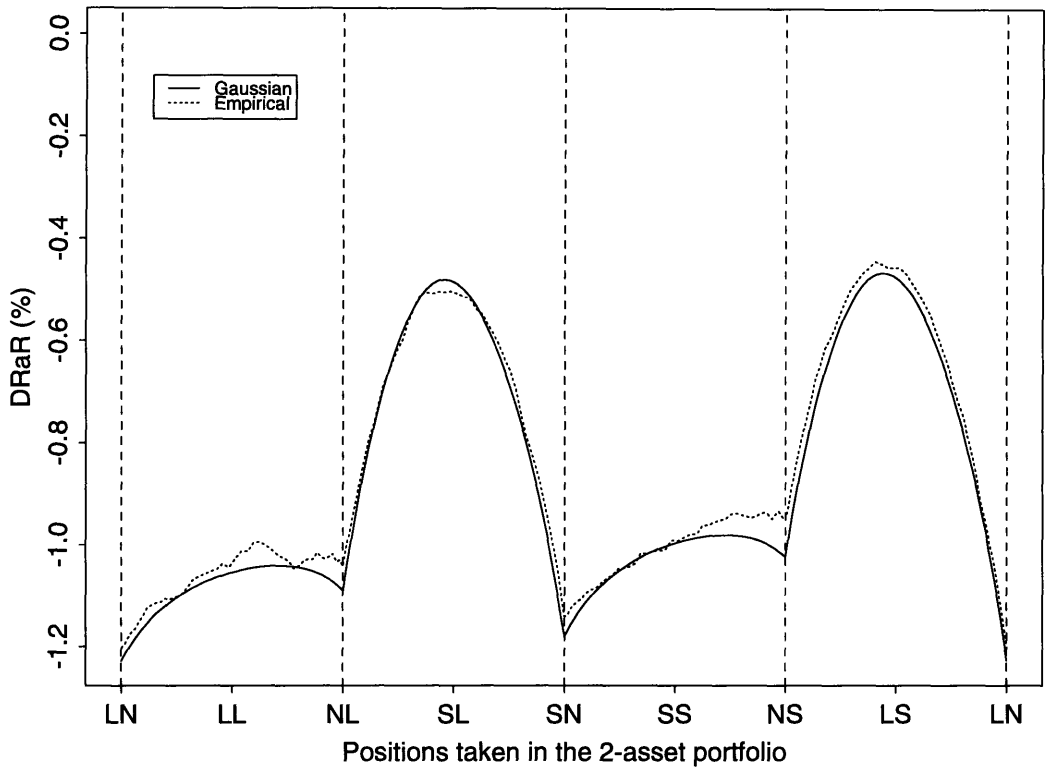

tolerance level. Also, the portfolio that has a long position in either DEM or JPY is slightly riskier than the portoflio that has a short position in either of them.

The sample mean $\bar{\mathbf{z}}(\mathbf{w}, m)$ in Equation 3.10 is the same as the MLE for the Gaussian mean, $\mathbf{w}'\hat{\mu}$. With the same portfolio return expectation estimate, we can directly compare the riskiness of the portfolio under the Gaussian and the empirical distribution assumptions by comparing EPMV with the historical volatility.

While the historical portfolio volatility is a symmetric function in $\mathbf{w}$, i.e. $\sigma(\mathbf{w}) = \sigma(-\mathbf{w})$, the EPMV is able to quantify aysmmetry and kurtosis of historical data on a Gaussian scale. Asymmetry is shown by considering the long and short positions of a portfolio together. In Figure 3-3, skewed asymmetry is shown by the different EPMV curves for long and short positions. In the same figure, kurtosis of data is shown by the EPMV of both long and short USD/DEM portfolios increasing and crossing over the MLE volatility.

Figure 3-3: Comparison of the EPMV for both long & short USD/DEM portfolios at 60% to 100% tolerance levels

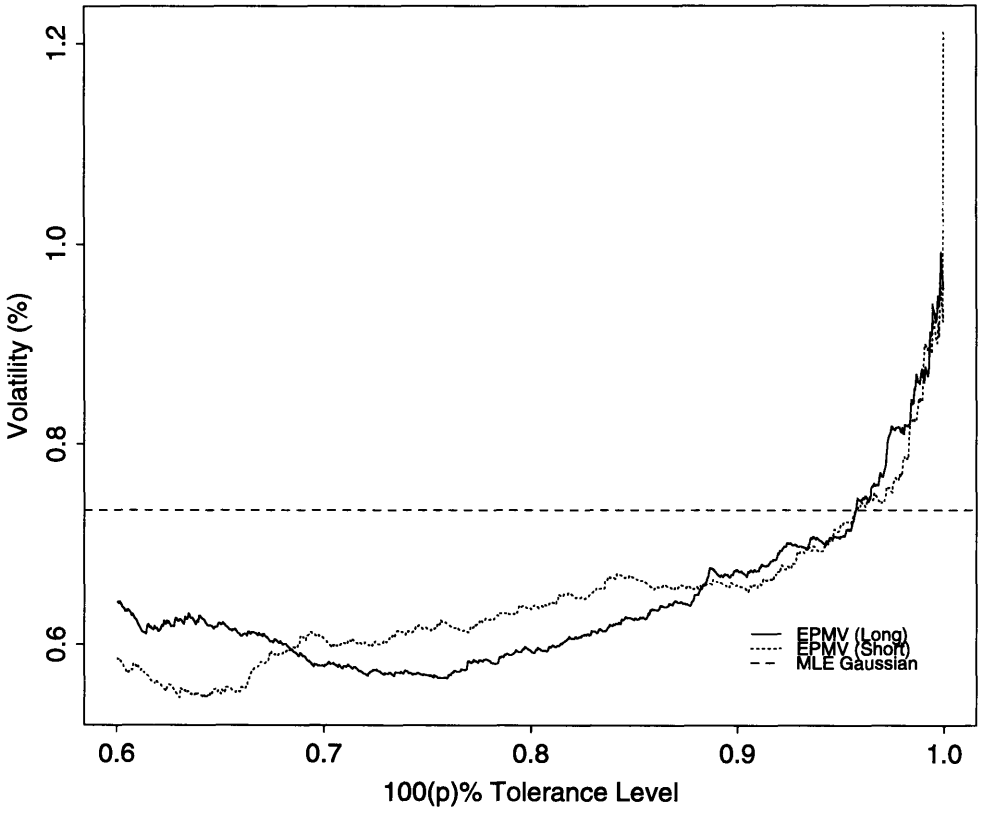

Figure 3-4: $\hat{\sigma}(\mathbf{w})$ and $\tilde{\sigma}(\mathbf{w}/95\%)$ for USD/DEM & USD/JPY, $\mathbf{w} \in \mathcal{W}$

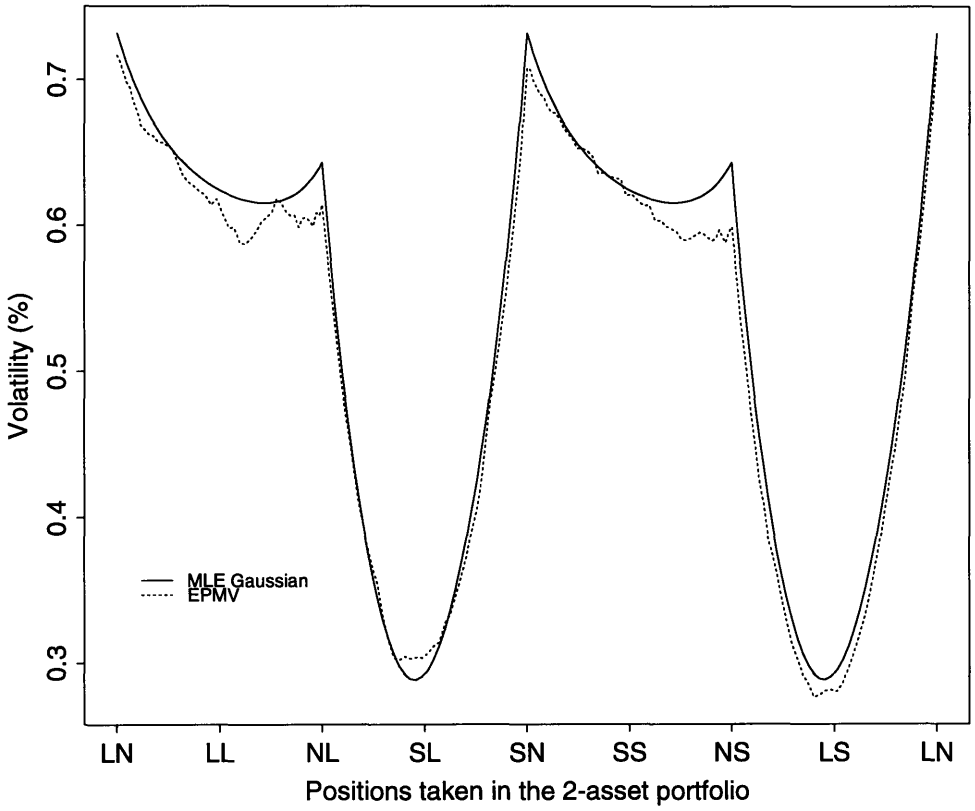

Figure 3-4 illustrates the EPMV at the 95% tolerance level and MLE volatility estimates of portfolios with weighting $\mathbf{w} \in \mathcal{W}$ that hold USD/DEM and USD/JPY. The x-axis is the same as that in Figure 3-2, representing positions taken in USD/DEM and USD/JPY respectively. We see that the curve under the Gaussian assumption shows symmetry in the long and short positions of the same asset. This is expected because $\hat{\sigma}(\mathbf{w}) = \hat{\sigma}(-\mathbf{w})$. However, the curve under the empirical distribution assumption is able to capture asymmetry. While the EPMV curve shows that the portfolio with a long position in USD/JPY is slightly riskier than the portfolio that shorts the same exchange rate at 95% tolerance level, the two curves are almost the same except in a few regions. This indicates that the MLE Gaussian model gives a good evaluation of the empirical portfolio risk estimates for most portfolios at 95% tolerance level.

The worst matched region is around 'NS' i.e. a 100% short USD/JPY portfolio. The EPMV of this portfolio is about 0.6%, and the corresponding Gaussian historical volatility is about 0.64%. The relative difference is about 6%. The measure of volatility here is on a daily scale. When the volatilities are rescaled to the annual scale, the relative difference remains the same. Hence at 95% tolerance level, the MLE Gaussian model evaluates the empirical portfolio risk estimates to within roughly about 6% accuracy.

3.3 Induced Correlation

Given the volatilities of the two underlying assets, denoted σ_1 and σ_2 respectively, and the correlation between the two assets, denoted ρ, the volatility of a portfolio with weighting $\mathbf{w}$ is given by Equation 3.5. When the Equation is expanded, the portfolio volatility is

$$\sigma(\mathbf{w}) = \sqrt{(w_1\sigma_1)^2 + (w_2\sigma_2)^2 + 2w_1w_2\rho\sigma_1\sigma_2}. \tag{3.11}$$

If the portfolio has weighting $\mathbf{w}$ such that $w_1 \neq 0$ and $w_2 \neq 0$, we can express ρ in terms of the volatilities of the two assets and that of the portfolio,

$$\rho = \frac{\sigma(\mathbf{w})^2 - (w_1\sigma_1)^2 - (w_2\sigma_2)^2}{2w_1w_2\sigma_1\sigma_2}. \tag{3.12}$$

Under the Gaussian distribution assumption, this correlation between the two assets is independent of the portfolio weighting $\mathbf{w}$.

Under a nonparametric empirical distribution assumption, we define the *empirical percentile-matched correlation (EPMC)* for a 2-asset portfolio with weighting $\mathbf{w}$ as the correlation between the two assets such that the EPMV of the two assets and that of the portfolio are consistent in the correlation equation like 3.11. Due to the asymmetry example in the EPMV, (a long position and a short position of the same portfolio have different risk exposures), we have to assign the long position and the short position of an asset with different risk measures. For $w_1 \neq 0$ and $w_2 \neq 0$, let $\tilde{\rho}(\mathbf{w}/p)$ denote the *EPMC for portfolio with weighting* $\mathbf{w}$ *at the* $100(p)\%$ *tolerance level.* This correlation equation is induced from Equation 3.12 and is

$$\tilde{\rho}(\mathbf{w}/p) \equiv \frac{\{\tilde{\sigma}(\mathbf{w}/p)\}^2 - w_1^2\{\tilde{\sigma}(\mathbf{e}_1(\mathbf{w})/p)\}^2 - w_2^2\{\tilde{\sigma}(\mathbf{e}_2(\mathbf{w})/p)\}^2}{2w_1w_2\tilde{\sigma}(\mathbf{e}_1(\mathbf{w})/p)\tilde{\sigma}(\mathbf{e}_2(\mathbf{w})/p)}, \tag{3.13}$$

where

$$\mathbf{e}_1(\mathbf{w}) \equiv \{\mathbf{b} : b_1 = w_1/|w_1|, b_2 = 0\},$$
$$\mathbf{e}_2(\mathbf{w}) \equiv \{\mathbf{b} : b_2 = w_2/|w_2|, b_1 = 0\}.$$

Figure 3-5 displays the MLE correlation and the EPMC for portfolios with weightings $\mathbf{w} \in \mathcal{W}$ at the 95% tolerance level between USD/DEM and USD/JPY. The EPMC for different portfolios varies from below 0.5 to above 0.9. The graph is split into four panels separated by the vertical solid lines. In different panels, different EPMVs of the individual assets are used. The EPMC are undefined at the vertical solid lines. The MLE correlation is constant at about 0.65. Given any set of historical data bootstrapped from the Gaussian bivariate model with the MLE correlation, we would

Figure 3-5: MLE correlation and $\tilde{\rho}(\mathbf{w}/95\%)$ between USD/DEM & USD/JPY, $\mathbf{w} \in \mathcal{W}$

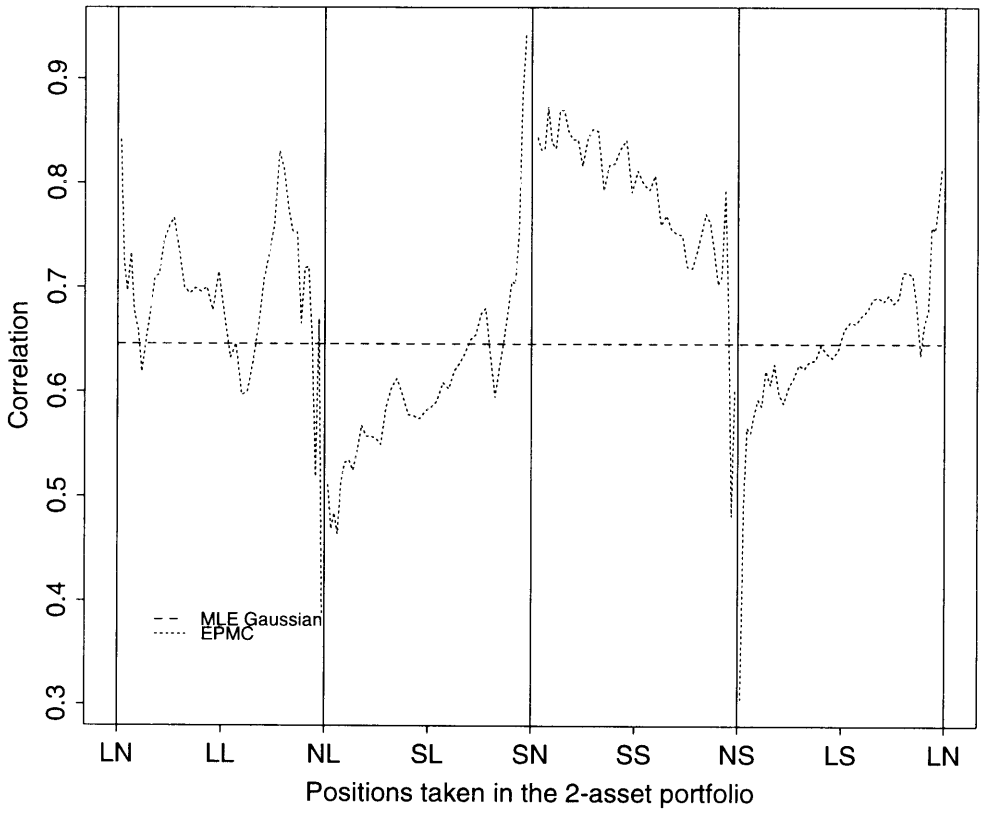

not expect to see a constant EPMC for different portfolios. This is due to sampling fluctuation. Here, we do not add on the goodness of fit of the MLE correlation to the historical data. We merely show the sampling fluctuation which occurs for the chosen historical data. Figure 3-5 shows that the EPMC for portfolios that short both assets are "on average" higher than the EPMC of the long portfolios of both assets. This indicates that DEM and JPY depreciates against USD together more often than they appreciate against USD at 95% tolerance level.

Because of the inherent sampling fluctuation, the EMPC is not a robust measure for the correlation between two assets in a portfolio. The estimate of correlation between two assets under an empirical distribution assumption is obtained via estimating the variance-covariance matrix that matches the EPMV of certain portfolios. This will be discussed in detail later in Section 3.5. Nonetheless, EPMC is a useful tool for detecting non-uniform correlation trends within the data.

3.4 Portfolio Risk Assessment under Stressful Market Conditions

The RaR at the $100(p)\%$ tolerance level is the measure of the maximum loss of a portfolio with weighting $\mathbf{w}$ given that the portfolio is *not* under $100(p)\%$ stressful conditions, as defined and explained in Section 3.2. In other words, RaR only estimates the worst scenario among all typical or non-disastrous return realizations of a portfolio over one trading day. It does not measure how much loss to expect from an atypical or disastrous return realization. Section 3.4.1 defines the *stress expected return* as the measure of the expected return of a portfolio given that a disastrous portfolio return is anticipated.

3.4.1 Stress Expected Return

For a given $p \in (0,1)$, we define *the 100(p)% stress expected return (SER) of a portfolio with weighting* $\mathbf{w}$ as the conditional expectation of $X(\mathbf{w})$ given that the

portfolio is subject to $100(p)\%$ stressful conditions. For the distribution of $X(\mathbf{w})$ with distribution function $F_{\mathbf{w}}(.)$, a portfolio is under $100(p)\%$ stressful conditions when it has a return realization $x(\mathbf{w})$ such that

$$x(\mathbf{w}) < F_{\mathbf{w}}^{-1}(1-p) \tag{3.14}$$

This follows from Equation 3.1 in Section 3.1.1.

Let $\nu(\mathbf{w}/p)$ denote the $100(p)\%$ SER of a portfolio with weighting $\mathbf{w}$. Then, from the definition of conditional expectation,

$$\nu(\mathbf{w}/p) = E(X(\mathbf{w})/X(\mathbf{w}) < F_{\mathbf{w}}^{-1}(1-p)) \tag{3.15}$$

The $100(p)\%$ SER of a portfolio with weighting $\mathbf{w}$ corresponds to an RaR of the portfolio at some $100(\pi(\mathbf{w}/p))\%$ tolerance level, $p < \pi(\mathbf{w}/p) \leq 1$. We define this $100(\pi(\mathbf{w}/p))\%$ tolerance level as *the* $100(p)\%$ *stress tolerance level of a portfolio with weighting* $\mathbf{w}$. A stress tolerance level indicates the seriousness of a stress expected return when compared to a typical return. Mathematically,

$$\pi(\mathbf{w}/p) = 1 - F_{\mathbf{w}}(\nu(\mathbf{w}/p)). \tag{3.16}$$

From the definition of $S(\mathbf{w}/p)$ given in Equation 3.3,

$$\begin{aligned} \nu(\mathbf{w}/p) &= F_{\mathbf{w}}^{-1}(1-\pi(\mathbf{w}/p)) \\ &= S(\mathbf{w}/\pi(\mathbf{w}/p)). \end{aligned} \tag{3.17}$$

3.4.2 Gaussian Case

Under the Gaussian assumption, i.e $X(\mathbf{w}) \sim N(\mathbf{w}'\mu, \mathbf{w}'\Sigma\mathbf{w})$, let $d = \Phi^{-1}(1-p)$. Let $\phi(.)$ be the standard Gaussian density function. Then, using the conditional expectation formula given by Equation 5.14 in Section 5.3, with $S(\mathbf{w}/p)$ replacing

the constant c in the formula,

$$\nu(\mathbf{w}/p) = \mathbf{w}'\mu - \frac{\sqrt{\mathbf{w}'\Sigma\mathbf{w}}\ \phi(d)}{1-p}, \tag{3.18}$$

and

$$\begin{aligned} \pi(\mathbf{w}/p) &= 1 - F_{\mathbf{w}}(\nu(\mathbf{w}/p)) \\ &= 1 - \Phi(\frac{\nu(\mathbf{w}/p) - \mathbf{w}'\mu}{\sqrt{\mathbf{w}'\Sigma\mathbf{w}}}). \end{aligned} \tag{3.19}$$

As in Section 3.2.2, given the bivariate sample $\mathbf{z}(k)$ $(k = 1, \ldots, m)$, we estimate (μ, Σ) with $(\hat{\mu}, \hat{\Sigma})$. Let $\hat{\nu}(\mathbf{w}/p)$ and $\hat{\pi}(\mathbf{w}/p)$ denote respectively the estimate of $\nu(\mathbf{w}/p)$ and $\pi(\mathbf{w}/p)$ using the MLE Gaussian parameters. Then,

$$\hat{\nu}(\mathbf{w}/p) = \mathbf{w}'\hat{\mu} - \frac{\sqrt{\mathbf{w}'\hat{\Sigma}\mathbf{w}}\ \phi(d)}{1-p}, \tag{3.20}$$

and

$$\hat{\pi}(\mathbf{w}/p) = 1 - \Phi(\frac{\hat{\nu}(\mathbf{w}/p) - \mathbf{w}'\hat{\mu}}{\sqrt{\mathbf{w}'\hat{\Sigma}\mathbf{w}}}). \tag{3.21}$$

3.4.3 Stress Volatility

Analogous to the percentile-matched volatility defined in Section 3.2.3, we define *the* $100(p)\%$ *stress PMV of a portfolio with weighting* $\mathbf{w}$ as the portfolio's PMV at the $100(p)\%$ stress tolerance level. Let $\varsigma(\mathbf{w}/p)$ denote this stress PMV. For convenience, the name of $100(p)\%$ stress PMV is simplified to $100(p)\%$ *stress volatility.* Then, for the portfolio return distribution with distribution function $F_{\mathbf{w}}(.)$ and mean $m(\mathbf{w})$,

$$\varsigma(\mathbf{w}/p) = \frac{F_{\mathbf{w}}^{-1}(1 - \pi(\mathbf{w}/p) - m(\mathbf{w})}{\Phi^{-1}(1 - \pi(\mathbf{w}/p))}. \tag{3.22}$$

The stress volatility is a measure of risk that matches with the conditional expectation of return under stressful market condition on a Gaussian scale.

3.4.4 Empirical Case

For the empirical distribution of $\mathbf{z}(\mathbf{w}, m)$ with distribution function $\tilde{F}_{\mathbf{w}}(.)$, let $\tilde{\nu}(\mathbf{w}/p)$, $\tilde{\pi}(\mathbf{w})/p)$ and $\tilde{\varsigma}(\mathbf{w}/p)$ denote respectively the estimate of $\nu(\mathbf{w}/p)$, $\pi(\mathbf{w}/p)$ and $\varsigma(\mathbf{w}/p)$. Then given $\tilde{\nu}(\mathbf{w}/p)$,

$$\tilde{\pi}(\mathbf{w}/p) = 1 - \tilde{F}_{\mathbf{w}}(\tilde{\nu}(\mathbf{w}/p)), \tag{3.23}$$

and

$$\begin{aligned} \tilde{\varsigma}(\mathbf{w}/p) &= \frac{\tilde{F}_{\mathbf{w}}^{-1}(1 - \tilde{\pi}(\mathbf{w}/p)) - \bar{\mathbf{z}}(\mathbf{w}, m)}{\Phi^{-1}(1 - \tilde{\pi}(\mathbf{w}/p))} \\ &= \frac{\tilde{\nu}(\mathbf{w}/p) - \bar{\mathbf{z}}(\mathbf{w}, m)}{\Phi^{-1}(1 - \tilde{\pi}(\mathbf{w}/p))}. \end{aligned} \tag{3.24}$$

Estimation of Empirical Stress Expected Return

There are different ways to specify the estimate of the empirical stress expected return, $\tilde{\nu}(\mathbf{w}/p)$. We propse the following method. Given the dataset $\mathbf{z}(\mathbf{w}, m)$ of portfolio returns, we first order the dataset. Denote the ordered dataset by $\dot{\mathbf{z}}(\mathbf{w}, m)$. For the given $p \in (0, 1)$, we calculate r as the rounded off integer of $m(1-p)$. Denote $\lfloor x \rfloor$ as the largest integer smaller than or equal to x, and $\lceil x \rceil$ as the smallest integer strictly larger than x. Then,

$$r = \begin{cases} \lfloor m(1-p) \rfloor & \text{if } m(1-p) - \lfloor m(1-p) \rfloor \leq 0.5, \\ \lceil m(1-p) \rceil & \text{if } \lceil m(1-p) \rceil - m(1-p) < 0.5. \end{cases} \tag{3.25}$$

We then extract the lowest r order statistics from $\dot{\mathbf{z}}(\mathbf{w}, m)$. This extracted sample is a Type-II censored sample; see Appendix A for a definition of Type-II censoring. We estimate the Gaussian parameters based on this Type-II censored sample, applying the theory of best linear unbiased estimators (BLUE) given in Section 5.2 in Chapter 5. We denote the BLUE of the Gaussian parameters by $(\ddot{\mu}(\mathbf{w}/p), \ddot{\sigma}^2(\mathbf{w}/p))$. We call these parameters *the* $100(p)\%$ *stress Gaussian parameters of a portfolio with weighting* $\mathbf{w}$. Let $d = (\tilde{F}_{\mathbf{w}}^{-1}(1-p) - \ddot{\mu}(\mathbf{w}/p))/\ddot{\sigma}(\mathbf{w}/p)$. Then, the empirical SER,

$\tilde{\nu}(\mathbf{w}/p)$, is computed using Equation 5.14 in Chapter 5 with $(\ddot{\mu}(\mathbf{w}/p), \ddot{\sigma}^2(\mathbf{w}/p))$. i.e.

$$\tilde{\nu}(\mathbf{w}/p) = \ddot{\mu}(\mathbf{w}/p) - \frac{\ddot{\sigma}(\mathbf{w}/p)\phi(d)}{\Phi(d)}. \tag{3.26}$$

The empirical SER, $\tilde{\nu}(\mathbf{w}/p)$, estimated in this way assumes that the distribution of $X(\mathbf{w})$ is Gaussian. Furthermore, it specifies the Gaussian distribution using only the empirical return data which were observed under the $100(p)\%$ stressful conditions. We could use distribution assumptions other than the Gaussian to compute $\tilde{\nu}(\mathbf{w}/p)$. Some examples are bivariate exponential, Cauchy and Weibull, which are all candidate models for the "tail" of financial returns distributions. For distributions other than the Gaussian, however, new conditional expectation formulae like Equation 5.14 must be derived.

3.4.5 MLE Gaussian vs Stress Gaussian

If the dataset $\mathbf{z}(\mathbf{w}, m)$ has leptokurtosis and the empirical frequency curve or histogram has higher density than the Gaussian density curve beyond the $100(1-p)^{th}$ empirical percentile, the stress Gaussian parameters $(\ddot{\mu}(\mathbf{w}/p), \ddot{\sigma}^2(\mathbf{w}/p))$ together approximate the empirical DRaR estimates of a portfolio with weighting $\mathbf{w}$ above the $100(p)\%$ tolerance level, $\tilde{S}(\mathbf{w}/p')$ $p < p' < 1$, much better than the MLE Gaussian parameters $(\hat{\mu}, \hat{\sigma}^2)$ do. Let $\ddot{S}(\mathbf{w}/p)$ denote the DRaR estimate of a portfolio with weighting $\mathbf{w}$ at the $100(p)\%$ tolerance level implied by the stress Gaussian parameters $(\ddot{\mu}(\mathbf{w}/p), \ddot{\sigma}^2(\mathbf{w}/p))$. Then,

$$\ddot{S}(\mathbf{w}/p) = \ddot{\mu}(\mathbf{w}/p) + \Phi^{-1}(1-p)\ddot{\sigma}(\mathbf{w}/p). \tag{3.27}$$

We illustrate how $\ddot{S}(\mathbf{w}/p)$ approximates $\tilde{S}(\mathbf{w}/p)$ much better than $\hat{S}(\mathbf{w}/p)$ in two ways. Figure 3-6 illustrates that the DRaR estimates of a long USD/DEM portfolio above 95% tolerance level are underestimated when the MLE Gaussian parameter estimates are used. The empirical DRaR estimates are consistently larger in magnitude. However, the stress Gaussian parameters estimates very well approximate the

Figure 3-6: The DRaR estimates of a long USD/DEM portfolio at above 95% tolerance levels under the empirical, MLE Gaussian and 95% stress Gaussian distribution assumptions

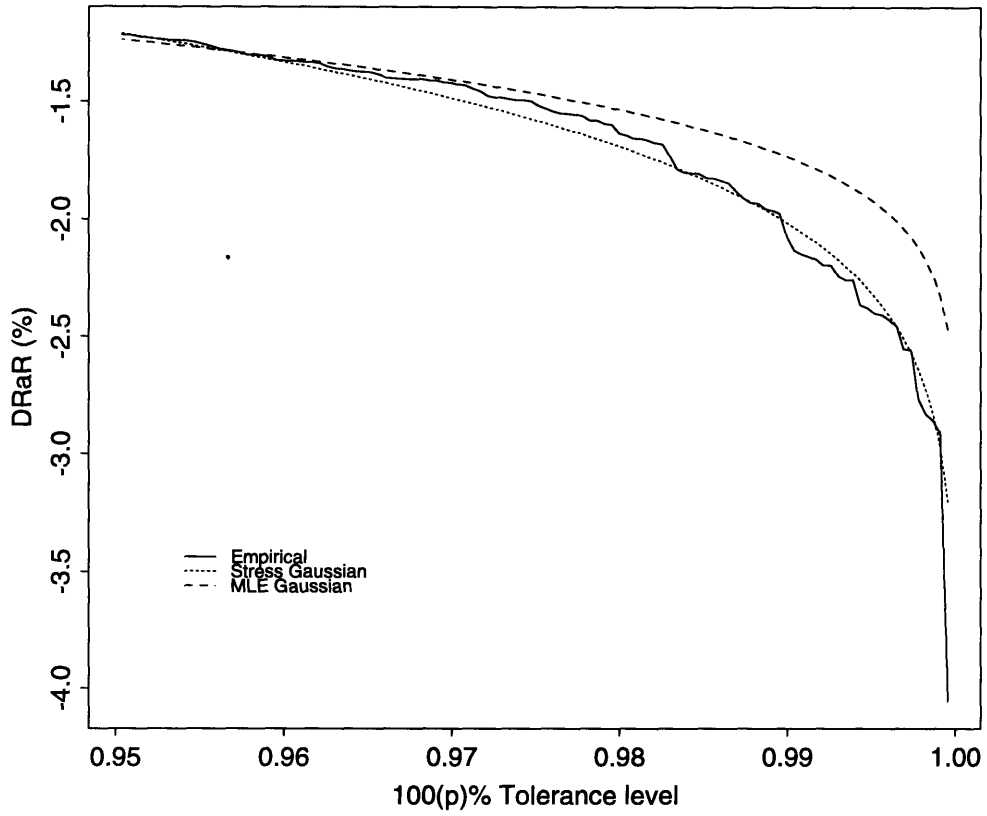

empirical DRaR estimates of the long USD/DEM portfolio above 95% tolerance level. This suggests that the empirical DRaR of a portfolio with weighting $\mathbf{w}$ at above the 95% tolerance level can be accurately estimated by the corresponding Gaussian DRaR estimates with the stress Gaussian parameters. Another way to illustrate the same point is given in Figure 3-7, which is a QQ-plot of the daily return data of USD/DEM plotted against the standard Gaussian quantiles. Kurtosis is shown by the inverted 'S' shape of the plot. Each of the fitted lines has the Gaussian mean estimate as the y-intercept on the y-axis and the Gaussian standard deviation estimate as the slope of the line. We see that the stress Gaussian parameter estimates fit the lower part of the curve better than the MLE Gaussian parameter estimates.

Figure 3-8 illustrates the 95% stress Gaussian parameter estimates of portfolios $\mathbf{w} \in \mathcal{W}$ that hold USD/DEM and USD/JPY in various long and short combinations.

Figure 3-7: Relationship between the 95% stress Gaussian parameters and the MLE Gaussian parameters of USD/DEM in a QQ-plot

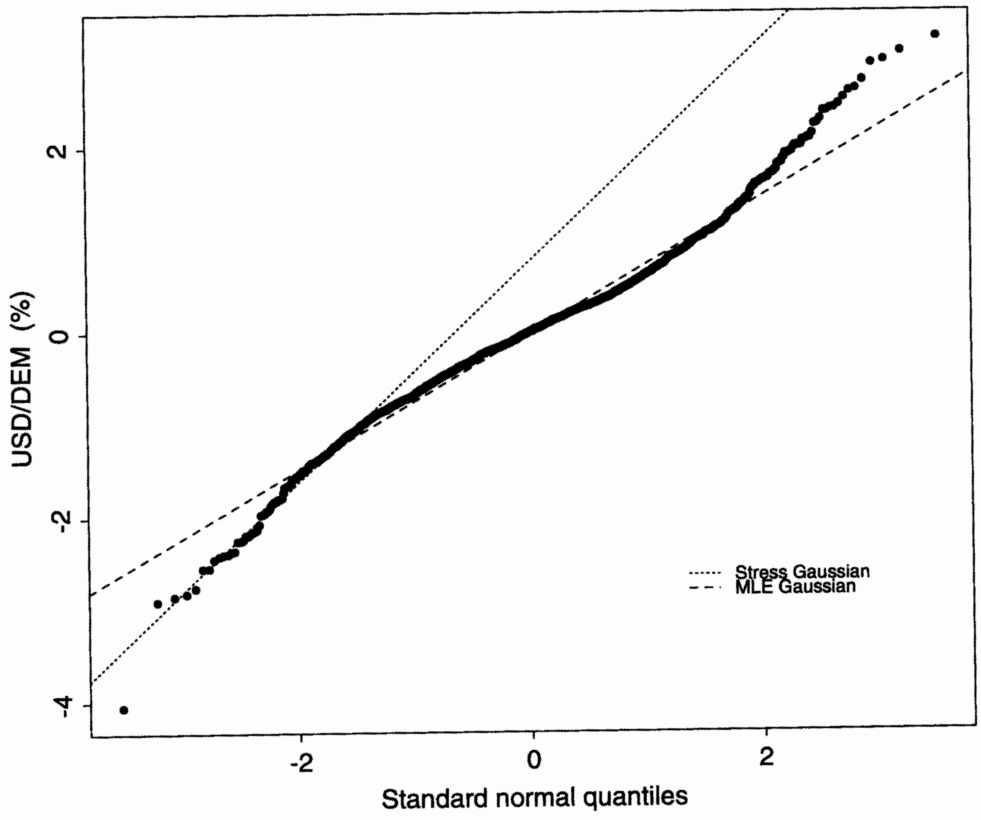

Figure 3-8: $(\ddot{\mu}(\mathbf{w}/95\%), \ddot{\sigma}^2(\mathbf{w}/95\%))$ for USD/DEM and USD/JPY, $\mathbf{w} \in \mathcal{W}$

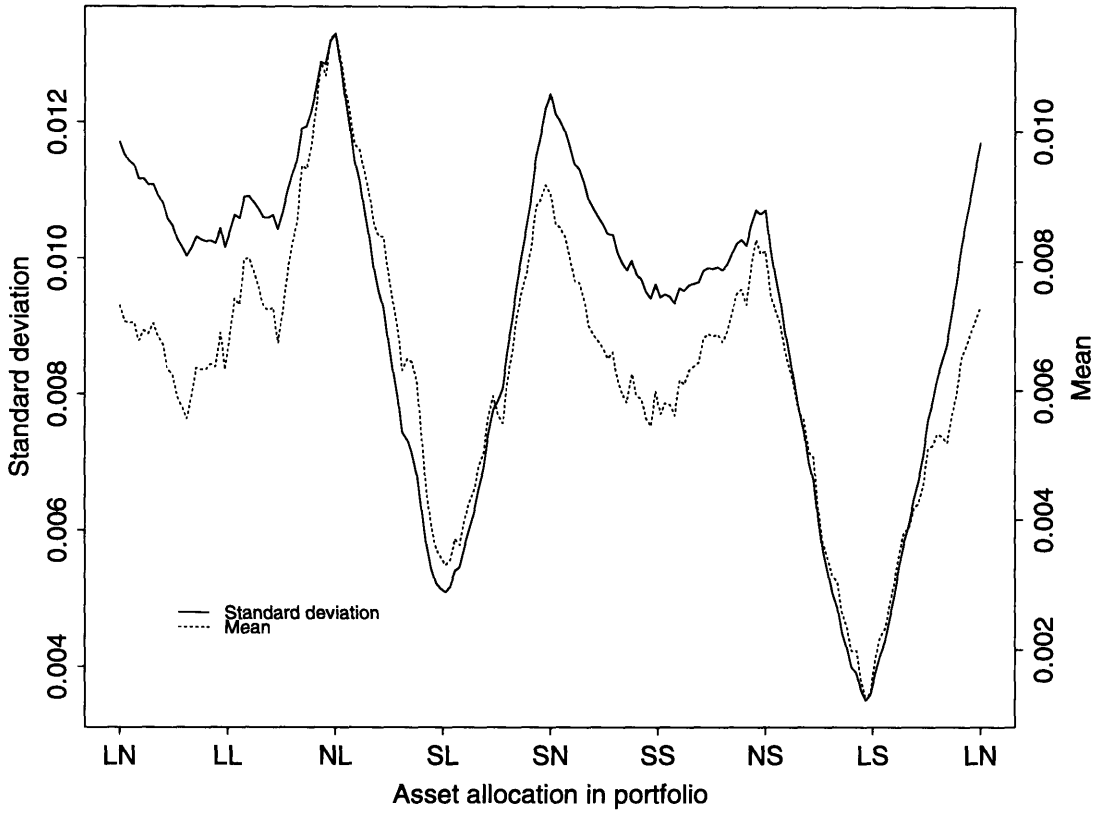

Taken alone each of these stress Gaussian parameters is useless in characterizing the risk of a portfolio. But together, they can very well characterize the risks in terms of the RaR of a portfolio at all tolerance levels above 95%.

Figure 3-9 illustrates how the 95% stress Gaussian parameters approximate the empirical DRaR of portfolios much better than the MLE Gaussian parameters for the tolerance level of 99%. Here, the portfolios with weightings $\mathbf{w} \in \mathcal{W}$ hold USD/DEM and USD/JPY.

Given a $p \in (0, 1)$, we estimate the $100(p)\%$ stress Gaussian parameters as described in Section 3.4.4. Hence, under different $100(p)\%$ stressful conditions, we have different estimates of the stress Gaussian parameters. Then, the SER and conditional standard deviation of return are computed using Equations 5.14 and 5.16 in Section 5.3 with the different stress Gaussian parameters.

Figure 3-10 illustrates respectively, for $0.95 < p < 1$, the $100(p)\%$ SER of a

Figure 3-9: $\hat{S}(\mathbf{w}/99\%)$, $\tilde{S}(\mathbf{w}/99\%)$ and $\ddot{S}(\mathbf{w}/99\%)$ for USD/DEM and USD/JPY, $\mathbf{w} \in \mathcal{W}$

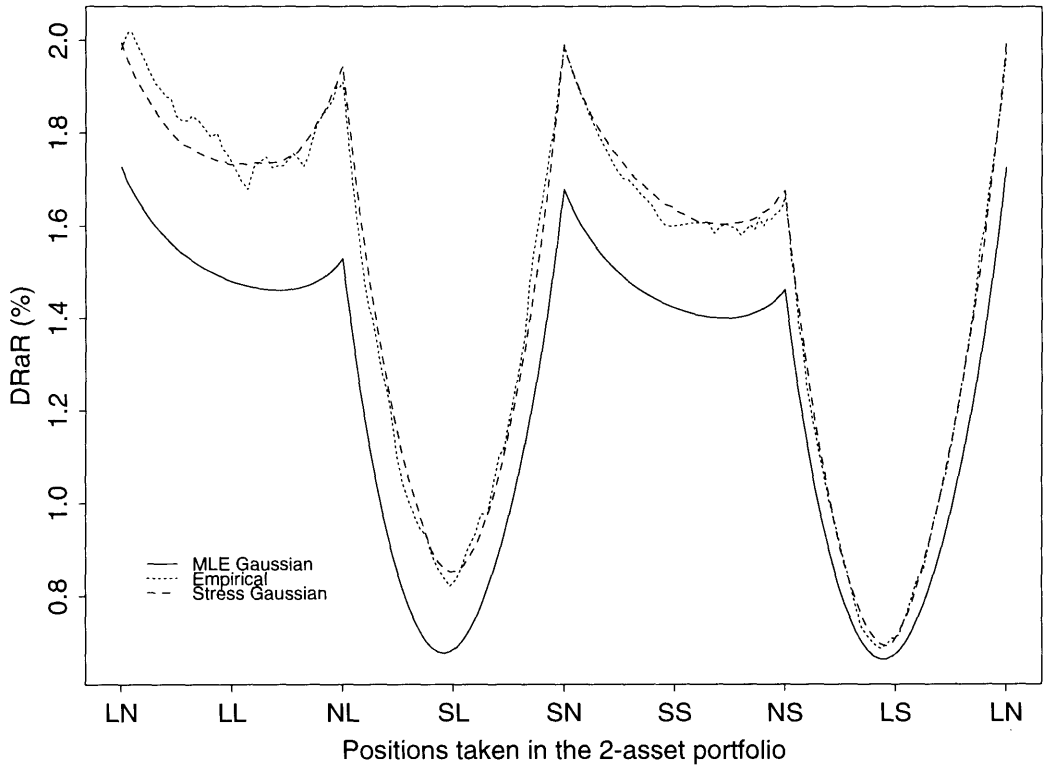

Figure 3-10: 100(p)% SER of a long USD/DEM portfolio and conditional standard deviation of USD/DEM return under 100(p)% stressful conditions, $0.95 < p < 1$

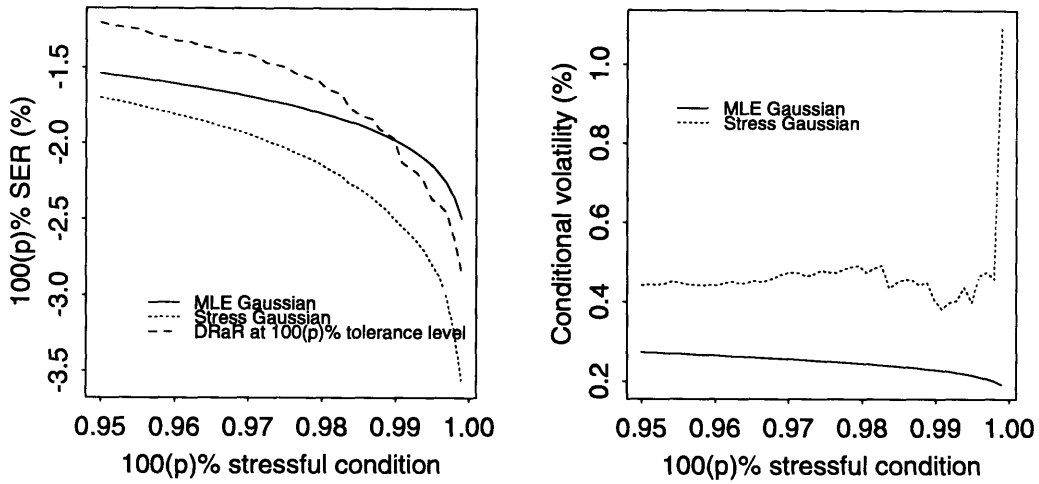

long USD/DEM portfolio and the conditional standard deviation of USD/DEM return under the different stressful conditions. Both the SER and conditional standard standard deviation are estimated using the MLE Gaussian parameters and the different 100(p)% stress Gaussian parameters. It is clear that the MLE Gaussian SER over-estimates the stress Gaussian SER. That is the MLE Gaussian model is not conservative enough in estimating the expected return of USD/DEM when a very negative return is anticipated. This is emphasized when the 100(p)% SERs estimated using the MLE and stress Gaussian parameters are plotted against the empirical RaR at the 100(p)% tolerance level ($0.95 < p < 1$) in Figure 3-11. This graph is another interpretation of the same plot in the graph on the left in Figure 3-10. By the crossing of the line 'y=x', we see how inappropriate it is to use the MLE Gaussian parameters to estimate the empirical SER.

Figure 3-12 illustrates the 95% stress volatility together with the EPMV at 95% tolerance level of portfolios with weightings $\mathbf{w} \in \mathcal{W}$ that hold USD/DEM and USD/JPY. It is intuitive to see that the stress volatility is larger than the EPMV.

Figure 3-11: $100(p)\%$ SER of a long USD/DEM portfolio estimated using MLE and stress Gaussian parameters plotted against the empirical RaR estimates at the 100(p)% tolerance level, $0.95 < p < 1$

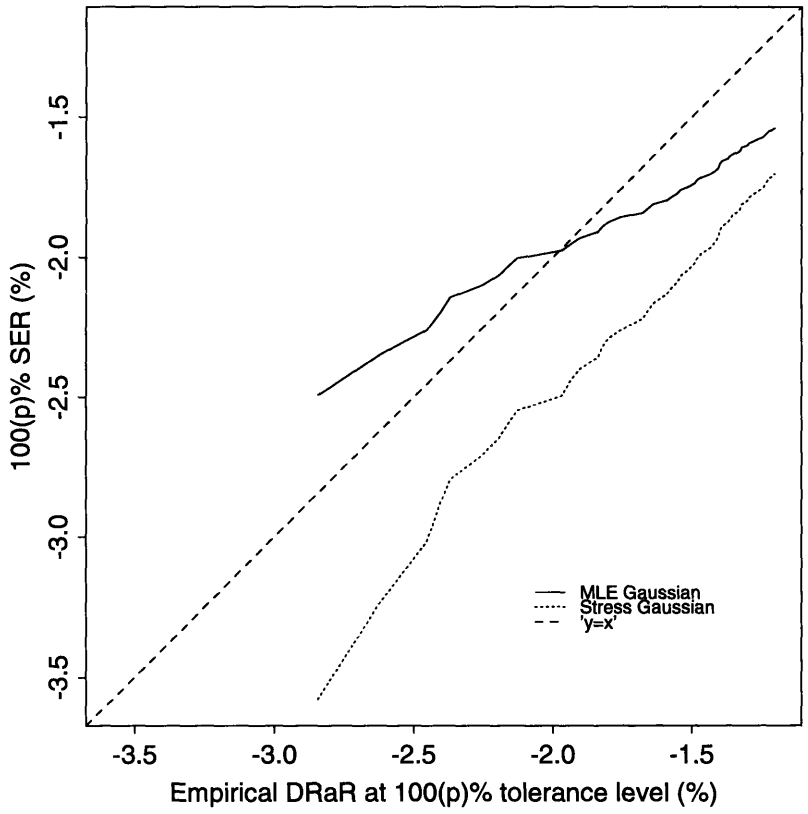

Figure 3-12: $\tilde{\varsigma}(\mathbf{w}/95\%)$ and $\tilde{\sigma}(\mathbf{w}/95\%)$ for USD/DEM and USD/JPY, $\mathbf{w} \in \mathcal{W}$

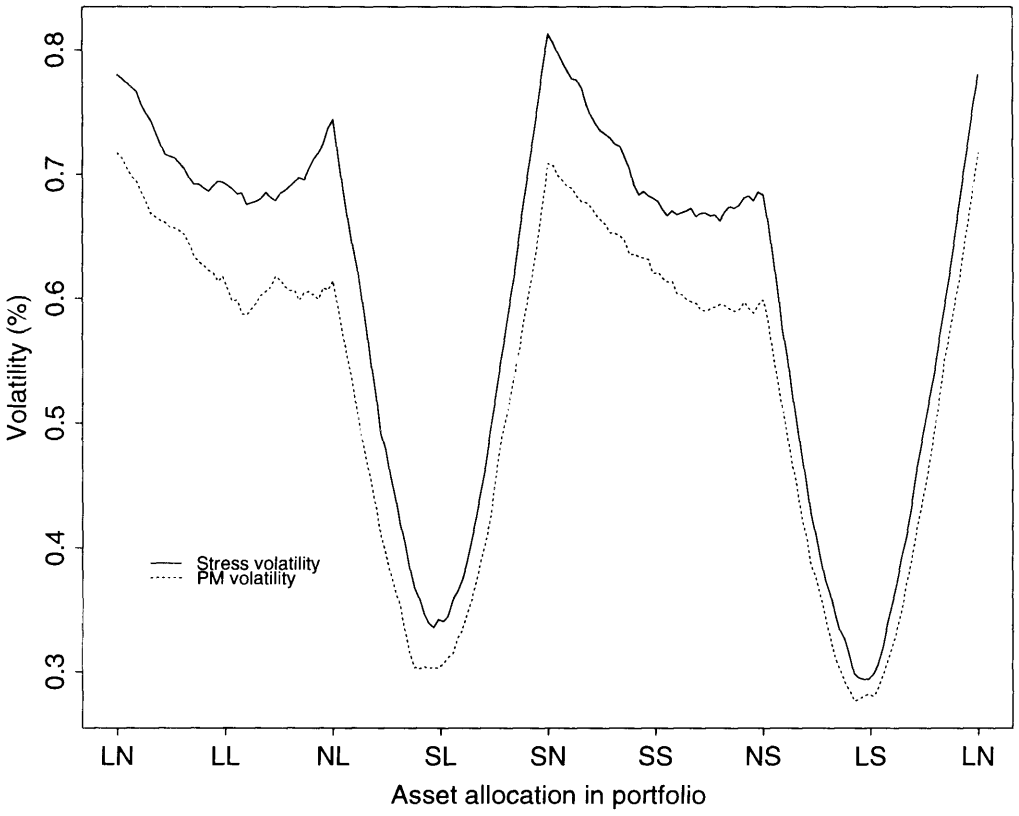

3.5 Generalized Variance-Covariance Matrices

Under the multivariate Gaussian assumption, the variance-covariance matrix Σ summarizes the risk exposure or volatility of any linear combination of the n underlying assets. Given an estimate of Σ (for example the MLE $\hat{\Sigma}$), we can derive estimation of the volatility of any portfolio with weighting $\mathbf{w}$ by Equation 3.7.

For a non-Gaussian distribution, the variance-covariance matrix Σ may provide a poor summary of the risk exposure of related portfolios. However, given the percentile-matched volatilities of portfolios with weightings $\mathbf{w} \in \mathcal{W}$ at the $100(p)\%$ tolerance level, we can induce correlation for individual portfolios. Grouping similar portfolios together, we propose below a method for estimating *the generalized variance-covariance matrix at the* $100(p)\%$ *tolerance level*, denoted $\Sigma(p)$. This matrix will summarize the PMVs of different portfolios at the $100(p)\%$ tolerance level under the general non-Gaussian distribution.

When the empirical distribution of $\mathbf{z}(k)$ $k = 1, \ldots, m$ is used to generate the different empirical portfolio return distributions, let $\tilde{\Sigma}(p)$ denote the estimate of $\Sigma(p)$. $\tilde{\Sigma}(p)$ is a positive definite matrix (any variance-covariance matrix is positive definite) that best matches with all the EPMVs of portfolios with weightings $\mathbf{w} \in \mathcal{W}$ at the $100(p)\%$ tolerance level. Mathematically, $\tilde{\Sigma}(p)$ is the solution of the following minimization problem

$$\begin{aligned} Min \quad & S(\Sigma/\mathcal{W}, p) \equiv \oint_{\mathbf{w}\in\mathcal{W}} d\mathbf{w} \left\{\sqrt{\mathbf{w}'\Sigma\mathbf{w}} - \tilde{\sigma}(\mathbf{w}/p)\right\}^2 \\ \textit{subject to} \quad & \Sigma \; p.d \end{aligned} \tag{3.28}$$

p.d. stands for 'positive definite'. Chapter 6 will discuss how to approximate solutions to this optimization problem using non-linear programming algorithms.

In order to capture the asymmetry of risk exposure and the varying correlation induced by different portfolios, we cannot have just one estimate of the generalized variance-covariance matrix. We use different estimates of the generalized variance-covariance matrix to match the PMVs of a group of portfolios with similar weightings $\mathbf{w}$. In Figure 1-1, different groups of portfolios with similar weightings are repre-

Figure 3-13: Fitting $\tilde{\sigma}(\mathbf{w}/99\%)$ for USD/DEM and USD/JPY, $\mathbf{w} \in \mathcal{W}$

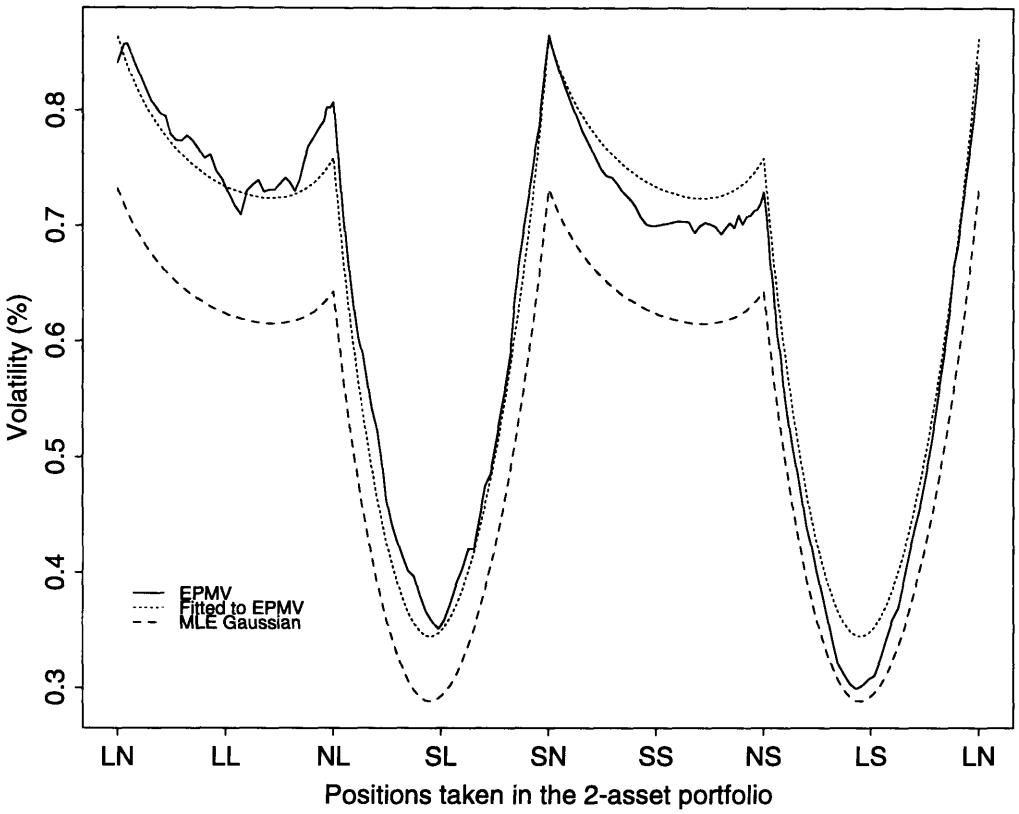

sented by different segments of $\mathcal{W}$. In doing so, we need to give new notations to the different estimates of the generalized variance-covariance matrix. These notations should identify the different collections of portfolios with similar weightings. Using Figure 1-1, the directions NE, NW, SW and SE, for eaxmple, can identify respectively the segments of $\mathcal{W}$ in the four quadrants, i.e. the segments in the first, second, third and fourth quadrant are respectively denoted $\mathcal{W}^{(NE)}, \mathcal{W}^{(NW)}, \mathcal{W}^{(SW)}$ and $\mathcal{W}^{(SE)}$, if we want to find the estimates of the generalized variance-covariance matrix matching the PMVs of portfolios with weightings $\mathbf{w}$ within each quadrant. Let $S(\Sigma/\mathcal{W}^{(NE)}, p), \ldots, S(\Sigma/\mathcal{W}^{(SE)}, p)$ denote the respective objective functions, and $\tilde{\Sigma}^{(NE)}(p), \ldots, \tilde{\Sigma}^{(SE)}(p)$ denote the respective solutions.

Figure 3-13 illustrates the EPMVs, the historical volatility estimates given by the MLE Gaussian model and the volatility estimates given by $\sqrt{\mathbf{w}'\tilde{\Sigma}(99\%)\mathbf{w}}$ of portfolios with weightings $\mathbf{w}$ that hold USD/DEM and USD/JPY. We see that some

Figure 3-14: Fitting $\tilde{\sigma}(\mathbf{w}/99\%)$ separately in the 4 quadrants of $\mathcal{W}$ for USD/DEM and USD/JPY

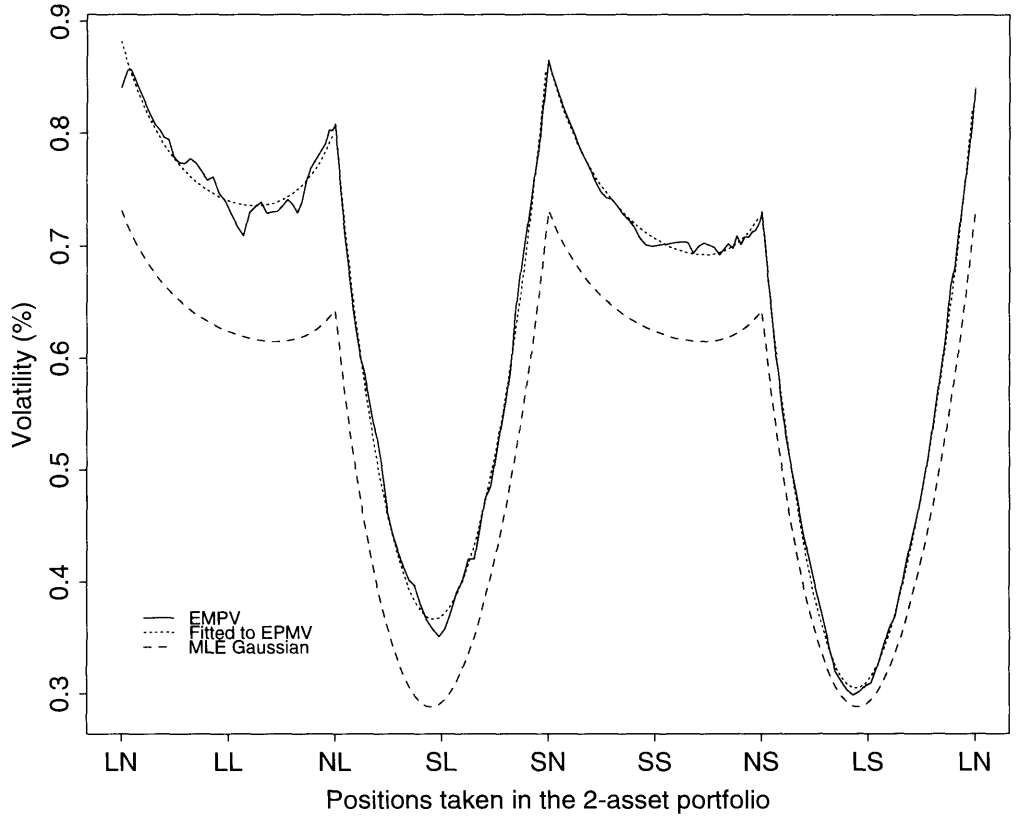

parts of $\tilde{\sigma}(\mathbf{w}/99\%)$ are not fitted well by $\tilde{\Sigma}(99\%)$. Figure 3-14 illustrates the fit of $\tilde{\sigma}(\mathbf{w}/99\%)$ separately in the 4 quadrants of $\mathcal{W}$. i.e. we are using the portfolio risk estimates given by the four matrices $\tilde{\Sigma}^{(NE)}(99\%), \ldots, \tilde{\Sigma}^{(SE)}(99\%)$ for the fitted curve. When compared to Figure 3-13, the fit in Figure 3-14 is much better. This illustrates that the asymmetry of risk in the empirical data at 99% tolerance level is not captured very well by $\tilde{\Sigma}(99\%)$, but is captured much better by the four matrices $\tilde{\Sigma}^{(NE)}(99\%), \ldots, \tilde{\Sigma}^{(SE)}(99\%)$.

It is interesting to compare the different matrices and illustrate by the comparison the skewed asymmetry and kurtosis features. Denote $vol1$ (in %) as the volatility estimate of the first variable (USD/DEM) given by a generalized variance-covariance matrix $\Sigma(p)$, $vol2$ (in %) as the volatility estimate of the second variable (USD/JPY) given by $\Sigma(p)$ and $corr$ as the correlation between the two variables (USD/DEM and USD/JPY) given by $\Sigma(p)$ i.e.

$$\begin{aligned} vol1 &= \sqrt{\{\Sigma(p)\}_{11}} \\ vol2 &= \sqrt{\{\Sigma(p)\}_{22}} \\ corr &= \frac{\{\Sigma(p)\}_{12}}{(vol1)(vol2)} \end{aligned}$$

Table 3.1 illustrates the values of $vol1$, $vol2$ and $corr$ given by the respective empirical generalized variance-covariance matrix estimates whose name is given in the first column. The name with just the two exchange rates represents the matrix $\tilde{\Sigma}(99\%)$. The name with the two exchange rates plus a direction, for example (NE) represents the matrix $\tilde{\Sigma}^{(NE)}(99\%)$. The sample variance-covariance matrix, named MLE, is for comparison to show kurtosis. Asymmetry at the $100(p)\%$ tolerance level is shown via the different volatility estimates of the same asset given by the four matrices $\tilde{\Sigma}^{(NE)}(p), \ldots, \tilde{\Sigma}^{(SE)}(p)$.

We see that the risk estimates of USD/DEM and USD/JPY at the 99% tolerance level based on the different generalized variance-covariance matrices are respectively larger than those implied by the maximum likelihood estimate of the variance-covariance matrix. This quantifies the evidence that the MLE Gaussian model under-

Table 3.1: Summary of the generalized variance-covariance matrices (empirical estimates) for USD/DEM and USD/JPY at 99% tolerance level

Matrix name	vol1(%)	vol2(%)	corr
USD/DEM , USD/JPY	0.863	0.758	0.636
USD/DEM , USD/JPY (NE)	0.882	0.808	0.540
USD/DEM , USD/JPY (NW)	0.887	0.808	0.624
USD/DEM , USD/JPY (SW)	0.863	0.731	0.568
USD/DEM , USD/JPY (SE)	0.854	0.731	0.700
MLE	0.732	0.643	0.645

estimate the risk exposure of USD/DEM and USD/JPY implied by the empirical data at the 99% tolerance level.

Results at both the 95% and 99% tolerance levels for other foreign exchange rates and equity indexes are given in Chapter 4.

3.6 Generalized Variance-Covariance Matrices For More Than Two Assets

When portfolios have holdings of n assets, the different risk exposures of different portfolios are summarized by an n-dimensional variance-covariance matrix. The results that we have generated so far are only in two dimensions. Because we can solve the minimization problem given by Equation 3.28 fast with a pair of assets, we use the two dimensional methods repeatedly to build the relavant variance-covariance matrix in n dimensions for modeling the risks of portfolios under non-Gaussian distribution assumptions. The algorithm to model the risk of a portfolio $\mathbf{w}$ at the $100(p)\%$ tolerance level under the empirical distribution assumption is given as follows.

Algorithm 3.1 *1. Given a portfolio* $\mathbf{w} = (w_1, \ldots, w_n)'$, $(w_j \neq 0 \quad \forall j)$ *identify the sign of each* w_j. *i.e. identify whether the portfolio has a long or short position in the* j^{th} *asset. For* $j = 1, \ldots, n$, *set* $s_j = +(-)$ *if* $w_j > (<)0$. *Denote* $\mathbf{s} = (s_1, \ldots, s_n)'$.

2. *Each of the n assets is identified with an integer from 1 to n. The j^{th} asset is identified by j. Among the n assets, choose in turn two assets from the n until all the* $\begin{pmatrix} n \\ 2 \end{pmatrix}$ *possible combinations have been chosen. Denote the k^{th} combination* $(x_1^{(k)}, x_2^{(k)})$, $k \in C_2^n \equiv \{1, \ldots, \begin{pmatrix} n \\ 2 \end{pmatrix}\}$. $x_i^{(k)} \in \{1, \ldots, n\}$, $i = 1, 2$.

3. *For each $k \in C_2^n$, estimate the EPMVs of portfolios with weightings $\mathbf{w} \in \mathcal{W}$ at the $100(p)\%$ tolerance level.*

4. *For each $k \in C_2^n$, if the portfolio's holding in $x_1^{(k)}$ is positive (negative), set $i_1^{(k)} = E$ (W); if the portfolio's holding in $x_2^{(k)}$ is positive (negative), set $i_2^{(k)} = N$ (S). Solve the problem given in Equation 3.28 with $S(\Sigma/\mathcal{W}^{(i_2^{(k)} i_1^{(k)})}, p)$ as the objective function. Denote the solution of the problem $\tilde{\Sigma}^{(i_2^{(k)} i_1^{(k)})}(p)$.*

5. *Set, for $i = 1, 2$,*

$$\tilde{\sigma}^2(x_i^{(k)}) = \{\tilde{\Sigma}^{(i_2^{(k)} i_1^{(k)})}(p)\}_{ii}, \tag{3.29}$$

and

$$\begin{aligned} \tilde{\rho}(x_1^{(k)}, x_2^{(k)}) &= \frac{\{\tilde{\Sigma}^{(i_2^{(k)} i_1^{(k)})}(p)\}_{12}}{\sqrt{\tilde{\sigma}^2(x_1^{(k)})\tilde{\sigma}^2(x_2^{(k)})}}, \\ \tilde{\rho}(x_2^{(k)}, x_1^{(k)}) &= \frac{\{\tilde{\Sigma}^{(i_2^{(k)} i_1^{(k)})}(p)\}_{21}}{\sqrt{\tilde{\sigma}^2(x_1^{(k)})\tilde{\sigma}^2(x_2^{(k)})}}. \end{aligned} \tag{3.30}$$

Note $\tilde{\rho}(x_1^{(k)}, x_2^{(k)}) = \tilde{\rho}(x_2^{(k)}, x_1^{(k)})$.

6. *Denote the n-dimensional generalized variance-covariance matrix as $\tilde{\Sigma}_n(\mathbf{s}/p)$. For $j = 1, \ldots, n$, set*

$$\{\tilde{\Sigma}_n(\mathbf{s}/p)\}_{jj} = \frac{1}{n-1}\Big(\sum_{\{k \in C_2^n : x_1^{(k)} = j\}} \tilde{\sigma}^2(x_1^{(k)}) + \sum_{\{k \in C_2^n : x_2^{(k)} = j\}} \tilde{\sigma}^2(x_2^{(k)})\Big), \tag{3.31}$$

and for $1 \leq i \leq n$, $1 \leq j \leq n$ such that $i \neq j$ set

$$\{\tilde{\Sigma}_n(\mathbf{s}/p)\}_{ij} = \tilde{\rho}(i, j)\sqrt{\{\tilde{\Sigma}^{(i_2^{(k)} i_1^{(k)})}(p)\}_{11}\{\tilde{\Sigma}^{(i_2^{(k)} i_1^{(k)})}(p)\}_{22}} \tag{3.32}$$

The algorithm assembles the different 2×2 matrices together into an $n \times n$ matrix. The i^{th} diagonal element of the $n \times n$ matrix is the average of the $n-1$ variance estimates for the i^{th} asset from the $(n-1)$ 2×2 generalized variance-covariance matrices that involve the i^{th} asset. The (i,j) element off the diagonal is the covariance of assets i and j such that the correlation between the assets estimated by the corresponding 2×2 generalized variance-covariance matrix involving the two assets is maintained. In this way, the n-dimensional generalized variance-covariance matrix remains positive definite.

Instead of showing an $n \times n$ generalized variance-covariance matrix directly, a more informative way to show the matrix is to use the correlation matrix with the diagonal elements of 1's replaced by the respective volatility estimates of the individual assets. The volatility estimate of the i^{th} asset is the square root of the i^{th} element in the diagonal of the $n \times n$ generalized variance-covariance matrix. The i^{th} column and row of the matrix are respectively named $\{i^{th}\ asset\ name\}^{s_i}$ where $s_i = +(-)$ if the portfolio is long (short) in the i^{th} asset.

Table 3.2 illustrates the information of the generalized variance-covariance matrix that characterizes the risk at 99% tolerance level of any portfolio that has long positions in all of the four equity indexes. Table 3.3 illustrates a similar matrix but for portfolios that short all of the four equity indexes. The two tables are generated from results given in Table 4.3 in Chapter 4.

From the two tables, we see evidence of asymmetry in the four equity indexes. The downside risk of each equity index is larger than the upside risk. Also the correlations between pairs of indexes are more positive when the estimates are focusing on accurately measuring downside risks versus upside risks. This shows that the indexes more frequently slump together than climb together.

Table 3.4 is the variance-covariance matrix estimated by maximum likelihood. Comparing this matrix with those in Tables 3.2 and 3.3, we see that leptokurtosis is evident and symmetric across all equity indexes except SP500, in which case asymmetric leptokurtosis occurs only on the downside.

Table 3.2: The generalized variance-covariance matrix (empirical estimate) at 99% tolerance level for portfolios that have long positions of all of the four equity indexes

	$SP500^+$	$NIKKEI^+$	DAX^+	$CAC\text{-}40^+$
$SP500^+$	1.340	0.180	0.340	0.340
$NIKKEI^+$	0.180	1.370	0.440	0.420
DAX^+	0.340	0.440	1.761	0.616
$CAC\text{-}40^+$	0.340	0.420	0.616	1.539

Table 3.3: The generalized variance-covariance matrix (empirical estimate) at 99% tolerance level for portfolios that have short positions of all of the four equity indexes

	$SP500^-$	$NIKKEI^-$	DAX^-	$CAC\text{-}40^-$
$SP500^-$	1.094	-0.020	0.028	-0.032
$NIKKEI^-$	-0.020	1.276	-0.072	0.140
DAX^-	0.028	-0.072	1.649	0.000
$CAC\text{-}40^-$	-0.032	0.140	0.000	1.216

Table 3.4: The MLE variance-covariance matrix for the four equity indexes

	SP500	NIKKEI	DAX	CAC-40
SP500	1.238	0.124	0.201	0.133
NIKKEI	0.124	1.109	0.303	0.316
DAX	0.201	0.303	1.415	0.432
CAC-40	0.133	0.316	0.432	1.175

3.7 Stress Variance-Covariance Matrices

Analogous to a generalized variance-covariance matrix at the $100(p)\%$ tolerance level, which is summarizing the PMVs of different portfolios at the $100(p)\%$ tolerance level, *the* $100(p)\%$ *stress variance-covariance matrix* is the matrix that summarizes the $100(p)\%$ stress volatilities of different portfolios. Let $\Omega(p)$ denote this $100(p)\%$ stress variance-covariance matrix.

Under the empirical distribution assumption, let $\tilde{\Omega}(p)$ denote the estimate of $\Omega(p)$. Mathematically $\tilde{\Omega}(p)$ is the solution of a problem similar to that given by Equation 3.28. This particular problem is

$$\begin{aligned} Min \quad & R(\Sigma/\mathcal{W},p) \equiv \oint_{\mathbf{w}\in\mathcal{W}} d\mathbf{w}\,\{\sqrt{\mathbf{w}'\Sigma\mathbf{w}} - \tilde{\varsigma}(\mathbf{w}/p)\}^2 \\ subject\ to \quad & \Sigma\ p.d \end{aligned} \tag{3.33}$$

The only difference between this problem and the one given by Equation 3.28 is that the constant term in the objective function is different. Before, it was the EPMV. In this problem, the constant is the empirical stress volatility estimated by the stress Gaussian parameters.

As before, we try to capture asymmetry of risk exposure and the varying correlation by solving the problem within different segments of $\mathcal{W}$. Let $\tilde{\Omega}^{(NE)}(p),\ldots,\tilde{\Omega}^{(SE)}(p)$ denote respectively the different empirical $100(p)\%$ stress variance-covariance estimates. The information of a matrix is summarized the same way as for the generalized variance-covariance matrix using *vol*1, *vol*2, and *corr*. Further, we can apply Algorithm 3.1 to build the relavant empirical $n \times n$ stress variance-covariance matrix estimate. The different steps are estimating the empirical $100(p)\%$ stress volatilities of portfolios with weightings $\mathbf{w} \in \mathcal{W}$ instead of step 3; and solving Problem 3.33 rather than Problem 3.28 in step 4.

Table 3.5 shows the information of the empirical 95% stress variance-covariance matrices estimates of portfolios that hold USD/DEM and USD/JPY. When the results of this table are compared to the results in Table 4.5, we see that the volatility estimates given by the stress matrices lie between those given by the respective gen-

Table 3.5: Summary of the 95% stress variance-covariance matrices (empirical estimates) for USD/DEM and USD/JPY

Matrix name	vol1(%)	vol2(%)	corr
USD/DEM , USD/JPY (NE)	0.783	0.731	0.620
USD/DEM , USD/JPY (NW)	0.813	0.755	0.628
USD/DEM , USD/JPY (SW)	0.817	0.693	0.620
USD/DEM , USD/JPY (SE)	0.784	0.682	0.668
MLE	0.732	0.643	0.645

erlized matrices at 95% and 99% tolerance level. This suggests that the 95% stress tolerance level will typically lie between 95% and 99%. (closer to 99% than 95%). Moreover, we see from Table 3.5 that the volatility estimates given by the stress matrices are all greater than the respective MLE estimates. This implies that under the 95% stressful conditions, the risk of each individual asset is larger than that estimated by the MLE Gaussian model.

Tables 3.6 and 3.7 are the respective 95% stress variance-covariance matrix (empirical estimate) of the portfolios that have either long or short positions in all of the four equity indexes. When compared to the respective generalized variance-covariance matrix (empirical estimate) at the 99% tolerance level, we see that all the volatility estimates of the indiviual indexes (elements on the digonal of the matrix) are lower in the stress matrix, with the exception of that of $SP500^{+}$. This implies that the 95% stress tolerance level of a long portfolio of the SP500 index is beyond the 99% level under the empirical distribution assumption. This may be because of the 1987 crash when the one-day realized return was -20.4%, which lowers the SER and consequently increases the stress tolerance level.

By comparing Tables 3.6 and 3.7 with Table 3.4, asymmetric leptokurtosis on the downside is evident for all the indexes except Nikkei which has symmetric leptokurtosis.

Results using the two dimensional methods for other pairs of foreign exchage rates with the USD and the DEM and pairs of equity indexes are given in Chapter 4.

Table 3.6: The 95% stress variance-covariance matrix (empirical estimate) for portfolios that have long positions of all of the four equity indexes

	$SP500^+$	$NIKKEI^+$	DAX^+	$CAC\text{-}40^+$
$SP500^+$	1.410	0.088	0.168	0.220
$NIKKEI^+$	0.088	1.325	0.292	0.336
DAX^+	0.168	0.292	1.645	0.360
$CAC\text{-}40^+$	0.220	0.336	0.360	1.420

Table 3.7: The 95% stress variance-covariance matrix (empirical estimate) for portfolios that have short positions of all of the four equity indexes

	$SP500^-$	$NIKKEI^-$	DAX^-	$CAC\text{-}40^-$
$SP500^-$	1.060	0.120	0.164	0.004
$NIKKEI^-$	0.120	1.136	0.164	0.180
DAX^-	0.164	0.164	1.409	0.204
$CAC\text{-}40^-$	0.004	0.180	0.204	1.140

Chapter 4

Applications to Foreign Exchange and Equity Index Returns

4.1 Introduction

This chapter presents results for datasets other than the USD/DEM and USD/JPY exchange rates. These datasets have already been introduced and described in Section 2.2. While many results could be presented, we give only the information summary of the 2×2 generalized and stress variance-covariance matrices.

4.2 Generalized Variance-Covariance Matrices Results

This section presents the results of estimating the 2×2 generalized variance-covariance matrices as in Table 3.1 in Section 3.5 for other pairs of foreign exchange rates at both the 95% and 99% tolerance levels. Table 4.1 presents the results for pairs of foreign exchange rates chosen from the seven currencies with the DEM. Table 4.2 presents the results for pairs of foreign exchange rates chosen from the eight curreicies with the USD. Table 4.3 presents the results for pairs of equity indexes chosen from the four equity indexes.

Table 4.1: Summary of the generalized variance-covariance matrices (empirical estimates) for pairs of exchange rates with the DEM at 95% and 99% tolerance levels

	95% tolerance level			99% tolerance level		
Matrix name	vol1 (%)	vol2 (%)	corr	vol1 (%)	vol2 (%)	corr
USD , CHF	0.712	0.263	0.036	0.866	0.289	-0.024
USD , CHF (NE)	0.708	0.277	0.000	0.886	0.319	-0.104
USD , CHF (NW)	0.711	0.261	0.028	0.870	0.304	-0.040
USD , CHF (SW)	0.714	0.257	0.056	0.861	0.287	-0.100
USD , CHF (SE)	0.724	0.261	0.060	0.890	0.289	0.160
USD , ESP	0.731	0.258	-0.204	0.864	0.421	-0.148
USD , ESP (NE)	0.728	0.243	-0.196	0.899	0.338	-0.260
USD , ESP (NW)	0.717	0.238	-0.320	0.871	0.383	-0.052
USD , ESP (SW)	0.706	0.244	0.000	0.885	0.534	-0.280
USD , ESP (SE)	0.719	0.263	-0.316	0.921	0.554	0.220
USD , FRF	0.721	0.103	-0.260	0.878	0.138	-0.176
USD , FRF (NE)	0.721	0.100	-0.280	0.907	0.137	-0.316
USD , FRF (NW)	0.719	0.105	-0.240	0.868	0.134	-0.196
USD , FRF (SW)	0.706	0.092	-0.080	0.868	0.155	-0.240
USD , FRF (SE)	0.730	0.105	-0.236	0.883	0.162	0.000
USD , ITL	0.731	0.247	-0.204	0.873	0.392	-0.100
USD , ITL (NE)	0.725	0.218	-0.176	0.905	0.360	-0.276
USD , ITL (NW)	0.718	0.220	-0.340	0.876	0.372	-0.020
USD , ITL (SW)	0.700	0.232	0.068	0.874	0.452	-0.160
USD , ITL (SE)	0.734	0.252	-0.240	0.903	0.473	0.144
USD , JPY	0.718	0.584	-0.312	0.872	0.658	-0.336
USD , JPY (NE)	0.715	0.595	-0.300	0.888	0.731	-0.388
USD , JPY (NW)	0.703	0.581	-0.368	0.903	0.703	-0.236
USD , JPY (SW)	0.724	0.573	-0.320	0.869	0.617	-0.380
USD , JPY (SE)	0.725	0.575	-0.316	0.873	0.643	-0.220
USD , GBP	0.717	0.455	0.208	0.861	0.550	0.140
USD , GBP (NE)	0.717	0.474	0.268	0.889	0.583	-0.020
USD , GBP (NW)	0.710	0.477	0.144	0.858	0.594	0.140
USD , GBP (SW)	0.715	0.417	0.200	0.885	0.550	0.040
USD , GBP (SE)	0.717	0.434	0.260	0.887	0.538	0.288
CHF , ESP	0.267	0.244	0.064	0.299	0.438	-0.060
CHF , ESP (NE)	0.264	0.234	0.016	0.304	0.350	0.060
CHF , ESP (NW)	0.260	0.238	0.040	0.281	0.340	0.020
CHF , ESP (SW)	0.261	0.255	0.180	0.306	0.524	-0.280
CHF , ESP (SE)	0.262	0.244	-0.040	0.310	0.539	-0.056

Table 4.1: Summary of the generalized variance-covariance matrices (empirical estimates) for pairs of exchange rates with the DEM at 95% and 99% tolerance levels

	95% tolerance level			99% tolerance level		
Matrix name	vol1 (%)	vol2 (%)	corr	vol1 (%)	vol2 (%)	corr
CHF , FRF	0.265	0.099	0.076	0.297	0.146	-0.012
CHF , FRF (NE)	0.265	0.094	0.080	0.312	0.139	-0.004
CHF , FRF (NW)	0.266	0.098	0.116	0.283	0.128	-0.036
CHF , FRF (SW)	0.264	0.099	0.120	0.287	0.152	-0.060
CHF , FRF (SE)	0.264	0.100	0.020	0.302	0.161	-0.080
CHF , ITL	0.264	0.234	0.068	0.293	0.406	0.016
CHF , ITL (NE)	0.269	0.220	0.076	0.303	0.363	0.068
CHF , ITL (NW)	0.260	0.213	0.040	0.287	0.378	0.164
CHF , ITL (SW)	0.263	0.246	0.100	0.300	0.459	-0.200
CHF , ITL (SE)	0.267	0.254	0.036	0.312	0.441	-0.020
CHF , JPY	0.260	0.580	0.096	0.302	0.657	0.008
CHF , JPY (NE)	0.259	0.588	0.148	0.317	0.685	-0.060
CHF , JPY (NW)	0.254	0.583	0.080	0.282	0.693	0.000
CHF , JPY (SW)	0.257	0.573	0.100	0.283	0.619	0.148
CHF , JPY (SE)	0.258	0.571	0.040	0.318	0.629	0.040
CHF , GBP	0.262	0.442	-0.076	0.291	0.568	-0.048
CHF , GBP (NE)	0.261	0.465	-0.056	0.305	0.608	-0.120
CHF , GBP (NW)	0.260	0.468	-0.116	0.276	0.597	-0.120
CHF , GBP (SW)	0.257	0.421	-0.060	0.285	0.539	-0.052
CHF , GBP (SE)	0.259	0.414	-0.100	0.311	0.531	0.040
ESP , FRF	0.243	0.103	0.412	0.423	0.145	0.412
ESP , FRF (NE)	0.234	0.093	0.560	0.329	0.135	0.424
ESP , FRF (NW)	0.253	0.097	0.388	0.494	0.134	0.340
ESP , FRF (SW)	0.250	0.106	0.520	0.513	0.144	0.476
ESP , FRF (SE)	0.229	0.097	0.280	0.336	0.145	0.320
ESP , ITL	0.253	0.240	0.428	0.417	0.412	0.348
ESP , ITL (NE)	0.233	0.218	0.452	0.331	0.372	0.560
ESP , ITL (NW)	0.251	0.215	0.280	0.487	0.368	0.280
ESP , ITL (SW)	0.249	0.243	0.940	0.520	0.462	0.132
ESP , ITL (SE)	0.235	0.245	0.328	0.320	0.435	0.280
ESP , JPY	0.244	0.589	0.172	0.414	0.665	0.052
ESP , JPY (NE)	0.233	0.579	0.220	0.354	0.702	-0.048
ESP , JPY (NW)	0.240	0.589	0.060	0.521	0.706	0.120
ESP , JPY (SW)	0.258	0.577	0.236	0.508	0.651	-0.020
ESP , JPY (SE)	0.231	0.573	0.160	0.340	0.626	0.120

Table 4.1: Summary of the generalized variance-covariance matrices (empirical estimates) for pairs of exchange rates with the DEM at 95% and 99% tolerance levels

	95% tolerance level			99% tolerance level		
Matrix name	vol1 (%)	vol2 (%)	corr	vol1 (%)	vol2 (%)	corr
ESP , GBP	0.252	0.448	-0.248	0.419	0.566	-0.208
ESP , GBP (NE)	0.222	0.464	-0.120	0.335	0.606	-0.136
ESP , GBP (NW)	0.259	0.464	-0.380	0.530	0.597	-0.140
ESP , GBP (SW)	0.248	0.414	-0.120	0.498	0.529	-0.260
ESP , GBP (SE)	0.230	0.418	-0.412	0.337	0.542	-0.200
FRF , ITL	0.103	0.233	0.516	0.147	0.415	0.424
FRF , ITL (NE)	0.092	0.218	0.604	0.134	0.374	0.460
FRF , ITL (NW)	0.101	0.214	0.456	0.149	0.369	0.432
FRF , ITL (SW)	0.096	0.250	0.808	0.153	0.442	0.560
FRF , ITL (SE)	0.100	0.246	0.456	0.155	0.459	0.460
FRF , JPY	0.099	0.587	0.204	0.139	0.665	0.124
FRF , JPY (NE)	0.098	0.589	0.180	0.140	0.707	-0.024
FRF , JPY (NW)	0.098	0.587	0.140	0.152	0.708	0.120
FRF , JPY (SW)	0.094	0.577	0.360	0.155	0.628	0.132
FRF , JPY (SE)	0.096	0.580	0.220	0.130	0.631	0.220
FRF , GBP	0.102	0.441	-0.188	0.141	0.568	-0.128
FRF , GBP (NE)	0.090	0.459	0.020	0.133	0.613	-0.240
FRF , GBP (NW)	0.102	0.460	-0.280	0.138	0.593	-0.272
FRF , GBP (SW)	0.095	0.411	-0.100	0.152	0.539	-0.136
FRF , GBP (SE)	0.093	0.414	-0.380	0.143	0.536	-0.060
ITL , JPY	0.240	0.585	0.176	0.401	0.660	0.172
ITL , JPY (NE)	0.217	0.589	0.224	0.378	0.692	0.100
ITL , JPY (NW)	0.245	0.576	-0.040	0.431	0.717	0.180
ITL , JPY (SW)	0.241	0.573	0.344	0.458	0.636	0.100
ITL , JPY (SE)	0.210	0.573	0.164	0.369	0.637	0.276
ITL , GBP	0.243	0.450	-0.128	0.391	0.571	-0.088
ITL , GBP (NE)	0.207	0.465	0.080	0.365	0.609	-0.180
ITL , GBP (NW)	0.243	0.454	-0.400	0.445	0.605	0.040
ITL , GBP (SW)	0.250	0.419	-0.020	0.453	0.542	-0.180
ITL , GBP (SE)	0.213	0.420	-0.300	0.370	0.556	0.020
JPY , GBP	0.581	0.451	-0.176	0.648	0.565	-0.076
JPY , GBP (NE)	0.590	0.469	-0.136	0.699	0.604	-0.060
JPY , GBP (NW)	0.565	0.466	-0.248	0.627	0.603	-0.100
JPY , GBP (SW)	0.567	0.417	-0.136	0.620	0.553	-0.220
JPY , GBP (SE)	0.577	0.413	-0.292	0.695	0.539	0.056

Table 4.2: Summary of the generalized variance-covariance matrices (empirical estimates) for pairs of exchange rates with the USD at 95% and 99% tolerance levels

	95% tolerance level			99% tolerance level		
Matrix name	vol1 (%)	vol2 (%)	corr	vol1 (%)	vol2 (%)	corr
AUD , CAD	0.603	0.271	-0.272	0.758	0.315	-0.232
AUD , CAD (NE)	0.655	0.260	-0.240	0.873	0.313	-0.320
AUD , CAD (NW)	0.551	0.258	-0.308	0.669	0.310	-0.120
AUD , CAD (SW)	0.546	0.270	-0.240	0.673	0.368	-0.404
AUD , CAD (SE)	0.658	0.279	-0.292	0.887	0.362	0.000
AUD , CHF	0.608	0.790	-0.140	0.758	0.889	-0.160
AUD , CHF (NE)	0.666	0.808	-0.144	0.885	0.906	-0.232
AUD , CHF (NW)	0.554	0.785	-0.240	0.665	0.909	-0.100
AUD , CHF (SW)	0.551	0.784	-0.160	0.652	0.890	-0.208
AUD , CHF (SE)	0.665	0.785	-0.084	0.863	0.882	-0.092
AUD , DEM	0.611	0.711	-0.132	0.750	0.863	-0.144
AUD , DEM (NE)	0.668	0.722	-0.128	0.876	0.887	-0.184
AUD , DEM (NW)	0.565	0.708	-0.136	0.665	0.861	-0.084
AUD , DEM (SW)	0.545	0.707	-0.120	0.665	0.906	-0.300
AUD , DEM (SE)	0.649	0.709	-0.176	0.864	0.867	-0.108
AUD , FRF	0.612	0.685	-0.148	0.747	0.840	-0.168
AUD , FRF (NE)	0.669	0.690	-0.136	0.871	0.854	-0.224
AUD , FRF (NW)	0.566	0.688	-0.140	0.666	0.836	-0.084
AUD , FRF (SW)	0.541	0.678	-0.120	0.653	0.862	-0.268
AUD , FRF (SE)	0.648	0.687	-0.172	0.877	0.868	-0.052
AUD , GBP	0.609	0.722	0.200	0.765	0.859	0.236
AUD , GBP (NE)	0.656	0.761	0.216	0.864	0.927	0.108
AUD , GBP (NW)	0.551	0.756	0.228	0.675	0.895	0.324
AUD , GBP (SW)	0.561	0.681	0.204	0.657	0.859	0.188
AUD , GBP (SE)	0.661	0.690	0.160	0.888	0.839	0.280
AUD , ITL	0.607	0.675	-0.144	0.756	0.845	-0.184
AUD , ITL (NE)	0.660	0.662	-0.100	0.886	0.849	-0.264
AUD , ITL (NW)	0.558	0.666	-0.172	0.670	0.850	-0.080
AUD , ITL (SW)	0.550	0.679	-0.160	0.655	0.853	-0.240
AUD , ITL (SE)	0.651	0.683	-0.160	0.863	0.864	-0.112
AUD , JPY	0.611	0.616	-0.116	0.768	0.774	-0.108
AUD , JPY (NE)	0.656	0.605	0.028	0.864	0.806	-0.028
AUD , JPY (NW)	0.548	0.620	-0.216	0.664	0.811	-0.104
AUD , JPY (SW)	0.552	0.601	-0.160	0.674	0.738	-0.260
AUD , JPY (SE)	0.671	0.602	-0.084	0.871	0.741	-0.024

Table 4.2: Summary of the generalized variance-covariance matrices (empirical estimates) for pairs of exchange rates with the USD at 95% and 99% tolerance levels

	95% tolerance level			99% tolerance level		
Matrix name	vol1 (%)	vol2 (%)	corr	vol1 (%)	vol2 (%)	corr
CAD , CHF	0.267	0.793	0.212	0.326	0.888	0.164
CAD , CHF (NE)	0.261	0.803	0.180	0.310	0.902	0.040
CAD , CHF (NW)	0.275	0.803	0.200	0.365	0.902	0.240
CAD , CHF (SW)	0.272	0.788	0.232	0.348	0.887	0.160
CAD , CHF (SE)	0.260	0.780	0.200	0.322	0.872	0.200
CAD , DEM	0.269	0.719	0.200	0.320	0.870	0.152
CAD , DEM (NE)	0.259	0.715	0.188	0.307	0.879	-0.004
CAD , DEM (NW)	0.274	0.718	0.184	0.370	0.899	0.280
CAD , DEM (SW)	0.269	0.704	0.360	0.353	0.895	0.080
CAD , DEM (SE)	0.253	0.710	0.140	0.327	0.867	0.240
CAD , FRF	0.272	0.689	0.220	0.320	0.846	0.156
CAD , FRF (NE)	0.261	0.696	0.200	0.309	0.856	-0.016
CAD , FRF (NW)	0.276	0.686	0.200	0.366	0.851	0.272
CAD , FRF (SW)	0.272	0.678	0.328	0.361	0.884	-0.020
CAD , FRF (SE)	0.254	0.685	0.156	0.323	0.848	0.240
CAD , GBP	0.266	0.720	-0.204	0.326	0.861	-0.208
CAD , GBP (NE)	0.263	0.754	-0.252	0.316	0.883	-0.176
CAD , GBP (NW)	0.270	0.757	-0.224	0.357	0.903	-0.200
CAD , GBP (SW)	0.268	0.675	-0.108	0.364	0.857	-0.360
CAD , GBP (SE)	0.262	0.680	-0.200	0.307	0.856	-0.024
CAD , ITL	0.270	0.680	0.200	0.323	0.837	0.192
CAD , ITL (NE)	0.253	0.664	0.276	0.307	0.854	0.040
CAD , ITL (NW)	0.269	0.661	0.116	0.371	0.854	0.328
CAD , ITL (SW)	0.274	0.680	0.272	0.356	0.867	0.096
CAD , ITL (SE)	0.254	0.684	0.164	0.323	0.846	0.240
CAD , JPY	0.275	0.616	0.072	0.322	0.769	0.060
CAD , JPY (NE)	0.253	0.617	0.220	0.311	0.832	-0.060
CAD , JPY (NW)	0.270	0.614	-0.088	0.365	0.800	0.036
CAD , JPY (SW)	0.277	0.594	0.124	0.352	0.751	-0.080
CAD , JPY (SE)	0.258	0.603	0.056	0.324	0.729	0.212
CHF , DEM	0.792	0.713	0.940	0.895	0.868	0.948
CHF , DEM (NE)	0.810	0.713	0.920	0.896	0.888	0.980
CHF , DEM (NW)	0.787	0.717	0.944	0.887	0.867	0.952
CHF , DEM (SW)	0.789	0.703	0.912	0.890	0.867	0.904
CHF , DEM (SE)	0.793	0.714	0.936	0.892	0.850	0.932

Table 4.2: Summary of the generalized variance-covariance matrices (empirical estimates) for pairs of exchange rates with the USD at 95% and 99% tolerance levels

	95% tolerance level			99% tolerance level		
Matrix name	vol1 (%)	vol2 (%)	corr	vol1 (%)	vol2 (%)	corr
CHF , FRF	0.795	0.684	0.928	0.896	0.844	0.932
CHF , FRF (NE)	0.808	0.696	0.872	0.906	0.861	0.880
CHF , FRF (NW)	0.795	0.689	0.936	0.894	0.840	0.940
CHF , FRF (SW)	0.780	0.684	0.944	0.891	0.838	0.928
CHF , FRF (SE)	0.795	0.685	0.924	0.899	0.846	0.920
CHF , GBP	0.789	0.717	-0.784	0.890	0.882	-0.784
CHF , GBP (NE)	0.801	0.751	-0.792	0.889	0.889	-0.748
CHF , GBP (NW)	0.788	0.762	-0.648	0.896	0.906	-0.744
CHF , GBP (SW)	0.781	0.689	-0.792	0.881	0.845	-0.792
CHF , GBP (SE)	0.798	0.680	-0.824	0.888	0.861	-0.844
CHF , ITL	0.790	0.671	0.880	0.905	0.851	0.880
CHF , ITL (NE)	0.804	0.659	0.900	0.907	0.851	0.932
CHF , ITL (NW)	0.797	0.678	0.892	0.878	0.830	0.876
CHF , ITL (SW)	0.787	0.681	0.848	0.887	0.852	0.928
CHF , ITL (SE)	0.797	0.678	0.876	0.895	0.843	0.852
CHF , JPY	0.791	0.615	0.644	0.881	0.758	0.636
CHF , JPY (NE)	0.803	0.628	0.584	0.892	0.809	0.580
CHF , JPY (NW)	0.774	0.618	0.596	0.907	0.802	0.632
CHF , JPY (SW)	0.794	0.594	0.736	0.887	0.715	0.616
CHF , JPY (SE)	0.790	0.605	0.652	0.885	0.725	0.680
DEM , FRF	0.717	0.689	0.984	0.876	0.854	0.984
DEM , FRF (NE)	0.719	0.694	0.948	0.882	0.858	1.000
DEM , FRF (NW)	0.709	0.689	0.984	0.874	0.846	0.984
DEM , FRF (SW)	0.708	0.681	1.000	0.866	0.863	0.960
DEM , FRF (SE)	0.720	0.685	0.984	0.876	0.854	0.984
DEM , GBP	0.713	0.713	-0.804	0.867	0.875	-0.812
DEM , GBP (NE)	0.724	0.747	-0.808	0.882	0.899	-0.796
DEM , GBP (NW)	0.716	0.761	-0.716	0.873	0.892	-0.840
DEM , GBP (SW)	0.713	0.690	-0.816	0.869	0.844	-0.836
DEM , GBP (SE)	0.715	0.684	-0.824	0.861	0.866	-0.760
DEM , ITL	0.717	0.669	0.928	0.882	0.853	0.928
DEM , ITL (NE)	0.721	0.656	0.952	0.888	0.857	0.952
DEM , ITL (NW)	0.717	0.669	0.932	0.861	0.827	0.920
DEM , ITL (SW)	0.716	0.683	0.856	0.863	0.852	0.972
DEM , ITL (SE)	0.725	0.681	0.932	0.871	0.848	0.916

Table 4.2: Summary of the generalized variance-covariance matrices (empirical estimates) for pairs of exchange rates with the USD at 95% and 99% tolerance levels

	95% tolerance level			99% tolerance level		
Matrix name	vol1 (%)	vol2 (%)	corr	vol1 (%)	vol2 (%)	corr
DEM , JPY	0.716	0.620	0.652	0.863	0.758	0.636
DEM , JPY (NE)	0.716	0.614	0.700	0.882	0.805	0.540
DEM , JPY (NW)	0.697	0.619	0.592	0.887	0.808	0.624
DEM , JPY (SW)	0.716	0.595	0.780	0.863	0.731	0.568
DEM , JPY (SE)	0.710	0.608	0.648	0.854	0.731	0.700
FRF , GBP	0.685	0.719	-0.804	0.853	0.876	-0.816
FRF , GBP (NE)	0.692	0.746	-0.804	0.845	0.892	-0.780
FRF , GBP (NW)	0.684	0.764	-0.724	0.872	0.885	-0.848
FRF , GBP (SW)	0.680	0.688	-0.804	0.848	0.849	-0.840
FRF , GBP (SE)	0.680	0.681	-0.872	0.843	0.865	-0.752
FRF , ITL	0.692	0.670	0.936	0.861	0.856	0.928
FRF , ITL (NE)	0.694	0.660	0.940	0.863	0.844	1.000
FRF , ITL (NW)	0.685	0.666	0.936	0.846	0.837	0.916
FRF , ITL (SW)	0.679	0.678	0.976	0.851	0.854	0.996
FRF , ITL (SE)	0.693	0.677	0.936	0.838	0.850	0.912
FRF , JPY	0.691	0.620	0.636	0.833	0.752	0.624
FRF , JPY (NE)	0.688	0.621	0.620	0.828	0.803	0.600
FRF , JPY (NW)	0.672	0.620	0.572	0.877	0.810	0.628
FRF , JPY (SW)	0.690	0.588	0.820	0.847	0.729	0.524
FRF , JPY (SE)	0.678	0.607	0.636	0.833	0.732	0.696
GBP , ITL	0.719	0.676	-0.764	0.877	0.843	-0.780
GBP , ITL (NE)	0.744	0.689	-0.772	0.894	0.828	-0.752
GBP , ITL (NW)	0.677	0.655	-0.892	0.866	0.838	-0.720
GBP , ITL (SW)	0.690	0.682	-0.768	0.838	0.827	-0.772
GBP , ITL (SE)	0.752	0.677	-0.760	0.895	0.848	-0.868
GBP , JPY	0.724	0.620	-0.544	0.858	0.757	-0.520
GBP , JPY (NE)	0.731	0.624	-0.492	0.909	0.784	-0.496
GBP , JPY (NW)	0.677	0.622	-0.620	0.836	0.814	-0.480
GBP , JPY (SW)	0.685	0.601	-0.532	0.841	0.721	-0.588
GBP , JPY (SE)	0.765	0.593	-0.584	0.893	0.746	-0.368
ITL , JPY	0.675	0.622	0.604	0.831	0.761	0.608
ITL , JPY (NE)	0.663	0.623	0.644	0.842	0.809	0.516
ITL , JPY (NW)	0.673	0.620	0.564	0.842	0.806	0.560
ITL , JPY (SW)	0.679	0.599	0.700	0.855	0.718	0.572
ITL , JPY (SE)	0.656	0.606	0.592	0.814	0.740	0.676

Table 4.3: Summary of the generalized variance-covariance matrices (empirical estimates) for pairs of equity indexes at 95% and 99% tolerance levels

	95% tolerance level			99% tolerance level		
Matrix name	vol1 (%)	vol2 (%)	corr	vol1 (%)	vol2 (%)	corr
SP500 , NIKKEI	1.001	0.896	0.136	1.202	1.341	0.112
SP500 , NIKKEI (NE)	1.013	0.952	0.180	1.286	1.412	0.180
SP500 , NIKKEI (NW)	0.985	0.928	0.140	1.090	1.386	0.180
SP500 , NIKKEI (SW)	0.982	0.840	0.080	1.112	1.317	-0.020
SP500 , NIKKEI (SE)	1.013	0.861	0.148	1.318	1.209	-0.044
SP500 , DAX	1.008	1.221	0.148	1.222	1.674	0.156
SP500 , DAX (NE)	1.010	1.290	0.160	1.406	1.656	0.340
SP500 , DAX (NW)	0.947	1.278	0.100	1.117	1.778	0.120
SP500 , DAX (SW)	0.977	1.133	0.220	1.065	1.617	0.028
SP500 , DAX (SE)	1.018	1.158	0.116	1.331	1.683	0.260
SP500 , CAC-40	0.974	1.142	0.048	1.242	1.385	0.104
SP500 , CAC-40 (NE)	1.013	1.154	0.080	1.325	1.544	0.340
SP500 , CAC-40 (NW)	0.975	1.193	0.084	1.087	1.517	0.024
SP500 , CAC-40 (SW)	0.968	1.129	-0.112	1.103	1.192	-0.032
SP500 , CAC-40 (SE)	1.031	1.139	0.220	1.294	1.201	0.020
NIKKEI , DAX	0.913	1.225	0.248	1.282	1.703	0.272
NIKKEI , DAX (NE)	0.967	1.302	0.320	1.317	1.833	0.440
NIKKEI , DAX (NW)	0.862	1.247	0.200	1.320	1.816	0.420
NIKKEI , DAX (SW)	0.862	1.149	0.164	1.275	1.670	-0.072
NIKKEI , DAX (SE)	0.895	1.168	0.164	1.418	1.668	0.340
NIKKEI , CAC-40	0.908	1.130	0.216	1.291	1.368	0.336
NIKKEI , CAC-40 (NE)	0.978	1.168	0.260	1.380	1.537	0.420
NIKKEI , CAC-40 (NW)	0.865	1.153	0.208	1.299	1.592	0.440
NIKKEI , CAC-40 (SW)	0.882	1.117	0.028	1.234	1.208	0.140
NIKKEI , CAC-40 (SE)	0.938	1.123	0.248	1.373	1.266	0.404
DAX , CAC-40	1.226	1.132	0.316	1.721	1.361	0.392
DAX , CAC-40 (NE)	1.307	1.161	0.328	1.790	1.536	0.616
DAX , CAC-40 (NW)	1.167	1.182	0.352	1.722	1.645	0.500
DAX , CAC-40 (SW)	1.164	1.107	0.220	1.661	1.248	0.000
DAX , CAC-40 (SE)	1.293	1.128	0.348	1.807	1.236	0.460

4.3 Stress Variance-Covariance Matrices Results

This section presents the results of the 2×2 empirical stress variance-covariance matrices estimates for pairs of foreign exchange rates with the USD and DEM respectively and for pairs of equity indexes under 95% stressful condition. Table 4.4 presents the results for pairs of foreign exchange rates chosen from the six curreicies with the DEM. Table 4.5 presents the results for pairs of foreign exchange rates chosen from the eight curreicies with the USD. Table 4.6 presents the results for pairs of equity indexes chosen from the four equity indexes. The estimates from the MLE Gaussian model are also included for comparison. We see that across nearly all different assets, the MLE estimate of the individual asset's volatility is smaller than that implied by any empirical stress variance-covariance matrix estimate that involves the asset.

Table 4.4: Summary of the 95% stress variance-covariance matrices (empirical estimates) for pairs of foreign exchange rates with the DEM

Matrix name	vol1 (%)	vol2 (%)	corr
USD , CHF (NE)	0.791	0.293	0.028
USD , CHF (NW)	0.827	0.299	0.052
USD , CHF (SW)	0.815	0.277	-0.036
USD , CHF (SE)	0.791	0.280	0.072
USD , CHF MLE	0.734	0.272	0.001
USD , ESP (NE)	0.802	0.323	-0.200
USD , ESP (NW)	0.805	0.329	-0.160
USD , ESP (SW)	0.814	0.414	-0.128
USD , ESP (SE)	0.802	0.419	-0.140
USD , ESP MLE	0.737	0.347	-0.171
USD , FRF (NE)	0.795	0.118	-0.140
USD , FRF (NW)	0.814	0.126	-0.220
USD , FRF (SW)	0.813	0.147	-0.216
USD , FRF (SE)	0.800	0.142	-0.160
USD , FRF MLE	0.737	0.128	-0.202
USD , ITL (NE)	0.796	0.317	-0.204
USD , ITL (NW)	0.806	0.325	-0.080
USD , ITL (SW)	0.809	0.418	-0.140
USD , ITL (SE)	0.801	0.407	-0.120
USD , ITL MLE	0.737	0.331	-0.141
USD , JPY (NE)	0.783	0.660	-0.284
USD , JPY (NW)	0.811	0.670	-0.248
USD , JPY (SW)	0.813	0.604	-0.344
USD , JPY (SE)	0.787	0.618	-0.360
USD , JPY MLE	0.734	0.600	-0.327
USD , GBP (NE)	0.798	0.580	0.040
USD , GBP (NW)	0.819	0.588	0.260
USD , GBP (SW)	0.811	0.499	0.088
USD , GBP (SE)	0.797	0.498	0.264
USD , GBP MLE	0.734	0.474	0.208
CHF , ESP (NE)	0.290	0.323	0.064
CHF , ESP (NW)	0.278	0.325	0.100
CHF , ESP (SW)	0.283	0.413	-0.088
CHF , ESP (SE)	0.291	0.416	-0.136
CHF , ESP MLE	0.269	0.341	-0.008

Table 4.4: Summary of the 95% stress variance-covariance matrices (empirical estimates) for pairs of foreign exchange rates with the DEM

Matrix name	vol1 (%)	vol2 (%)	corr
CHF , FRF (NE)	0.295	0.125	0.040
CHF , FRF (NW)	0.275	0.125	0.060
CHF , FRF (SW)	0.280	0.143	0.000
CHF , FRF (SE)	0.293	0.146	-0.012
CHF , FRF MLE	0.269	0.126	0.040
CHF , ITL (NE)	0.293	0.318	0.048
CHF , ITL (NW)	0.275	0.316	0.036
CHF , ITL (SW)	0.282	0.414	-0.080
CHF , ITL (SE)	0.297	0.407	-0.012
CHF , ITL MLE	0.269	0.326	0.005
CHF , JPY (NE)	0.299	0.674	-0.036
CHF , JPY (NW)	0.284	0.657	0.116
CHF , JPY (SW)	0.278	0.603	0.152
CHF , JPY (SE)	0.297	0.611	0.052
CHF , JPY MLE	0.268	0.595	0.103
CHF , GBP (NE)	0.297	0.582	-0.168
CHF , GBP (NW)	0.279	0.577	-0.028
CHF , GBP (SW)	0.276	0.499	-0.112
CHF , GBP (SE)	0.293	0.496	-0.024
CHF , GBP MLE	0.268	0.473	-0.081
ESP , FRF (NE)	0.320	0.129	0.344
ESP , FRF (NW)	0.411	0.129	0.400
ESP , FRF (SW)	0.409	0.139	0.500
ESP , FRF (SE)	0.317	0.141	0.360
ESP , FRF MLE	0.337	0.125	0.384
ESP , ITL (NE)	0.320	0.317	0.364
ESP , ITL (NW)	0.400	0.319	0.280
ESP , ITL (SW)	0.409	0.409	0.420
ESP , ITL (SE)	0.324	0.406	0.380
ESP , ITL MLE	0.337	0.325	0.358
ESP , JPY (NE)	0.330	0.671	0.000
ESP , JPY (NW)	0.418	0.669	0.076
ESP , JPY (SW)	0.413	0.620	0.064
ESP , JPY (SE)	0.322	0.614	0.220
ESP , JPY MLE	0.341	0.600	0.114

Table 4.4: Summary of the 95% stress variance-covariance matrices (empirical estimates) for pairs of foreign exchange rates with the DEM

Matrix name	vol1 (%)	vol2 (%)	corr
ESP , GBP (NE)	0.329	0.580	-0.264
ESP , GBP (NW)	0.415	0.582	-0.212
ESP , GBP (SW)	0.414	0.497	-0.236
ESP , GBP (SE)	0.315	0.500	-0.232
ESP , GBP MLE	0.341	0.476	-0.264
FRF , ITL (NE)	0.123	0.313	0.516
FRF , ITL (NW)	0.138	0.315	0.380
FRF , ITL (SW)	0.142	0.410	0.520
FRF , ITL (SE)	0.133	0.409	0.360
FRF , ITL MLE	0.125	0.325	0.352
FRF , JPY (NE)	0.127	0.670	0.076
FRF , JPY (NW)	0.143	0.672	0.160
FRF , JPY (SW)	0.141	0.618	0.160
FRF , JPY (SE)	0.124	0.619	0.220
FRF , JPY MLE	0.126	0.600	0.151
FRF , GBP (NE)	0.125	0.580	-0.200
FRF , GBP (NW)	0.142	0.585	-0.120
FRF , GBP (SW)	0.140	0.497	-0.148
FRF , GBP (SE)	0.128	0.499	-0.100
FRF , GBP MLE	0.126	0.475	-0.194
ITL , JPY (NE)	0.324	0.668	0.140
ITL , JPY (NW)	0.412	0.680	0.200
ITL , JPY (SW)	0.410	0.615	0.140
ITL , JPY (SE)	0.317	0.615	0.220
ITL , JPY MLE	0.326	0.600	0.158
ITL , GBP (NE)	0.321	0.580	-0.184
ITL , GBP (NW)	0.411	0.592	-0.008
ITL , GBP (SW)	0.404	0.506	-0.140
ITL , GBP (SE)	0.313	0.498	-0.088
ITL , GBP MLE	0.326	0.475	-0.166
JPY , GBP (NE)	0.668	0.576	-0.152
JPY , GBP (NW)	0.613	0.577	-0.056
JPY , GBP (SW)	0.608	0.504	-0.180
JPY , GBP (SE)	0.670	0.495	-0.020
JPY , GBP MLE	0.595	0.473	-0.165

Table 4.5: Summary of the 95% stress variance-covariance matrices (empirical estimates) for pairs of foreign exchange rates with the USD

Matrix name	vol1 (%)	vol2 (%)	corr
AUD , CAD (NE)	0.795	0.299	-0.312
AUD , CAD (NW)	0.623	0.289	-0.260
AUD , CAD (SW)	0.635	0.315	-0.292
AUD , CAD (SE)	0.800	0.317	-0.152
AUD , CAD MLE	0.638	0.280	-0.228
AUD , CHF (NE)	0.809	0.857	-0.180
AUD , CHF (NW)	0.631	0.873	-0.100
AUD , CHF (SW)	0.636	0.852	-0.224
AUD , CHF (SE)	0.797	0.870	-0.060
AUD , CHF MLE	0.639	0.793	-0.150
AUD , DEM (NE)	0.801	0.788	-0.136
AUD , DEM (NW)	0.622	0.800	-0.144
AUD , DEM (SW)	0.633	0.814	-0.240
AUD , DEM (SE)	0.797	0.833	-0.040
AUD , DEM MLE	0.638	0.734	-0.150
AUD , FRF (NE)	0.805	0.758	-0.156
AUD , FRF (NW)	0.622	0.764	-0.156
AUD , FRF (SW)	0.638	0.817	-0.292
AUD , FRF (SE)	0.797	0.813	-0.048
AUD , FRF MLE	0.638	0.706	-0.160
AUD , GBP (NE)	0.795	0.816	0.188
AUD , GBP (NW)	0.631	0.837	0.280
AUD , GBP (SW)	0.618	0.802	0.184
AUD , GBP (SE)	0.810	0.797	0.240
AUD , GBP MLE	0.638	0.741	0.213
AUD , ITL (NE)	0.807	0.761	-0.200
AUD , ITL (NW)	0.619	0.751	-0.196
AUD , ITL (SW)	0.632	0.809	-0.216
AUD , ITL (SE)	0.799	0.814	-0.060
AUD , ITL MLE	0.638	0.726	-0.139
AUD , JPY (NE)	0.801	0.743	-0.104
AUD , JPY (NW)	0.621	0.725	-0.140
AUD , JPY (SW)	0.636	0.682	-0.220
AUD , JPY (SE)	0.797	0.681	-0.072
AUD , JPY MLE	0.638	0.643	-0.120

Table 4.5: Summary of the 95% stress variance-covariance matrices (empirical estimates) for pairs of foreign exchange rates with the USD

Matrix name	vol1 (%)	vol2 (%)	corr
CAD , CHF (NE)	0.286	0.872	0.096
CAD , CHF (NW)	0.330	0.868	0.248
CAD , CHF (SW)	0.320	0.864	0.088
CAD , CHF (SE)	0.305	0.860	0.252
CAD , CHF MLE	0.281	0.793	0.170
CAD , DEM (NE)	0.285	0.792	0.136
CAD , DEM (NW)	0.322	0.794	0.196
CAD , DEM (SW)	0.315	0.816	0.160
CAD , DEM (SE)	0.302	0.812	0.236
CAD , DEM MLE	0.280	0.734	0.173
CAD , FRF (NE)	0.282	0.761	0.180
CAD , FRF (NW)	0.322	0.764	0.200
CAD , FRF (SW)	0.316	0.809	0.116
CAD , FRF (SE)	0.302	0.805	0.272
CAD , FRF MLE	0.280	0.706	0.180
CAD , GBP (NE)	0.295	0.829	-0.220
CAD , GBP (NW)	0.311	0.832	-0.240
CAD , GBP (SW)	0.321	0.793	-0.248
CAD , GBP (SE)	0.288	0.794	-0.108
CAD , GBP MLE	0.280	0.741	-0.211
CAD , ITL (NE)	0.283	0.754	0.200
CAD , ITL (NW)	0.327	0.752	0.240
CAD , ITL (SW)	0.310	0.803	0.192
CAD , ITL (SE)	0.300	0.802	0.228
CAD , ITL MLE	0.280	0.726	0.163
CAD , JPY (NE)	0.292	0.738	-0.020
CAD , JPY (NW)	0.323	0.741	0.032
CAD , JPY (SW)	0.316	0.691	-0.028
CAD , JPY (SE)	0.292	0.688	0.140
CAD , JPY MLE	0.280	0.643	0.057
CHF , DEM (NE)	0.875	0.796	0.908
CHF , DEM (NW)	0.856	0.791	0.948
CHF , DEM (SW)	0.864	0.810	0.896
CHF , DEM (SE)	0.866	0.814	0.936
CHF , DEM MLE	0.793	0.733	0.938

Table 4.5: Summary of the 95% stress variance-covariance matrices (empirical estimates) for pairs of foreign exchange rates with the USD

Matrix name	vol1 (%)	vol2 (%)	corr
CHF , FRF (NE)	0.874	0.762	0.904
CHF , FRF (NW)	0.853	0.762	0.940
CHF , FRF (SW)	0.867	0.798	0.844
CHF , FRF (SE)	0.873	0.796	0.920
CHF , FRF MLE	0.793	0.704	0.922
CHF , GBP (NE)	0.866	0.842	-0.768
CHF , GBP (NW)	0.862	0.832	-0.736
CHF , GBP (SW)	0.851	0.792	-0.796
CHF , GBP (SE)	0.861	0.784	-0.820
CHF , GBP MLE	0.793	0.740	-0.771
CHF , ITL (NE)	0.867	0.752	0.924
CHF , ITL (NW)	0.853	0.750	0.876
CHF , ITL (SW)	0.866	0.792	0.796
CHF , ITL (SE)	0.864	0.802	0.840
CHF , ITL MLE	0.793	0.725	0.835
CHF , JPY (NE)	0.864	0.735	0.560
CHF , JPY (NW)	0.855	0.750	0.620
CHF , JPY (SW)	0.866	0.696	0.528
CHF , JPY (SE)	0.858	0.682	0.668
CHF , JPY MLE	0.792	0.642	0.643
DEM , FRF (NE)	0.789	0.757	0.996
DEM , FRF (NW)	0.804	0.767	0.984
DEM , FRF (SW)	0.809	0.804	0.964
DEM , FRF (SE)	0.800	0.793	0.980
DEM , FRF MLE	0.734	0.706	0.979
DEM , GBP (NE)	0.783	0.827	-0.760
DEM , GBP (NW)	0.822	0.839	-0.764
DEM , GBP (SW)	0.796	0.795	-0.828
DEM , GBP (SE)	0.799	0.786	-0.764
DEM , GBP MLE	0.734	0.741	-0.799
DEM , ITL (NE)	0.787	0.750	0.960
DEM , ITL (NW)	0.804	0.758	0.924
DEM , ITL (SW)	0.813	0.809	0.840
DEM , ITL (SE)	0.794	0.800	0.892
DEM , ITL MLE	0.734	0.726	0.893

Table 4.5: Summary of the 95% stress variance-covariance matrices (empirical estimates) for pairs of foreign exchange rates with the USD

Matrix name	vol1 (%)	vol2 (%)	corr
DEM , JPY (NE)	0.783	0.731	0.620
DEM , JPY (NW)	0.813	0.755	0.628
DEM , JPY (SW)	0.817	0.693	0.620
DEM , JPY (SE)	0.784	0.682	0.668
DEM , JPY MLE	0.732	0.643	0.645
FRF , GBP (NE)	0.759	0.828	-0.760
FRF , GBP (NW)	0.812	0.837	-0.760
FRF , GBP (SW)	0.788	0.802	-0.832
FRF , GBP (SE)	0.761	0.786	-0.800
FRF , GBP MLE	0.706	0.741	-0.798
FRF , ITL (NE)	0.756	0.750	1.000
FRF , ITL (NW)	0.790	0.763	0.928
FRF , ITL (SW)	0.810	0.805	0.820
FRF , ITL (SE)	0.765	0.801	0.888
FRF , ITL MLE	0.706	0.726	0.895
FRF , JPY (NE)	0.756	0.727	0.628
FRF , JPY (NW)	0.799	0.754	0.616
FRF , JPY (SW)	0.807	0.698	0.536
FRF , JPY (SE)	0.760	0.682	0.656
FRF , JPY MLE	0.704	0.643	0.635
GBP , ITL (NE)	0.828	0.761	-0.732
GBP , ITL (NW)	0.786	0.750	-0.764
GBP , ITL (SW)	0.795	0.794	-0.756
GBP , ITL (SE)	0.841	0.794	-0.744
GBP , ITL MLE	0.741	0.726	-0.745
GBP , JPY (NE)	0.833	0.744	-0.516
GBP , JPY (NW)	0.787	0.736	-0.504
GBP , JPY (SW)	0.789	0.679	-0.592
GBP , JPY (SE)	0.835	0.688	-0.460
GBP , JPY MLE	0.739	0.643	-0.544
ITL , JPY (NE)	0.753	0.725	0.620
ITL , JPY (NW)	0.796	0.751	0.556
ITL , JPY (SW)	0.811	0.686	0.616
ITL , JPY (SE)	0.750	0.687	0.640
ITL , JPY MLE	0.724	0.643	0.590

Table 4.6: Summary of the 95% stress variance-covariance matrices (empirical estimates) for pairs of equity indexes

Matrix name	vol1 (%)	vol2 (%)	corr
SP500 , NIKKEI (NE)	1.390	1.331	0.088
SP500 , NIKKEI (NW)	1.086	1.323	0.164
SP500 , NIKKEI (SW)	1.067	1.139	0.120
SP500 , NIKKEI (SE)	1.396	1.115	0.120
SP500 , NIKKEI MLE	1.238	1.109	0.124
SP500 , DAX (NE)	1.425	1.605	0.180
SP500 , DAX (NW)	1.105	1.645	0.140
SP500 , DAX (SW)	1.044	1.403	0.168
SP500 , DAX (SE)	1.388	1.415	0.260
SP500 , DAX MLE	1.238	1.415	0.201
SP500 , CAC-40 (NE)	1.410	1.393	0.220
SP500 , CAC-40 (NW)	1.104	1.405	0.028
SP500 , CAC-40 (SW)	1.069	1.135	0.004
SP500 , CAC-40 (SE)	1.361	1.113	0.100
SP500 , CAC-40 MLE	1.238	1.175	0.133
NIKKEI , DAX (NE)	1.326	1.658	0.300
NIKKEI , DAX (NW)	1.177	1.648	0.396
NIKKEI , DAX (SW)	1.142	1.407	0.164
NIKKEI , DAX (SE)	1.276	1.419	0.280
NIKKEI , DAX MLE	1.109	1.415	0.303
NIKKEI , CAC-40 (NE)	1.318	1.420	0.340
NIKKEI , CAC-40 (NW)	1.196	1.434	0.424
NIKKEI , CAC-40 (SW)	1.126	1.143	0.180
NIKKEI , CAC-40 (SE)	1.272	1.115	0.300
NIKKEI , CAC-40 MLE	1.109	1.175	0.316
DAX , CAC-40 (NE)	1.654	1.421	0.400
DAX , CAC-40 (NW)	1.482	1.428	0.480
DAX , CAC-40 (SW)	1.417	1.148	0.200
DAX , CAC-40 (SE)	1.610	1.136	0.420
DAX , CAC-40 MLE	1.415	1.175	0.432

Chapter 5

Estimation of Return at Risk and Stress Expected Return

5.1 Introduction

This chapter includes the two different methods to estimate the two respective portfolio risk measures under normal and stressful market conditions. Estimation of the return at risk measure under normal market conditions is discussed in the last section of this chapter. Estimation of the stress expected return under stressful market conditions is discussed in Sections 5.2 and 5.3. As defined in Chapter 3, the stress expected return of a portfolio is the conditional expectation of the portfolio return given that it is smaller than a threshold. As we assume that the portfolio return distribution is Gaussian, the conditional expectation of a Gaussian variable given that it is smaller than a constant is formulated in Section 5.3. The Gaussian parameters used in the conditional expectation formula are estimated using best linear unbiased estimation (BLUE) for Gaussian parameters based on a Type-II censored sample. Readers can refer to Appendix A for a defintion of Type-II censoring.

Section 5.2 reviews the BLUE for the location and scale parameter family of distributions based on a Type-II censored sample, which is quoted from Balakrishnan *et al* (pages 80-83) . The idea was first used by Wilk and Shapiro (1965) for the Gaussian distribution based on complete samples. In their paper, they could only

claim to calculate the expectations and covariances of the order statistics of standard Gaussian samples up to size n=30. The calculation of means and product moments of Gaussian order statistics for sample sizes up to 20 were prepared by Teichroew (1956) . Sarhan and Greenberg (1956) have tabulated the variances and covariances to ten decimals for $n \leq 20$. These tables have been extended to $n \leq 50$ by Tietjen *et al* (1977) .

As I need to work with sample size as large as 2500, I really have to rely on other sources or methods like the David-Johnson approximation which is described in section A.5. An algorithm to estimate the variance-covariance matrix of the Gaussian order statistics of a Type-II censored sample is given in Section 5.2.1. This algorithm works with complete samples of any size as long as the size of the Type-II censored sample is not too large for the computer to handle. A DECstation 5000/25, for example, can easily handle a matrix multiplication with 100×100 matrices. Therefore, the algorithm when implemented on the DECstation 5000/25 can work well with a Type-II censored sample of size 100 from any complete sample of any size. The algorithm is based on the findings presented at the end of Appendix A.

Section 5.4 reviews how to estimate the population or empirical quantiles. This section provides the background information for estimating an empirical daily return at risk. This estimation step is included in the process of generating a generalized variance-covariance matrix.

5.2 BLUEs of the Location and Scale Parameters

Let μ and σ denote respectively the location and scale parameters of a distribution that belongs to the location and scale parameter family of distributions. An example in this family is a Gaussian distribution. Given a sample of size n, and known censoring limits r and s such that $r < s$, let $X_{r+1:n} \leq X_{r+2:n} \leq \ldots \leq X_{n-s:n}$ be a Type-II censored sample from a location-scale parameter distribution. Let us denote $Z_{i:n} = (X_{i:n} - \mu)/\sigma \;\; (r+1 \leq i \leq n-s)$ and, $E(Z_{i:n}) = \alpha_{i:n} \;\; (r+1 \leq i \leq n-s)$ and

$Cov(Z_{i:n}, Z_{j:n}) = \beta_{i,j:n}$ $(r+1 \leq i \leq j \leq n-s)$. We use the notations

$$\mathbf{X} = (X_{r+1:n}, X_{r+2:n}, \ldots, X_{n-s:n})', \tag{5.1}$$

$$\boldsymbol{\alpha} = (\alpha_{r+1:n}, \alpha_{r+2:n}, \ldots, \alpha_{n-s:n})', \tag{5.2}$$

and

$$\boldsymbol{\beta} = \begin{bmatrix} \beta_{r+1,r+1:n} & \beta_{r+1,r+2:n} & \cdots & \beta_{r+1,n-s:n} \\ \beta_{r+2,r+1:n} & \beta_{r+2,r+2:n} & \cdots & \beta_{r+2,n-s:n} \\ \vdots & \vdots & \ddots & \vdots \\ \beta_{n-s,r+1:n} & \beta_{n-s,r+2:n} & \cdots & \beta_{n-s,n-s:n} \end{bmatrix}. \tag{5.3}$$

In addition, let $\mathbf{1}$ denote a column vector of $(n-r-s)$ ones.

Following Lloyd (1952), let us consider the generalized variance given by

$$\begin{aligned} &(\mathbf{X} - \mu\mathbf{1} - \sigma\boldsymbol{\alpha})'\boldsymbol{\beta}^{-1}(\mathbf{X} - \mu\mathbf{1} - \sigma\boldsymbol{\alpha}) \\ &= \mathbf{X}'\boldsymbol{\beta}^{-1}\mathbf{X} - \mu\mathbf{1}'\boldsymbol{\beta}^{-1}\mathbf{X} - \sigma\boldsymbol{\alpha}'\boldsymbol{\beta}^{-1}\mathbf{X} - \mu\mathbf{X}'\boldsymbol{\beta}^{-1}\mathbf{1} + \mu^2\mathbf{1}'\boldsymbol{\beta}^{-1}\mathbf{1} \\ &\quad +\mu\sigma\boldsymbol{\alpha}'\boldsymbol{\beta}^{-1}\mathbf{1} - \sigma\mathbf{X}'\boldsymbol{\beta}^{-1}\boldsymbol{\alpha} + \mu\sigma\mathbf{1}'\boldsymbol{\beta}^{-1}\boldsymbol{\alpha} + \sigma^2\boldsymbol{\alpha}'\boldsymbol{\beta}^{-1}\boldsymbol{\alpha} \\ &= \mathbf{X}'\boldsymbol{\beta}^{-1}\mathbf{X} + \mu^2\mathbf{1}'\boldsymbol{\beta}^{-1}\mathbf{1} + \sigma^2\boldsymbol{\alpha}'\boldsymbol{\beta}^{-1}\boldsymbol{\alpha} - 2\mu\mathbf{1}'\boldsymbol{\beta}^{-1}\mathbf{X} \\ &\quad -2\sigma\boldsymbol{\alpha}'\boldsymbol{\beta}^{-1}\mathbf{X} + 2\mu\sigma\boldsymbol{\alpha}'\boldsymbol{\beta}^{-1}\mathbf{1}. \end{aligned} \tag{5.4}$$

By minimizing the expression of the generalized variance in Equation 5.4 with respect to μ and σ, we obtain the equations

$$\mu\mathbf{1}'\boldsymbol{\beta}^{-1}\mathbf{1} + \sigma\boldsymbol{\alpha}'\boldsymbol{\beta}^{-1}\mathbf{1} = \mathbf{1}'\boldsymbol{\beta}^{-1}\mathbf{X}, \tag{5.5}$$

and

$$\mu\boldsymbol{\alpha}'\boldsymbol{\beta}^{-1}\mathbf{1} + \sigma\boldsymbol{\alpha}'\boldsymbol{\beta}^{-1}\boldsymbol{\alpha} = \boldsymbol{\alpha}'\boldsymbol{\beta}^{-1}\mathbf{X}. \tag{5.6}$$

Upon solving Equations 5.5 and 5.6, we derive the BLUEs of μ and σ

$$\begin{aligned} \mu^* &= \left\{ \frac{\boldsymbol{\alpha}'\boldsymbol{\beta}^{-1}\boldsymbol{\alpha}\mathbf{1}'\boldsymbol{\beta}^{-1} - \boldsymbol{\alpha}'\boldsymbol{\beta}^{-1}\mathbf{1}\boldsymbol{\alpha}'\boldsymbol{\beta}^{-1}}{(\boldsymbol{\alpha}'\boldsymbol{\beta}^{-1}\boldsymbol{\alpha})(\mathbf{1}'\boldsymbol{\beta}^{-1}\mathbf{1}) - (\boldsymbol{\alpha}'\boldsymbol{\beta}^{-1}\mathbf{1})^2} \right\} \mathbf{X} \\ &= -\boldsymbol{\alpha}'\boldsymbol{\Delta}\mathbf{X}, \end{aligned} \tag{5.7}$$

and

$$\begin{aligned}\sigma^* &= \left\{\frac{\mathbf{1}'\boldsymbol{\beta}^{-1}\mathbf{1}\boldsymbol{\alpha}'\boldsymbol{\beta}^{-1} - \mathbf{1}'\boldsymbol{\beta}^{-1}\boldsymbol{\alpha}\mathbf{1}'\boldsymbol{\beta}^{-1}}{(\boldsymbol{\alpha}'\boldsymbol{\beta}^{-1}\boldsymbol{\alpha})(\mathbf{1}'\boldsymbol{\beta}^{-1}\mathbf{1}) - (\boldsymbol{\alpha}'\boldsymbol{\beta}^{-1}\mathbf{1})^2}\right\}\mathbf{X} \\ &= \mathbf{1}'\boldsymbol{\Delta}\mathbf{X}, \end{aligned} \tag{5.8}$$

where $\boldsymbol{\Delta}$ is a skew-symmetric matrix of order $n - r - s$ given by

$$\boldsymbol{\Delta} = \left\{\frac{\boldsymbol{\beta}^{-1}(\mathbf{1}\boldsymbol{\alpha}' - \boldsymbol{\alpha}\mathbf{1}')\boldsymbol{\beta}^{-1}}{(\boldsymbol{\alpha}'\boldsymbol{\beta}^{-1}\boldsymbol{\alpha})(\mathbf{1}'\boldsymbol{\beta}^{-1}\mathbf{1}) - (\boldsymbol{\alpha}'\boldsymbol{\beta}^{-1}\mathbf{1})^2}\right\}. \tag{5.9}$$

Furthermore, from Equations 5.7 and 5.8 we obtain the variances and covariances of the estimators to be

$$Var(\mu^*) = \sigma^2\left\{\frac{\boldsymbol{\alpha}'\boldsymbol{\beta}^{-1}\boldsymbol{\alpha}}{(\boldsymbol{\alpha}'\boldsymbol{\beta}^{-1}\boldsymbol{\alpha})(\mathbf{1}'\boldsymbol{\beta}^{-1}\mathbf{1}) - (\boldsymbol{\alpha}'\boldsymbol{\beta}^{-1}\mathbf{1})^2}\right\}, \tag{5.10}$$

$$Var(\sigma^*) = \sigma^2\left\{\frac{\mathbf{1}'\boldsymbol{\beta}^{-1}\mathbf{1}}{(\boldsymbol{\alpha}'\boldsymbol{\beta}^{-1}\boldsymbol{\alpha})(\mathbf{1}'\boldsymbol{\beta}^{-1}\mathbf{1}) - (\boldsymbol{\alpha}'\boldsymbol{\beta}^{-1}\mathbf{1})^2}\right\}, \tag{5.11}$$

and

$$Cov(\mu^*, \sigma^*) = -\sigma^2\left\{\frac{\boldsymbol{\alpha}'\boldsymbol{\beta}^{-1}\mathbf{1}}{(\boldsymbol{\alpha}'\boldsymbol{\beta}^{-1}\boldsymbol{\alpha})(\mathbf{1}'\boldsymbol{\beta}^{-1}\mathbf{1}) - (\boldsymbol{\alpha}'\boldsymbol{\beta}^{-1}\mathbf{1})^2}\right\}. \tag{5.12}$$

For the complete sample case ($r = s = 0$) in which the population distribution is symmetric, some simplification in the Equations 5.7 to 5.12 is possible. In fact, the BLUE μ^* in Equation 5.7 becomes the sample mean for the Gaussian distribution. For a proof of this result, interested readers may refer to Lloyd (1952) .

In this thesis, we apply this BLUE theory to estimate the mean and variance of a Gaussian distribution. $\boldsymbol{\alpha}$ and $\boldsymbol{\beta}$ for a Type-II censored sample of Gaussian order statistics are obtained with the algorithm given in the following section.

5.2.1 Approximation of α and β for a Type-II censored sample of Gaussian order statistics

As suggested at the end of the Section A.5, the procedure to approximate $\boldsymbol{\alpha}$ and $\boldsymbol{\beta}$ is as follows:

Algorithm 5.1 *1. Use Equations A.31 and A.32 to approximate $\alpha_{i:n}$ and $\beta_{i,i:n}$, $1 \leq i \leq n$. We will denote here the approximations $\tilde{\alpha_{i:n}}$ and $\tilde{\beta_{i,i:n}}$ respectively.*

2. $\boldsymbol{\alpha}$ is given by $(\tilde{\alpha_{r+1:n}}, \ldots, \tilde{\alpha_{n-s:n}})$

3. The elements $\beta_{i,j:n}$ of $\boldsymbol{\beta}$ $(r+1 \leq i < j \leq n-s)$ are given by:

$$\beta_{i,j:n} = \sqrt{\frac{i(n+1-j)}{j(n+1-i)}\tilde{\beta_{i,i:n}}\tilde{\beta_{j,j:n}}} \tag{5.13}$$

4. Use symmetry to obtain the other elements of the matrix.

5.3 Conditional Expectation and Variance of a Gaussian Variable

This section computes the conditional expectation and variance of a one-dimensional Gaussian variable $X \sim N(\mu, \sigma^2)$ given that $X < c$ where c is a real constant.

Let $d = (c-\mu)/\sigma$. The conditional first moment or expectation is given as

$$\begin{aligned} E((X/X<c)/\mu,\sigma^2) &= \frac{E(X1_{\{X<c\}}/\mu,\sigma^2)}{E(1_{\{X<c\}}/\mu,\sigma^2)} \\ &= \frac{1}{\Phi(d)\sqrt{2\pi\sigma^2}}\int_{-\infty}^{c} xe^{-\frac{(x-\mu)^2}{2\sigma^2}}\,dx \\ &= \frac{1}{\Phi(d)\sqrt{2\pi}}\int_{-\infty}^{d}(\sigma z+\mu)e^{-\frac{z^2}{2}}\,dz \\ &= \mu - \frac{\sigma\phi(d)}{\Phi(d)}. \end{aligned} \tag{5.14}$$

The conditional second moment is given by

$$\begin{aligned} E((X^2/X<c)/\mu,\sigma^2) &= \frac{E(X^2 1_{\{X<c\}}/\mu,\sigma^2)}{E(1_{\{X<c\}}/\mu,\sigma^2)} \\ &= \frac{1}{\Phi(d)\sqrt{2\pi\sigma^2}}\int_{-\infty}^{c} xe^{-\frac{(x-\mu)^2}{2\sigma^2}}\,dx \\ &= \frac{1}{\Phi(d)\sqrt{2\pi}}\int_{-\infty}^{d}(\sigma z+\mu)^2 e^{-\frac{z^2}{2}}\,dz \\ &= \mu^2 - \frac{2\mu\sigma\phi(d)}{\Phi(d)} + (\frac{\sigma\phi(d)}{\Phi(d)})^2. \end{aligned} \tag{5.15}$$

The conditional variance is given by

$$\begin{aligned} Var((X/X<c)/\mu,\sigma^2) &= E((X^2/X<c)/\mu,\sigma^2) - \{E((X/X<c)/\mu,\sigma^2)\}^2 \\ &= \sigma^2(1 - \frac{d\phi(d)}{\Phi(d)} - \frac{\phi(d)^2}{\Phi(d)^2}). \end{aligned} \tag{5.16}$$

5.4 Estimation of Population Quantiles

For a population with known distribution and distribution function $F(.)$, a quantile function, denoted $G(.)$, is defined for $0 \leq u \leq 1$ by

$$G(u) = F^{-1}(u) = \inf\{x : F(x) \geq u\} \tag{5.17}$$

Based on a random sample of size n from a population with distribution function $F(.)$, an estimate of $F(.)$ is given by the empirical distribution function $F_n(.)$ defined by

$$F_n(x) = \begin{cases} 0, & \text{for } x < X_{1:n}, \\ (i-1)/n & \text{for } X_{i-1:n} \leq x < X_{i:n}, \\ 1, & \text{for } x \geq X_{n:n}. \end{cases} \tag{5.18}$$

when the corresponding order statistics are $X_{1:n} \leq X_{2:n} \leq \cdots \leq X_{n:n}$.

It is well known that $F_n(x) \to F(x)$ in probability. So a natural estimate function $G(u)$ in Equation 5.17 is given by the sample quantile function $G_n(u)$ defined by

$$G_n(u) = F_n^{-1}(u) = \inf\{x : F_n(x) \geq u\}$$
$$= X_{i:n}, \quad \text{for } \tfrac{i-1}{n} < u \leq \tfrac{i}{n}. \tag{5.19}$$

The above sample quantile function has been studied in detail by Csörgo and Revesz (1981) . They have established several properties of the empirical distribution function $F_n(x)$. It should be noted that $G_n(u)$ gives a nonparametric estimate of $G(u)$ that is based on a single order statistics, regardless of the form of the population distribution $F(x)$. A modified estimate of $G(u)$ has been proposed by Parzen (1979) that uses adjacent order statistics and is given by

$$\tilde{G}_n(u) = n(\frac{i}{n} - u)X_{i-1:n} + n(u - \frac{i-1}{n})X_{i:n}, \quad \text{for } \tfrac{i-1}{n} < u \leq \tfrac{i}{n}. \tag{5.20}$$

This estimate is based on linear interpolation of adjacent order statistics.

The algorithm in the S-PLUS language to compute an empirical quantile is based on this estimate by Parzen. The empirical quantile estimation for all the results of this thesis uses this algorithm in S-PLUS.

Chapter 6

Estimation of Generalized and Stress Variance-Covariance Matrices

6.1 Introduction

In this chapter, we focus our attention on nonlinear programming algorithms that approximate solutions to the minimization problem specified in Equation 3.28 or 3.33.

In Section 6.2, we discuss how to discretize the contour integral into a finite sum, and the minimization problem specified in Equation 3.28 or 3.33 is replaced by a nonlinear program.

Section 6.5 presents the general idea of a three-dimensional uniform search algorithm, which is used to solve the nonlinear program. This algorithm is an extension of the one-dimensional uniform search algorithm which is reviewed in Sections 6.3 and 6.4.

Section 6.6 proves that the objective function is strictly quasiconvex. Consequently, the algorithm can converge to an approximate solution in a finite number of steps. The proof makes use of several lemmas which are also presented in this section.

Section 6.7 illustrates the possible choices of variable space for 2×2 positive

definite matrices.

Section 6.8 presents the three-dimensional uniform search algorithm to solve the nonlinear program.

6.2 Problem Context in Finite Dimensions

Let $\mathcal{C}$ denote a general open or closed contour. $\mathcal{C}$ can be a closed contour, e.g. $\mathcal{C} = \mathcal{W}$ or $\mathcal{C}$ can be an open contour, e.g. $\mathcal{C} = \mathcal{W}^{(NE)}$. The minimization problem that we seek to solve is either Problem 3.28 or 3.33. Suppose we use Problem 3.28.

$$\begin{aligned} Min \quad & S(\Sigma/\mathcal{C}, p) = \oint_{\mathbf{w}\in\mathcal{C}} d\mathbf{w} \{\sqrt{\mathbf{w}'\Sigma\mathbf{w}} - \tilde{\sigma}(\mathbf{w}/p)\}^2 \\ \textit{subject to} \quad & \Sigma \ p.d \end{aligned}$$

Since it is difficult to obtain an analytic solution to the above problem in its infinite dimensions, we approximate the problem with a nonlinear program in finite dimensions. We choose a finite set of $\mathbf{w} \in \mathcal{C}$. We denote the set $\mathcal{B}_n = \{\mathbf{w}_1, \mathbf{w}_2, \cdots, \mathbf{w}_n\}$. Let $k > 0$ denote a constant positive real number. If we choose $\mathcal{B}_n$ such that $\|\mathbf{w}_{i+1} - \mathbf{w}_i\|_2 = k \ i = 1, \ldots, n-1$ for an open contour $\mathcal{C}$, (in addition, $\|\mathbf{w}_1 - \mathbf{w}_n\|_2 = k$ for a closed contour $\mathcal{C}$), then the objective function is approximated by the sum

$$\oint_{\mathbf{w}\in\mathcal{C}} d\mathbf{w} \{\sqrt{\mathbf{w}'\Sigma\mathbf{w}} - \tilde{\sigma}(\mathbf{w}/p)\}^2 \simeq \sum_{i=1}^{n} \{\sqrt{\mathbf{w}_i'\Sigma\mathbf{w}_i} - \tilde{\sigma}(\mathbf{w}_i/p)\}^2 k \tag{6.1}$$

Since k is a constant, we can simplify with the approximation problem, which is given as

$$\begin{aligned} Min \quad & \tilde{S}(\Sigma/\mathcal{B}_n, p) \equiv \textstyle\sum_{i=1}^{n} \{\sqrt{\mathbf{w}_i'\Sigma\mathbf{w}_i} - \tilde{\sigma}(\mathbf{w}_i/p)\}^2 \\ \textit{subject to} \quad & \Sigma \ p.d., \end{aligned}$$

where $\tilde{\sigma}(\mathbf{w}_i/p), i = 1, \ldots, n$ are the empirical percentile-matched volatilites of portfolios with weightings $\mathbf{w}_i$ at $100(p)\%$ tolerance level. In this optimization problem context, they are a set of constants that depend only on i. Hence, we simplify

the notation of $\tilde{\sigma}(\mathbf{w}_i/p)$ to c_i. Let $f_i(\Sigma)$ denote the i^{th} element in the sum. i.e. $f_i(\Sigma) = \sqrt{\mathbf{w}_i'\Sigma\mathbf{w}_i} - c_i$. The finite nonlinear program for the approximation problem is then given as

$$\begin{aligned} Min \quad & \tilde{S}(\Sigma/\mathcal{B}_n, p) = \textstyle\sum_{i=1}^{n}(f_i(\Sigma))^2 \\ subject\ to \quad & \Sigma\ p.d. \end{aligned} \tag{6.2}$$

Any feasible Σ is a positive definite 2×2 matrix. Suppose

$$\Sigma = \begin{pmatrix} x_1 & x_2 \\ x_2 & x_3 \end{pmatrix} \tag{6.3}$$

Let $\mathbf{x} = (x_1, x_2, x_3)'$. The positive definite constraint can be expressed as

$$\begin{aligned} x_1 &> 0 \\ x_3 &> 0 \\ x_2^2 &< x_1 x_3. \end{aligned} \tag{6.4}$$

As this is a problem in three dimensions, i.e. three degrees of freedom, if $n = 3$ i.e. $\mathcal{B}_3$ consists of only three points, we can completely solve the three simultaneous linear equations given as, for $\mathbf{w}_i = (a_i, b_i)'$ and $i = 1, 2, 3$,

$$\sqrt{a_i^2 x_1 + 2a_i b_i x_2 + b_i^2 x_3} - c_i = 0. \tag{6.5}$$

When $n > 3$, we solve this problem by using multi-line search algorithms without using derivatives. One example is the uniform search. To make use of the capabilities of S-PLUS language, we can more efficiently perform a uniform search over a three dimensional grid instead of sequential uniform search in one dimension. Before we describe how the uniform search over a three dimensional grid works, we review the theory in line search and the one-dimensional uniform search algorithm, which are quoted from Bazaraa *et al* (pages 266-268).

6.3 Line Search Without Using Derivatives

One-dimensional line search is the backbone of many algorithms for solving nonlinear programming problems. Many nonlinear programming algorithms proceed as follows. Given a point $\mathbf{x}_k$, find a direction vector $\mathbf{d}_k$ and then a suitable step size λ_k, yielding a new point $\mathbf{x}_{k+1} = \mathbf{x}_k + \lambda_k \mathbf{d}_k$. The new point $\mathbf{x}_{k+1}$ presumably yields improvement in value of the objective function. This process is then repeated. Finding the step size λ_k involves solving the subproblem to minimize $f(\mathbf{x}_k + \lambda \mathbf{d}_k)$, which is a one-dimensional search problem in the variable λ. The minimization may be over all real λ, nonnegative λ, or λ such that $\mathbf{x}_k + \lambda \mathbf{d}_k$ is feasible.

Consider a function θ of one variable λ to be minimized. One approach to minimizing θ is to set the derivative θ' equal to 0 and then solve for λ. Note, however, that θ is usually defined implicitly in terms of a function f of several variables. In particular, given the vectors $\mathbf{x}$ and $\mathbf{d}$, $\theta(\lambda) = f(\mathbf{x} + \lambda \mathbf{d})$. If f is not differentiable, then θ will not be differentiable. If f is differentiable, then $\theta'(\lambda) = \mathbf{d}' \nabla f(\mathbf{x} + \lambda \mathbf{d})$. To find a point λ with $\theta'(\lambda) = 0$, we have to solve the equation $\mathbf{d}' \nabla f(\mathbf{x} + \lambda \mathbf{d}) = 0$, which is usually nonlinear in λ. Furthermore, λ satisfying $\theta'(\lambda) = 0$ is not necessarily a minimum; it may be a local minimum, a local maximum, or even a saddle point. For these reasons, and except for some special cases, we avoid minimizing θ by letting its derivative be equal to zero. Instead, we resort to some numerical techniques for minimizing the function θ.

In this section, we discuss a method that does not use derivatives for minimizing a function θ of one variable over a closed bounded interval. This method falls under the category of simultaneous line search problems, in which case the candidate points $\mathbf{x}_k$, at which the objective function is evaluated, are determined before the line search begins.

6.3.1 The Interval of Uncertainty

Consider the line search problem to minimize $\theta(\lambda)$ subject to $a \leq \lambda \leq b$. Since the exact location of the minimum of θ over $[a, b]$ is not known, this interval is called

the *interval of uncertainty.* During the search procedure if we can exclude portions of this interval that do not contain the minimum, then the interval of uncertainty is reduced. In general, $[a, b]$ is called the interval of uncertainty if a minimum point $\bar{\lambda}$ lies in $[a, b]$, though its exact value is not known. Theorem 6.3.1 below shows that if the function is strictly quasiconvex, then the interval of uncertainty can be reduced by evaluating θ at two points within the interval. The following is the definition of a quasiconvex function.

Definition 6.3.1 *Let $f : S \to E_1$, where S is a nonempty convex set in E_n. The function f is said to be strictly quasiconvex if, for each $\mathbf{x}_1$ and $\mathbf{x}_2 \in S$ with $f(\mathbf{x}_1) \neq f(\mathbf{x}_2)$, the following inequality is true:*

$$f[\lambda \mathbf{x}_1 + (1 - \lambda)\mathbf{x}_2] < \max\{f(\mathbf{x}_1), f(\mathbf{x}_2)\} \quad \textit{for each } \lambda \in (0, 1) \tag{6.6}$$

Theorem 6.3.1 *Let $\theta : E_1 \to E_1$ be strictly quasiconvex over the interval $[a, b]$. Let $\lambda, \mu \in [a, b]$ be such that $\lambda < \mu$. If $\theta(\lambda) > \theta(\mu)$, then $\theta(z) \geq \theta(\mu)$ for all $z \in [a, \lambda)$. If $\theta(\lambda) \leq \theta(\mu)$, then $\theta(z) \geq \theta(\lambda)$ for all $z \in (\mu, b]$.*

The proof of this theorem can be found in Bazaraa *et al* (page 267) . From the above theorem, under strict quasiconvexity if $\theta(\lambda) > \theta(\mu)$, the new interval of uncertainty is $[\lambda, b]$. On the other hand, if $\theta(\lambda) \leq \theta(\mu)$, the new interval of uncertainty is $[a, \mu]$. These two cases are illustrated in Figure 6-1.

6.4 An Example of a Simultaneous Search: Uniform Search

Uniform search is an example of simultaneous search, where we decide beforehand the points at which the functional evaluations are to be made. The interval of uncertainty $[a_1, b_1]$ is divided into smaller subintervals via the *grid points* $a_1 + k\delta$ for $k = 1, \ldots, n$, where $b_1 = a_1 + (n + 1)\delta$, as illustrated in Figure 6-2. The function θ is evaluated at

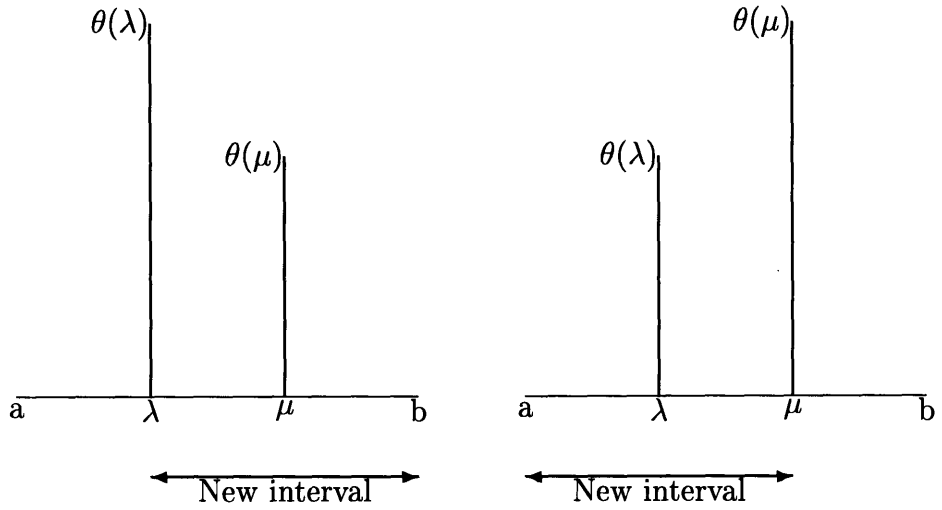

Figure 6-1: Reducing the interval of uncertainty

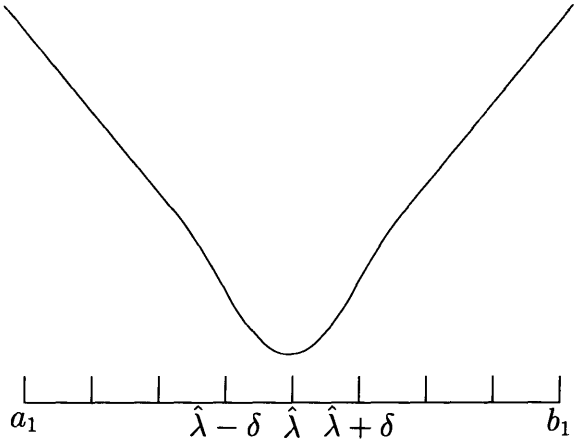

Figure 6-2: Uniform search

each of the n grid points. Let $\hat{\lambda}$ be a grid point with the smallest value of θ. If θ is strictly quasiconvex, it follows that a minimum of θ lies in the interval $[\hat{\lambda}-\delta, \hat{\lambda}+\delta]$.

6.4.1 The Choice of the Grid Length δ

We see that the interval of uncertainty $[a_1, b_1]$ is reduced, after n functional evaluations, to an interval of length of 2δ. Noting that $n = [(b_1 - a_1)/\delta] - 1$, if we desire a small final interval of uncertainty, then a large number n of function evaluations must be made. One technique that is often used to reduce the computational effort

is to utilize a large grid size first and then switch to a finer grid size.

6.5 Three-dimensional Uniform Search

We extend the one-dimensional uniform search described in Section 6.4 to three dimesions. The interval of uncertainty is now a cube represented by $[(a_1, a_2, a_3), (b_1, b_2, b_3)] \equiv \{(x_1, x_2, x_3) : a_i \leq x_i \leq b_i \;\; i = 1, 2, 3\}$. The cube is divided into smaller subcubes via the grid points $(a_1 + k_1\delta_1, a_2 + k_2\delta_2, a_3 + k_3\delta_3)$ for $k_i = 1, \ldots, n_i \;\; i = 1, 2, 3$, where $b_i = a_i + (n_i + 1)\delta_i \;\; i = 1, 2, 3$. The objective function is evaluated at each of the $n_1 n_2 n_3$ grid points. Let $\hat{\lambda} = (\hat{\lambda}_1, \hat{\lambda}_2, \hat{\lambda}_3)$ be a grid point with the smallest value of the objective function. If the objective function is strictly quasiconvex in each of its variable, it follows that a minimum of the objective lies in the cube $[\hat{\lambda} - (\delta_1, \delta_2, \delta_3), \hat{\lambda} + (\delta_1, \delta_2, \delta_3)]$ which will become the new interval of uncertainty in the next step of the three-dimensional uniform search. The proof of this uses Theorem 6.3.1 three times for the three variables.

6.6 Convex Functions and Generalizations

We need to prove that the objective function is a strictly quasiconvex function before we can use the uniform search algorithm. We prove it by using a few lemmas stated as follows.

Lemma 6.6.1 *Let S be a nonempty open set in E_n, and let $f : S \to E_1$ be a convex function on S. Then, f is strictly quasiconvex.*

Proof: *Suppose, given $\mathbf{x}_1$, $\mathbf{x}_2 \in S$ with $f(\mathbf{x}_1) \neq f(\mathbf{x}_2)$ and $\lambda \in (0, 1)$,*

$$\begin{aligned} f(\lambda\mathbf{x}_1 + (1-\lambda)\mathbf{x}_2) &\leq \lambda f(\mathbf{x}_1) + (1-\lambda) f(\mathbf{x}_2) \\ &< \lambda \max\{f(\mathbf{x}_1), f(\mathbf{x}_2)\} + (1-\lambda)\max\{f(\mathbf{x}_1), f(\mathbf{x}_2)\} \\ &= \max\{f(\mathbf{x}_1), f(\mathbf{x}_2)\} \square \end{aligned}$$

Lemma 6.6.2 *Let S be a nonempty open set in E_n, and let $f_i : S \to E_1,\ \ i = 1, \ldots, n$ be convex functions on S. Then, $F_n = \sum_{i=1}^{n} f_i$ is also convex on S.*

Proof: *We prove by induction. The statement is obviously true for $n = 1$. Suppose the statement is true for some k such that $1 \leq k < n$. Then given $\mathbf{x}_1,\ \mathbf{x}_2 \in S$ and $\lambda \in (0, 1)$,*

$$\begin{aligned} F_{k+1}(\lambda \mathbf{x}_1 + (1-\lambda)\mathbf{x}_2) &= F_k(\lambda \mathbf{x}_1 + (1-\lambda)\mathbf{x}_2) + f_{k+1}(\lambda \mathbf{x}_1 + (1-\lambda)\mathbf{x}_2) \\ &\leq \lambda F_k(\mathbf{x}_1) + (1-\lambda)F_k(\mathbf{x}_2) + \lambda f_{k+1}(\mathbf{x}_1) + (1-\lambda) f_{k+1}(\mathbf{x}_2) \\ &= \lambda F_{k+1}(\mathbf{x}_1) + (1-\lambda)F_{k+1}(\mathbf{x}_2) \square \end{aligned}$$

The two lemmas together imply that in order to prove the objective function $\tilde{S}(\Sigma/\mathcal{B}_n, p)$ given in 6.2 is a strictly quasiconvex function, it is sufficient to prove that each $f_i(\Sigma),\ \ i = 1, \ldots, n$ is convex.

Lemma 6.6.3 *$f_i(\Sigma)$ is convex in the space of positive definite matrices.*

Proof: *Suppose given Σ_1 and Σ_2 which are both positive definite, $\lambda \in (0, 1)$, and $i = 1, \ldots, n$*

$$\begin{aligned} f_i(\lambda\Sigma_1 + (1-\lambda)\Sigma_2) &= \{\sqrt{\mathbf{w}_i'[\lambda\Sigma_1 + (1-\lambda)\Sigma_2]\mathbf{w}_i} - c_i\}^2 \\ &= \mathbf{w}_i'(\lambda\Sigma_1 + (1-\lambda)\Sigma_2)\mathbf{w}_i - 2c_i\sqrt{\mathbf{w}_i'(\lambda\Sigma_1 + (1-\lambda)\Sigma_2)\mathbf{w}_i} + c_i^2 \\ &= \lambda(\mathbf{w}_i'\Sigma_1\mathbf{w}_i) + (1-\lambda)(\mathbf{w}_i'\Sigma_2\mathbf{w}_i) \\ &\quad -2c_i\sqrt{\lambda(\mathbf{w}_i'\Sigma_1\mathbf{w}_i) + (1-\lambda)(\mathbf{w}_i'\Sigma_2\mathbf{w}_i)} + \lambda c_i^2 + (1-\lambda)c_i^2 \end{aligned}$$

Now given that the $c_i,\ \ i = 1, \ldots, n$ are the volatility estimates which are always > 0, and $\sqrt{x}$ is a concave function in $x \in (0, \infty)$, it follows from the last equality that

$$\begin{aligned} f_i(\lambda\Sigma_1 + (1-\lambda)\Sigma_2) &\leq \lambda(\mathbf{w}_i'\Sigma_1\mathbf{w}_i) + (1-\lambda)(\mathbf{w}_i'\Sigma_2\mathbf{w}_i) - 2c_i(\lambda\sqrt{\mathbf{w}_i'\Sigma_1\mathbf{w}_i} \\ &\quad +(1-\lambda)\sqrt{\mathbf{w}_i'\Sigma_2\mathbf{w}_i}) + \lambda c_i^2 + (1-\lambda)c_i^2 \\ &= \lambda(\sqrt{\mathbf{w}_i'\Sigma_1\mathbf{w}_i} - c_i)^2 + (1-\lambda)(\sqrt{\mathbf{w}_i'\Sigma_2\mathbf{w}_i} - c_i)^2 \\ &= \lambda f_i(\Sigma_1) + (1-\lambda) f_i(\Sigma_2) \square \end{aligned}$$

6.7 Variable Space

In a three-dimensional uniform search step, we search over the a bounded grid in the space of (x_1, x_2, x_3). For convenient implementation of the uniform search, there are other candidates for the best variable space to be used. The following are two possible variable spaces for consideration.

1. Keep x_1 and x_3 as before. Let $\rho = x_2/\sqrt{x_1 x_3}$. The variable space is (x_1, x_3, ρ). All the constraints are the same, except the last one becomes $\rho^2 < 1$. In this form, ρ^2 lies in the bounded interval $(-1, 1)$. If we know whether the c_i are lying in a positively or negatively correlated elliptical shape, we can further constrain ρ to the range $[0, 1)$ or $(-1, 0]$. We need to provide an initial bound for x_1 and x_3.

2. The variable space is $(\lambda_1, \lambda_2, \theta)$ where the two λ's are the eigenvalues of the matrix Σ and $(cos\ \theta, sin\ \theta)'$ is the eigenvector associated with the larger eigenvalue. Suppose λ_1 is the larger eigenvalue. The transformation of Σ is given as

$$\Sigma = R_\theta \begin{pmatrix} \lambda_1 & 0 \\ 0 & \lambda_2 \end{pmatrix} R_{-\theta} \tag{6.7}$$

where R_θ is the orthogonal matrix that rotates around the origin through and angle θ in the anti-clockwise direction. The constraints become

$$\begin{aligned} \lambda_1 &> 0 \\ \lambda_2 &> 0 \\ \lambda_1 &\geq \lambda_2 \\ \theta &\geq 0 \\ \theta &< \pi \end{aligned}$$

If we know whether the c_i are lying in a positively or negatively correlated elliptical shape, we can further constrain θ to the range $(0, \frac{\pi}{2})$ or $(\frac{\pi}{2}, \pi)$. In any case, θ is bounded. We just need to provide initial upper bound for λ_1.

6.8 The Algorithm

The algorithm that is used to solve Problem 6.2 is a three-dimensional uniform search over the variable space (x_1, x_3, ρ). The algorithm is given as

Algorithm 6.1 • **Initialization Step:**

1. *Set Σ_0 to be the sample variance-covariance matrix, and $k = 0$.*
2. *Define L_0 and U_0 as*

$$L_0 \equiv \min_{i=1,\ldots,n} \frac{\sqrt{\mathbf{w}_i' \Sigma_0 \mathbf{w}_i}}{c_i},$$
$$U_0 \equiv \max_{i=1,\ldots,n} \frac{\sqrt{\mathbf{w}_i' \Sigma_0 \mathbf{w}_i}}{c_i}.$$

3. *Define $\Sigma_0^{(U)} \equiv (U_0)^2 \Sigma_0$ and $\Sigma_0^{(L)} \equiv (L_0)^2 \Sigma_0$. The first three-dimensional grid is then $G_0 \equiv [(\Sigma_0^{(L)})_{11}, (\Sigma_0^{(L)})_{22}, -1], [(\Sigma_0^{(U)})_{11}, (\Sigma_0^{(U)})_{22}, 1]$. Go to the main step.*

• **Main Step:**

1. *Perform the three-dimensional uniform search (Section 6.5) to search for the minimizing Σ in the three dimensional grid given by G_k. Denote the minimizing Σ as Σ_{k+1}.*
2. *If each element of the matrix $\Sigma_k^{(U)} - \Sigma_k^{(L)}$ has absolute value smaller than l,* and *if $|\tilde{S}(\Sigma_{k+1}/\mathcal{B}_n, p) - \tilde{S}(\Sigma_k/\mathcal{B}_n, p)| < \epsilon$, stop. The minimizing matrix is Σ_{k+1} and lies in the interval $[\Sigma_k^{(L)}, \Sigma_k^{(U)}]$. Otherwise, set $k = k + 1$. Generate G_k as described in Section 6.5. Go to step 1 of the Main step.*

Figure 6-3: Initial lower and upper bounds for fitting $\tilde{\sigma}(\mathbf{w}/95\%)$ for portfolios that hold USD/DEM and USD/JPY, $\mathbf{w} \in \mathcal{W}$

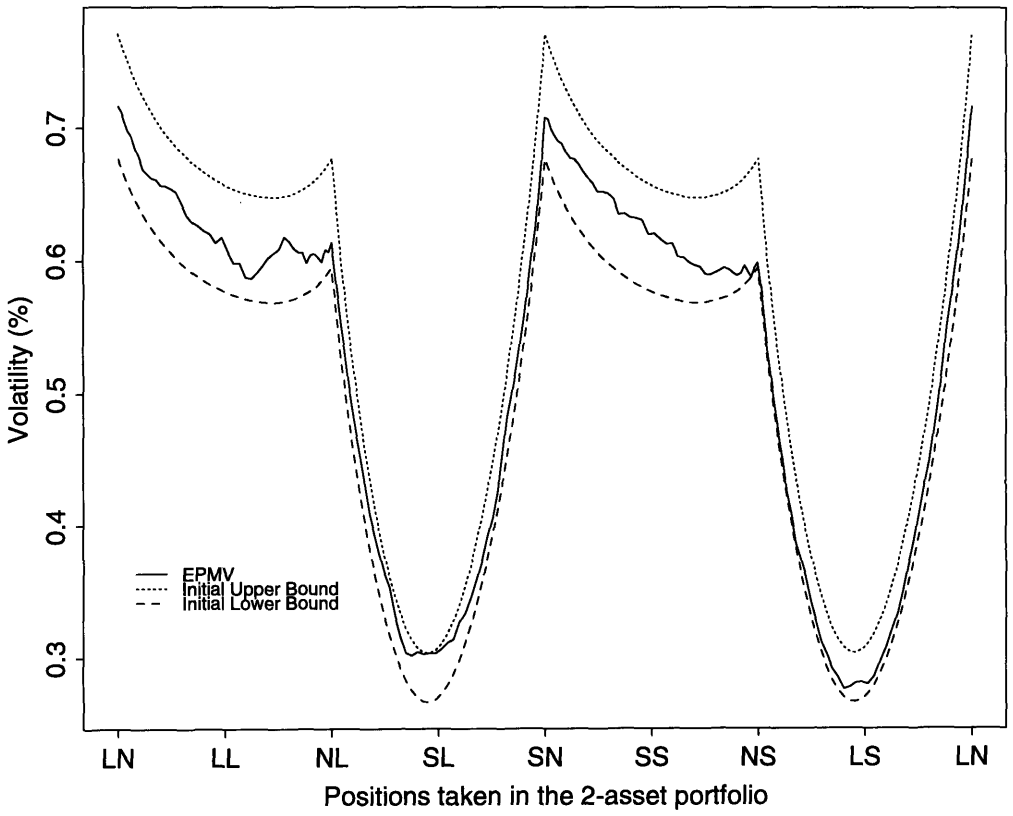

Figure 6-3 illustrates the initial upper and lower bounds for the empirical percentile-matched volatilities at 95% tolerance level for portfolios with weightings $\mathbf{w} \in \mathcal{W}$ that hold USD/DEM and USD/JPY.

Appendix A

Univariate Ordered Statistics

A.1 Introduction

In this appendix, we review the basic theory of order statistics and the David and Johnson's approximation for the moments of order statistics from a known continuous distribution. The reviewed materials are selectively quoted from Chapters 2 and 3 of Balakrishnan *et al* (1991) . The end of this appendix includes a new approximation method to compute the variance-covariance matrix for standard Gaussian order statistics. This new method has made a breakthrough in the best linear unbiased estimation for the Gaussian distribution parameters. Before, although the David and Johnson approximation method can approximate the variance-covariance matrix for standard Gaussian order statistics, it is computationally not fast enough for sample sizes as large as like 2000, which is roughly the size of a sample of 9 years' daily closing prices. Given a sample of size n, the order of magnitude of the number of computations needed to use the David and Johnson approximation method to compute the approximating variance-covariance matrix for order statistics is $O(n^2)$. The new method's order of magnitude, however, is only $O(n)$. This new method is used in Chapter 5 for the best linear unbiased estimation of the Gaussian parameters.

Section A.2 provides descriptions of Type-I and Type-II censored samples.

In Section A.3, starting with the joint distribution of all n order statistics, we derive the joint distribution of two order statistics and the marginal distribution of a

single order statistic.

By making use of these results, we then present some fundamental formulae that are necessary for the computation of single and product moments of order statistics in Section A.4. Next, we consider the uniform distribution and derive the closed forms of the moments and product moments of order statistics from uniform samples. Further, we present some identities of the moments and product moments of order statistics for symmetric distributions about zero. This helps reduce the amount of computation for the standard Gaussian distribution.

In Section A.5, we review the David-Johnson (1954) approximation for the moments of order statistics from an arbitrary continuous distribution. This method of approximation, based on the probability integral transformation and the explicit expressions of the moments of uniform order statistics, provides a simple and practical method of approximating the single and the product moments of order statistics for large random samples from known distributions. A detailed account of this and some other methods of approximation for the moments of order statistics may be found in the monograph on this topic by Arnold and Balakrishnan (1989) . At the end of this section, it is shown that there is no need to use David-Johnson approximation to obtain the variance-covariance matrix for order statistics of the standard Gaussian distribution. A good enough approximation of this matrix can be obtained by using the correlation matrix for order statistics of the uniform distribution, which is in closed form.

A.2 Censored Data

By censored data we shall mean that, in a potential sample of size n, a known number of observations is missing at either end (single censoring) or at both ends (double censoring). In Type-I censoring, the sample is curtailed below and/or above a fixed point. The number of censored observations is random. In Type-II censoring, the number of censored observations is known and the censoring fixed point is usually an empirical percentile of the complete sample. Both forms of censoring are different

from truncation, where the population rather than the sample is curtailed and the number of lost observations is unknown.

A.3 Basic Theory

A.3.1 Joint Distribution of n Order Statistics

Let $X_1, X_2, \ldots, X_n$ be independent, absolutely continuous random variables with common probability density function (pdf) $f(x)$ and cumulative distribution function (cdf) $F(x)$, and let $X_{1:n} \leq X_{2:n} \leq \ldots \leq X_{n:n}$ be the corresponding order statistics. Then, given the realizations of these n order statistics to be $x_{1:n} \leq x_{2:n} \leq \ldots \leq x_{n:n}$, the original variables X_i $(i = 1, 2, \ldots, n)$ are constrained to take on values $x_{i_k:n}$, which by symmetry carries equal and independent probability for each of the $n!$ permutations $(i_1, i_2, \ldots, i_n)$ of $(1, 2, \ldots, n)$. As a result, their joint density is

$$f_{1,2,\ldots,n:n}(x_{1:n}, x_{2:n}, \ldots, x_{n:n}) = \begin{cases} n! \prod_{i=1}^{n} f(x_{i:n}), & -\infty < x_{1:n} < x_{2:n} < \ldots < x_{n:n} < \infty \\ 0, & \text{otherwise.} \end{cases} \tag{A.1}$$

A.3.2 Distribution of a Single Order Statistic

Let us consider the order statistics $X_{i:n}$ and derive its density from Equation A.1. With the joint density of all n order statistics, we integrate out the variables $(X_{1:n}, \ldots, X_{i-1:n})$, $(X_{i+1:n}, \ldots, X_{n:n})$ in order to derive the marginal density function of $X_{i:n}$ $(1 \leq i \leq n)$ as

$$\begin{aligned} f_{i:n}(x_{i:n}) &= n! f(x_{i:n}) \\ &\quad \times \int_{-\infty}^{x_{i:n}} \cdots \int_{-\infty}^{x_{2:n}} f(x_{1:n}) \ldots f(x_{i-1:n}) dx_{1:n} \ldots dx_{i-1:n} \\ &\quad \times \int_{x_{i:n}}^{\infty} \cdots \int_{x_{i:n}}^{x_{i+2:n}} f(x_{i+1:n}) \ldots f(x_{n:n}) dx_{i+1:n} \ldots dx_{n:n}. \end{aligned} \tag{A.2}$$

Direct integration yields

$$\int_{-\infty}^{x_{i:n}} \cdots \int_{-\infty}^{x_{2:n}} f(x_{1:n}) \ldots f(x_{i-1:n}) dx_{1:n} \ldots dx_{i-1:n} = \frac{\{F(x_{i:n})\}^{i-1}}{(i-1)!}, \tag{A.3}$$

and

$$\int_{x_{i:n}}^{\infty} \cdots \int_{x_{i:n}}^{x_{i+2:n}} f(x_{i+1:n}) \ldots f(x_{n:n}) dx_{i+1:n} \ldots dx_{n:n} = \frac{\{1 - F(x_{i:n})\}^{n-i}}{(n-i)!}. \tag{A.4}$$

Upon substituting the expressions A.3 and A.4 for the two sets of integrals in Equation A.2, we obtain the marginal density function of $X_{i:n}$ $(1 \leq i \leq n)$ as

$$\begin{aligned} f_{i:n}(x_{i:n}) &= \frac{n!}{(i-1)!\,(n-i)!} \{F(x_{i:n})\}^{i-1} \{1 - F(x_{i:n})\}^{n-i} f(x_{i:n}), \\ &\quad \text{for } -\infty < x_{i:n} < \infty. \end{aligned} \tag{A.5}$$

A.3.3 Joint Distribution of Two Order Statistics

Let us consider the order statistics $X_{i:n}$ and $X_{j:n}$ $(1 \leq i < j \leq n)$ and derive their joint density from Equation A.1.

By considering the joint density of all n order statistics and integrating out the variables $(X_{1:n}, \ldots, X_{i-1:n})$, $(X_{i+1:n}, \ldots, X_{j-1:n})$, $(X_{j+1:n}, \ldots, X_{n:n})$, we derive the joint density function of $X_{i:n}$ and $X_{j:n}$ as

$$\begin{aligned} f_{i,j:n}(x_{i:n}, x_{j:n}) &= n! f(x_{i:n}) f(x_{j:n}) \\ &\quad \times \int_{-\infty}^{x_{i:n}} \cdots \int_{-\infty}^{x_{2:n}} f(x_{1:n}) \ldots f(x_{i-1:n}) dx_{1:n} \ldots dx_{i-1:n} \\ &\quad \times \int_{x_{i:n}}^{x_{j:n}} \cdots \int_{x_{i:n}}^{x_{i+2:n}} f(x_{i+1:n}) \ldots f(x_{j-1:n}) dx_{i+1:n} \ldots dx_{j-1:n} \\ &\quad \times \int_{x_{j:n}}^{\infty} \cdots \int_{x_{j:n}}^{x_{j+2:n}} f(x_{j+1:n}) \ldots f(x_{n:n}) dx_{j+1:n} \ldots dx_{n:n}. \end{aligned} \tag{A.6}$$

Direct integration yields

$$\int_{-\infty}^{x_{i:n}} \cdots \int_{-\infty}^{x_{2:n}} f(x_{1:n}) \ldots f(x_{i-1:n}) dx_{1:n} \ldots dx_{i-1:n} = \frac{\{F(x_{i:n})\}^{i-1}}{(i-1)!}, \tag{A.7}$$

$$\int_{x_{i:n}}^{x_{j:n}} \cdots \int_{x_{i:n}}^{x_{i+2:n}} f(x_{i+1:n}) \ldots f(x_{j-1:n}) dx_{i+1:n} \ldots dx_{j-1:n} = \frac{\{F(x_{j:n}) - F(x_{i:n})\}^{j-i-1}}{(j-i-1)!}, \tag{A.8}$$

and

$$\int_{x_{j:n}}^{\infty} \cdots \int_{x_{j:n}}^{x_{j+2:n}} f(x_{j+1:n}) \ldots f(x_{n:n}) dx_{j+1:n} \ldots dx_{n:n} = \frac{\{1 - F(x_{j:n})\}^{n-j}}{(n-j)!}. \tag{A.9}$$

Upon using the Equations A.7 - A.9 for the three sets of integrals in Equation A.6, we obtain the joint density function of $X_{i:n}$ and $X_{j:n}$ $(1 \leq i < j \leq n)$ as

$$\begin{aligned} & f_{i,j:n}(x_{i:n}, x_{j:n}) = \\ & \quad \frac{n!}{(i-1)!\,(j-i-1)!\,(n-j)!} \{F(x_{i:n})\}^{i-1} \{F(x_{j:n}) - F(x_{i:n})\}^{j-i-1} \\ & \quad \times \{1 - F(x_{j:n})\}^{n-j} f(x_{i:n}) f(x_{j:n}) \\ & \quad \text{for } -\infty < x_{i:n} < x_{j:n} < \infty. \end{aligned} \tag{A.10}$$

A.4 Moments and Other Expected Values

A.4.1 Some Basic Formulae

Let $X_1, X_2, \ldots, X_n$ be a random sample from a population with pdf $f(x)$ and cdf $F(x)$, and let $X_{1:n} \leq X_{2:n} \leq \ldots \leq X_{n:n}$ be the order statistics obtained from the above sample. Let $\alpha_{i:n}^{(k)}$ denote the single moment $E(X_{i:n}^k)$. We assume that $E(X_{i:n}^k)$ is finite, i.e. $E(|X_{i:n}^k|) < \infty$. Then, from the density function of $X_{i:n}$ in Equation A.5, we have for $i = 1, 2, \ldots, n$ and $k \geq 1$

$$\begin{aligned} \alpha_{i:n}^{(k)} &= E(X_{i:n}^k) = \int_{-\infty}^{\infty} x^k f_{i:n}(x)\, dx \\ &= \frac{n!}{(i-1)!\,(n-i)!} \int_{-\infty}^{\infty} x^k \{F(x)\}^{i-1} \{1 - F(x)\}^{n-i} f(x)\, dx, \end{aligned} \tag{A.11}$$

For convenience, let $\alpha_{i:n}$ denote $\alpha_{i:n}^{(1)}$. Then from the first two single moments of

$X_{i:n}$, we may compute the variance as

$$\beta_{i,i:n} = Var(X_{i:n}) = \alpha^{(2)}_{i:n} - \alpha^2_{i:n}, \quad 1 \leq i \leq n \tag{A.12}$$

Next, let $\alpha_{i,j:n}$ denote the product moment $E(X_{i:n}X_{j:n})$. Then, from the joint density function of $X_{i:n}$ and $X_{j:n}$ in Equation A.10, we have for $1 \leq i < j \leq n$

$$\begin{aligned}
\alpha_{i,j:n} &= E(X_{i:n}X_{j:n}) \\
&= \int_{-\infty}^{\infty} dx \int_{x}^{\infty} dy \;\; xy f_{i,j:n}(x,y) \\
&= \frac{n!}{(i-1)!\,(j-i-1)!\,(n-j)!} \int_{-\infty}^{\infty} dx \int_{x}^{\infty} dy \;\; xy\{F(x)\}^{i-1}\{F(y)-F(x)\}^{j-i-1} \\
&\quad \times\{1-F(y)\}^{n-j} f(x) f(y)
\end{aligned} \tag{A.13}$$

For convenience, let $\alpha_{i,i:n}$ denote $\alpha^{(2)}_{i:n}$. From the first two single moments and the above product moments, we may compute the covariance of $X_{i:n}$ and $X_{j:n}$ as

$$\beta_{i,j:n} = Cov(X_{i:n}, X_{j:n}) = \alpha_{i,j:n} - \alpha_{i:n}\alpha_{j:n}, \quad 1 \leq i < j \leq n \tag{A.14}$$

The correlation between $X_{i:n}$ and $X_{j:n}$ is

$$\begin{aligned}
\rho_{i,j:n} &= \frac{Cov(X_{i:n}, X_{j:n})}{\sqrt{Var(X_{i:n})Var(X_{j:n})}} \\
&= \frac{\beta_{i,j:n}}{\sqrt{\beta_{i,i:n}\beta_{j,j:n}}}
\end{aligned} \tag{A.15}$$

A.4.2 Results for the Uniform Distribution

Let $U_{1:n} \leq U_{2:n} \leq \ldots \leq U_{n:n}$ be the order statistics from a uniform (0,1) distribution. Then from Equation A.11, we get for $1 \leq i \leq n$ and $k \geq 1$

$$\begin{aligned}
\alpha^{(k)}_{i:n} &= E(U^k_{i:n}) \\
&= \frac{n!}{(i-1)!\,(n-i)!} \int_0^1 x^{k+i-1}(1-x)^{n-i}\, dx
\end{aligned}$$

$$
\begin{aligned}
&= \frac{n!}{(i-1)!}\frac{(k+i-1)!}{(n+k)!} \\
&= \frac{i(i+1)\ldots(i+k-1)}{(n+1)(n+2)\ldots(n+k)}
\end{aligned} \tag{A.16}
$$

Thus, by setting $p_i = i/(n+1)$ and $q_i = 1 - p_i$, we find from Equation A.16 that

$$
\alpha_{i:n} = E(U_{i:n}) = p_i \tag{A.17}
$$

and

$$
\begin{aligned}
\beta_{i,i:n} &= Var(U_{i:n}) \\
&= \frac{i(i+1)}{(n+1)(n+2)} - \frac{i^2}{(n+1)^2} \\
&= \frac{p_i q_i}{n+2}
\end{aligned} \tag{A.18}
$$

Similarly, from Equation A.13, we get for $1 \leq i < j \leq n$ and $k_1, k_2 \geq 1$

$$
\begin{aligned}
&\alpha_{i,j:n}^{(k_1,k_2)} \\
&= E(U_{i:n}^{k_1} U_{j:n}^{k_2}) \\
&= \frac{n!}{(i-1)!\,(j-i-1)!\,(n-j)!}\int_0^1 dx \int_x^1 dy\; x^{k_1+i-1}(y-x)^{j-i-1}y^{k_2}(1-y)^{n-j} \\
&= \frac{n!\,(k_1+i-1)!\,(k_1+k_2+j-1)!}{(i-1)!\,(k_1+j-1)!\,(n+k_1+k_2)!} \\
&= \frac{i(i+1)\ldots(i+k_1-1)(j+k_1)(j+k_1+1)\ldots(j+k_1+k_2-1)}{(n+1)(n+2)\ldots(n+k_1+k_2)}
\end{aligned} \tag{A.19}
$$

By setting $k_1 = k_2 = 1$ in Equation A.19, we immediately obtain for $1 \leq i < j \leq n$

$$
\alpha_{i,j:n} = \frac{i(j+1)}{(n+1)(n+2)}, \tag{A.20}
$$

which, when used with Equation A.17, yields for $1 \leq i < j \leq n$

$$
\begin{aligned}
\beta_{i,j:n} &= Cov(U_{i:n}, U_{j:n}) \\
&= \frac{i(j+1)}{(n+1)(n+2)} - \frac{ij}{(n+1)^2}
\end{aligned}
$$

$$= \frac{p_i q_j}{n+2} \tag{A.21}$$

and

$$\begin{aligned}\rho_{i,j:n} &= \frac{\beta_{i,j:n}}{\sqrt{\beta_{i,i:n}\beta_{j,j:n}}} \\ &= \sqrt{\frac{p_i q_j}{p_j q_i}} \\ &= \sqrt{\frac{i(n+1-j)}{(n+1-i)j}}\end{aligned} \tag{A.22}$$

Proceeding similarly, we derive for $1 \leq i_1 < i_2 < i_3 < i_4 \leq n$

$$\begin{aligned}&E(U_{i_1:n}^{k_1} U_{i_2:n}^{k_2} U_{i_3:n}^{k_3} U_{i_4:n}^{k_4}) = \\ &\quad \frac{n!\,(k_1+i_1-1)!\,(k_1+k_2+i_2-1)!}{(i_1-1)!\,(k_1+i_2-1)!\,(k_1+k_2+i_3-1)!} \\ &\times \frac{(k_1+k_2+k_3+i_3-1)!\,(k_1+k_2+k_3+k_4+i_4-1)!}{(k_1+k_2+k_3+i_4-1)!\,(n+k_1+k_2+k_3+k_4)!}.\end{aligned} \tag{A.23}$$

A.4.3 Some Identities for Symmetric Distributions about Zero

For distributions that are symmetric about zero, it may be noted from Equation A.5 that for $1 \leq i \leq n$

$$X_{i:n} \stackrel{d}{=} (-X)_{n-i+1:n}, \tag{A.24}$$

and from Equation A.10 that for $1 \leq i < j \leq n$

$$(X_{i:n}, X_{j:n}) \stackrel{d}{=} ((-X)_{n-i+1:n}, (-X)_{n-j+1:n}). \tag{A.25}$$

Therefore, for distributions which are symmetric about zero, we have the results for $1 \leq i \leq n$ and $k \geq 1$

$$\alpha_{n-i+1:n}^{(k)} = (-1)^k \alpha_{i:n}^{(k)}, \tag{A.26}$$

and for $1 \leq i < j \leq n$

$$\alpha_{n-j+1,n-i+1:n} = \alpha_{i,j:n}, \tag{A.27}$$

and

$$\begin{aligned} \beta_{n-j+1,n-i+1:n} &= \alpha_{n-j+1,n-i+1:n} - \alpha_{n-j+1:n}\alpha_{n-i+1:n} \\ &= \alpha_{i,j:n} - \alpha_{i:n}\alpha_{j:n} \\ &= \beta_{i,j:n}. \end{aligned} \tag{A.28}$$

A.5 David and Johnson's Approximation

The probability integral transformation $u = F(x)$ transforms the order statistics $X_{i:n}$ from a population with pdf $f(x)$ and cdf $F(x)$ into the uniform order statistics $U_{i:n}$ for $i = 1, 2, \ldots, n$. Conversely, the probability integral transformation $x = F^{-1}(u)$[1] transforms the order statistics $U_{i:n}$ from a uniform distribution into the order statistics $X_{i:n}$ for $i = 1, 2, \ldots, n$. By the latter transfomration, we get for $1 \leq i \leq n$

$$X_{i:n} \stackrel{d}{=} F^{-1}(U_{i:n}) = G(U_{i:n}). \tag{A.29}$$

By a Taylor series expansion around the point p_i as defined by Equation A.17, it follows from Equation A.29 that

$$\begin{aligned} X_{i:n} &= G_i + G_i'(U_{i:n} - p_i) + \frac{1}{2}G_i''(U_{i:n} - p_i)^2 \\ &\quad + \frac{1}{6}G_i'''(U_{i:n} - p_i)^3 + \frac{1}{24}G_i^{iv}(U_{i:n} - p_i)^4 + \ldots; \end{aligned} \tag{A.30}$$

here, G_i denotes $G(p_i)$, G_i' denotes $dG(u)/du|_{u=p_i}$, and similarly G_i'', G_i''', $G_i^{iv}, \ldots$, denote successive derivatives of $G(u)$ evaluated at $u = p_i$. Then, by taking expectation on both sides of Equation A.30 and by using the expressions of the central moments of uniform order statistics derived from Equation A.23 (written, however, in inverse powers of $(n + 2)$ by David and Johnson (1954) for simplicity and computational

[1] In general, for $u \in (0, 1)$, $F^{-1}(u) \equiv \inf\{x : F(x) \geq u\}$

ease), we obtain

$$\begin{aligned}\alpha_{i:n} \simeq\ & G_i + \frac{p_iq_i}{2(n+2)}G_i'' + \frac{p_iq_i}{(n+2)^2}\left[\frac{1}{3}(q_i-p_i)G_i''' + \frac{1}{8}p_iq_iG_i^{iv}\right] \\ & + \frac{p_iq_i}{(n+2)^3}\left[-\frac{1}{3}(q_i-p_i)G_i''' + \frac{1}{4}\{(q_i-p_i)^2 - p_iq_i\}G_i^{iv}\right. \\ & \left. + \frac{1}{6}p_iq_i(q_i-p_i)G_i^{v} + \frac{1}{48}p_i^2q_i^2G_i^{vi}\right], \end{aligned} \tag{A.31}$$

where q_i is as defined in Section A.4.2. Similarly, by taking expectation on the series expansion for $X_{i:n}^2$ obtained from Equation A.30, and then subtracting from it the expression of $\alpha_{i:n}^2$ obtained from Equation A.31, we get an approximate formula for the variance of $X_{i:n}$:

$$\begin{aligned}\beta_{i,i:n} \simeq\ & \frac{p_iq_i}{(n+2)}(G_i')^2 + \frac{p_iq_i}{(n+2)^2}\left[2(q_i-p_i)G_i'G_i'' + p_iq_i\left\{G_i'G_i''' + \frac{1}{2}(G_i'')^2\right\}\right] \\ & + \frac{p_iq_i}{(n+2)^3}\left[-2(q_i-p_i)G_i'G_i'' + \{(q_i-p_i)^2 - p_iq_i\}\right. \\ & \times\left\{2G_i'G_i''' + \frac{3}{2}(G_i'')^2\right\} + p_iq_i(q_i-p_i)\left\{\frac{5}{3}G_i'G_i^{iv} + 3G_i''G_i'''\right\} \\ & \left. + \frac{1}{4}p_i^2q_i^2\left\{G_i'G_i^{v} + 2G_i''G_i^{iv} + \frac{5}{3}(G_i''')^2\right\}\right]. \end{aligned} \tag{A.32}$$

Next, by taking expectation on the series expansion for $X_{i:n}X_{j:n}$ obtained from Equation A.30, and then subtracting from it the expression of $\alpha_{i:n}\alpha_{j:n}$ obtained from Equation A.31, we derive an approximate formula for the covariance of $X_{i:n}$ and $X_{j:n}$ $(1 \le i < j \le n)$:

$$\begin{aligned}\beta_{i,j:n} \simeq\ & \frac{p_iq_j}{(n+2)}G_i'G_j' + \frac{p_iq_j}{(n+2)^2}\left[(q_i-p_i)G_i''G_j' + (q_j-p_j)G_i'G_j''\right. \\ & \left. + \frac{1}{2}p_iq_iG_i'''G_j' + \frac{1}{2}p_jq_jG_i'G_j''' + \frac{1}{2}p_iq_jG_i''G_j''\right] \\ & + \frac{p_iq_j}{(n+2)^3}\left[-(q_i-p_i)G_i''G_j' - (q_j-p_j)G_i'G_j'' + \{(q_i-p_i)^2 - p_iq_i\}G_i'''G_j'\right. \\ & + \{(q_j-p_j)^2 - p_jq_j\}G_i'G_j''' + \left\{\frac{3}{2}(q_i-p_i)(q_j-p_j) + \frac{1}{2}p_jq_i\right. \\ & \left. -2p_iq_j\right\}G_i''G_j'' + \frac{5}{6}p_iq_i(q_i-p_i)G_i^{iv}G_j' + \frac{5}{6}p_jq_j(q_j-p_j)G_i'G_j^{iv} \\ & + \left\{p_iq_j(q_i-p_i) + \frac{1}{2}p_iq_i(q_j-p_j)\right\}G_i'''G_j'' + \{p_iq_j(q_j-p_j) \end{aligned}$$

$$+\frac{1}{2}p_jq_j(q_i-p_i)\Big\}G_i''G_j''' + \frac{1}{8}p_i^2q_i^2G_i^vG_j' + \frac{1}{8}p_j^2q_j^2G_i'G_j^v$$
$$+\frac{1}{4}p_i^2q_iq_jG_i^{iv}G_j'' + \frac{1}{4}p_ip_jq_j^2G_i''G_j^{iv}$$
$$+\frac{1}{12}(2p_i^2q_j^2+3p_ip_jq_iq_j)G_i'''G_j'''\Big]. \tag{A.33}$$

By using Equation A.22, the correlation between $X_{i:n}$ and $X_{j:n}$ $(1 \le i \le j \le n)$ is approximated by

$$\rho_{i,j:n} = \sqrt{\frac{i(n+1-j)}{j(n+1-i)}}\left[1-\frac{1}{4(n+2)}\left\{\frac{(G_i'')^2}{(G_i')^2}p_iq_i - \frac{2G_i''G_j''}{G_i'G_j'}p_iq_j + \frac{(G_j'')^2}{(G_j')^2}p_jq_j\right\}\right.$$
$$\left.+O(n^{-2})\right] \tag{A.34}$$

From Equations A.31 and A.34, as pointed out by Arnold and Balakrishnan (1989) , if both i, j and n increase with i/n, j/n remaining fixed, the asymptotic distribution of $X_{i:n}$ has the mean G_i which is $F^{-1}(E(U_{i:n}))$ and the asymptotic joint distribution of $X_{i:n}$ and $X_{j:n}$ has the correlation of the uniform order statistics.

As pointed out by David and Johnson (1954) , the evaluation of the derivatives of G_i is rather easy in most cases. First of all, we realize that

$$G_i' = \frac{dG(u)}{du}|_{u=p_i} = \frac{1}{f(F^{-1}(u))}|_{u=p_i} = \frac{1}{f(G_i)}, \tag{A.35}$$

which is just the reciprocal of the pdf of the population evaluated at G_i. The above expression of G_i' in Equation A.35 allows us to write down the higher derivatives of G_i without great difficulty in most cases.

A.5.1 Results for the Standard Gaussian Distribution

For the standard Gaussian distribution, by making use of the property $f'(x) = -xf(x)$ we get

$$G_i' = 1/f(G_i),$$

$$
\begin{aligned}
G_i'' &= G_i/\{f(G_i)\}^2, \\
G_i''' &= \{1+2(G_i)^2\}/\{f(G_i)\}^3, \\
G_i^{iv} &= G_i\{7+6(G_i)^2\}/\{f(G_i)\}^4, \\
G_i^{v} &= \{7+46(G_i)^2+24(G_i)^4\}/\{f(G_i)\}^5, \\
G_i^{vi} &= G_i\{127+326(G_i)^2+120(G_i)^4\}/\{f(G_i)\}^6,
\end{aligned}
$$

etc.

As illustrated by David and Johnson (1954) , and also by several other authors, this simple approximation procedure works well in most cases. However, this procedure may not provide satisfactory results for the extreme order statistics. In this case, the convergence of this approximation to the exact value may be very slow, and even nonexistent in some cases. An analysis of the error after a number of terms of the David-Johnson series for the expected values of Gaussian statistics is presented by Saw (1960) . Interested reader can compare the results in Table A.1 with results in Saw (1960). Table A.1 presents the relative error of $\alpha_{n:n}$ using Equation A.31 with the exact values taken from the tables of Hartner (1961) and Tippett (1925) . We see that the relative error decreases as n increases. Hence for the standard Gaussian distribution, we can sufficiently accurately approximate the expectations of the order statistics using the David and Johnson's approximation.

If one uses Equation A.34 up to the term $O(n^{-1})$ as an approximation to compute $\rho_{i,j:n}$, one would find that $\rho_{1,n:n}$ does not converge at all. Convergent results can be obtained by using Equation A.33 directly to compute $\rho_{i,j:n}$. This is illustrated in Table A.2. The relative error using the correlation of the uniform order statistics to approximate the correlation of the standard Gaussian order statistics computed by David and Johnson's approximation is defined as $(1 \leq i \leq j \leq n)$

$$
\varepsilon_{i,j:n} \equiv \frac{\rho_{i,j:n}^{DJ}}{\sqrt{\frac{i(n+1-j)}{j(n+1-i)}}} - 1. \tag{A.36}
$$

Table A.1: Approximations and relative errors for $\alpha_{n:n}$ in the standard Gaussian distribution

n	DJ's approx.	Exact value	Relative error
100	2.50905	2.50759	5.84e-4
200	2.74745	2.74604	5.14e-4
300	2.87915	2.87777	4.80e-4
400	2.96955	2.96818	4.61e-4
500	3.03806	3.03670	4.48e-4
600	3.09305	3.09170	4.38e-4
700	3.13889	3.13755	4.28e-4
800	3.17813	3.17679	4.22e-4
900	3.21239	3.21105	4.17e-4
1000	3.24277	3.24144	4.09e-4

The bounds given in the Table A.2 are

$$\begin{aligned} L(n) &\equiv \min_i \min_j \varepsilon_{i,j:n} \\ U(n) &\equiv \max_i \max_j \varepsilon_{i,j:n} \end{aligned} \tag{A.37}$$

From the results in Table A.2, it is easy to see that there is no need to use Equation A.33 to compute the variance-covariance matrix for the standard Gaussian order statistics of any sample sizes. One can simply use the uniform correlation matrix for the order statistics and derive the variance-covariance matrix for the standard Gaussian order statistics using the variances of the order statistics computed by Equation A.32. With this procedure, we can reduce amount of computation significantly and maintain a high degree of precision.

Table A.2: Relative error bounds of the correlation matrix approximation for the standard Gaussian order statistics

n	L(n)	U(n)	n	L(n)	U(n)
3	0.00e+00	1.92e-16	30	-9.29e-16	1.01e-15
4	-3.33e-16	1.67e-16	40	-3.49e-15	5.46e-16
5	-1.53e-15	0.00e+00	50	-1.32e-15	1.39e-15
6	-6.66e-16	3.04e-16	60	-8.74e-15	1.06e-15
7	-3.89e-16	2.98e-16	70	-2.67e-15	8.34e-16
8	-3.51e-16	2.94e-16	80	-1.25e-15	1.53e-15
9	-5.55e-16	5.09e-16	90	-5.93e-15	6.25e-16
10	-3.20e-16	3.22e-16	100	-3.61e-15	2.26e-15
11	-1.98e-15	5.25e-16	200	-8.01e-15	1.42e-15
12	-4.21e-16	5.86e-16	300	-1.13e-14	1.94e-15
13	-4.18e-16	3.61e-16	400	-1.32e-14	5.88e-15
14	-5.66e-16	5.87e-16	500	-1.88e-14	1.21e-14
15	-4.36e-16	4.48e-16	600	-2.15e-14	2.31e-15
16	-1.25e-15	6.66e-16	700	-1.07e-14	2.45e-14
17	-1.40e-15	4.86e-16	800	-1.33e-14	1.07e-14
18	-1.12e-15	3.34e-16	900	-3.91e-14	1.09e-14
19	-6.05e-16	1.19e-15	1000	-2.49e-14	3.19e-14
20	-2.50e-15	4.05e-16	2000		

Appendix B

S-PLUS Program Source Codes

The program source codes written in S-PLUS to generate this thesis' results are presented here in this appendix.

B.1 Transformation and Manipulation of Data

```
#dataconvert.src
#this file contains data manipulation functions

# file (character string) has format (date,vector of numeric data)
# in each row, with the headings in the first line
# n is the number of numeric fields in the file
# value is a matrix of simple returns(flag=1) or prices.
# column names=headings, row names = dates
# Inf or -Inf in the matrix represent missing data.

convert_function(file,flag,n){
temp_scan(file,what="")
name_temp[2:(1+n)]
temp_temp[(2+n):length(temp)]
```

```
temp_matrix(temp,byrow=T,ncol=(n+1))
date_temp[,1]
temp_temp[,2:(n+1)]
temp_as.numeric(temp)
temp_matrix(temp,ncol=n)
temp_ifelse(temp==0,NA,temp)
dimnames(temp)_list(date=date,name=name)
if(flag==1){
result_(temp[2:length(temp[,1]),]-temp[1:(length(temp[,1])-1),])/
temp[1:(length(temp[,1])-1),]
result_ifelse(result==Inf,NA,result)
result_ifelse(result==-Inf,NA,result)
temp_result
}
temp
}

#col= vector representing the column indices.
#this function eliminates the dates on which any one of the
#chosen columns has missing data
extract_function(x,col){
result_x[,col]
if(length(col)!=1)
for(i in c(1:length(col))){
index_(1:length(result[,i]))[is.na(result[,i])]
if(length(index)!=0)
result_result[-index,]
}
else{
index_(1:length(result))[is.na(result)]
```

```
if(length(index)!=0)
result_result[-index]
}
result
}
```

B.2 Estimation of the EPMV and Stress Volatility

```
#biorder.src

#stress = 1, stress volatility estimates, = 0, PM volatiltiy estimates
#bins = multiple of 180
#sc = 1, circle, = 2 diamond
#col=c(i,j) columns (2) of fxrate used i.e. pairs of assets
#p=e.g 95 for 95\% tolerance level or stress condition
#fxrate=fxrate(fx return data, 1985-1994 from BT),
#      =equity(4 equity indexes return data)
pea_function(fxrate,p,col,sc,bins,stress){
data_extract(fxrate,col)
x_data[,1]
y_data[,2]
v_var(data)
xname_dimnames(data)[[2]][1]
yname_dimnames(data)[[2]][2]
temp_empquan(x,y,p,xname,yname,0,sc,bins,stress)
angle_temp[-length(temp[,6]),6]
temp1_theoquan(x,y,v,p,temp[,1:2])
list(theo=temp1,emp=temp)
```

```
}

quantile1_function(x,p){
x_sort(x)
ind_p*length(x)
inf_floor(ind)
quan_(ind-inf)*x[inf+1]+(inf+1-ind)*x[inf]
quan
}

#bins = multiple of 180
#sc = 1, circle, = 2 diamond
empquan_function(x,y,p,xname,yname,flag,sc,bins,stress){
angle_c(0:(bins-1))/(bins/2)*pi
angle1_c(angle,angle[1])
if(sc==1)
alpha_cbind(cos(angle1),sin(angle1))
else{
temp_diam(bins/4,0)
alpha_temp$positions
angle1_temp$angle
angle_angle1[-length(angle1)]
}
data_cbind(x,y)
p_1-p/100
if(stress==1){
select_c(1:round(p*length(data)))
temp_DJcov(length(data[,1]),select)
a_temp$a
b_solve(temp$b)
```

```
one_rep(1,length(select))
ca_rep(a,length(select))
ca_matrix(ca,ncol=length(select),byrow=T)
delta_b%*%(ca-t(ca))%*%b
d2_as.numeric((t(a)%*%b%*%a)*(t(one)%*%b%*%one)-(t(a)%*%b%*%one)^2)
delta_delta/d2
}
r_c(1:3)
for(i in c(1:length(alpha[,1]))){
xdata_sort(data%*%alpha[i,])
if(stress==1){
x_xdata[select]
mu_-t(a)%*%delta%*%x
sigma_t(one)%*%delta%*%x
answer_tailev(mu,sigma,p)
tildep_length(xdata[xdata<=(answer$exp/100)])/length(xdata)
stresvol_(answer$exp/100-mean(xdata))/qnorm(tildep)
r_rbind(r,c(answer$exp/100,mean(xdata),stresvol))
}
else
r_rbind(r,c(quantile1(xdata,p),mean(xdata),
(quantile1(xdata,p)-mean(xdata))/qnorm(p)))
}
r_r[2:length(r[,1]),]
result_r[,1]*alpha
radius_-r[,1]
m_r[,2]

v1_c(NA,rep(r[1,3],length(angle)/4-1),NA,rep(r[(length(angle)/2+1),3],
length(angle)/4-1),NA,rep(r[(length(angle)/2+1),3],
```

```
length(angle)/4-1),NA,rep(r[1,3],length(angle)/4-1),NA)
v2_c(NA,rep(r[(length(angle)/4+1),3],length(angle)/4-1),NA,
rep(r[(length(angle)/4+1),3],length(angle)/4-1),NA,
rep(r[(length(angle)*3/4+1),3],length(angle)/4-1),NA,
rep(r[(length(angle)*3/4+1),3],length(angle)/4-1),NA)
rho_(r[,3]^2-alpha[,1]^2*v1^2-alpha[,2]^2*v2^2)/(2*alpha[,1]*
alpha[,2]*v1*v2)
if(flag==1)
plot(result,type="l",lty=2,xlab=xname,ylab=yname)
print("Estimation finished")
cbind(alpha,radius,result,angle1,r[,3],rho)
}

theoquan_function(x,y,v,p,alpha){
m_c(mean(x),mean(y))
ma_alpha%*%m
q_qnorm(1-p/100)
va_(alpha%*%v)*alpha
va_sqrt(va[,1]+va[,2])
va_ifelse(is.na(va),Inf,va)
r1_va*q+ma
r2_cbind(r1*alpha[,1],r1*alpha[,2])
r_v[1,2]/sqrt(v[1,1]*v[2,2])
list(value=-r1,position=r2,rho=r,iv=va)
}

#flag=1:plot the theoretical and empirical peanut on the same graph
#flag=2:plot the risk exposure at p% tolerance level or the stress
#tolerance level vs position of portfolio
#flag=3:plot the PM (stress) volatility vs position of portfolio
```

```
#flag=4:plot the PM correlation vs position of portfolio
#flag=0:no plots
#pea_pea(fxrate,p,col,2,180,stress)
peaplot_function(pea,fxrate,p,col,flag,a){
data_extract(fxrate,col)
xname_dimnames(data)[[2]][1]
yname_dimnames(data)[[2]][2]
temp1_pea$theo
temp_pea$emp
v_temp[c((0:4)*(length(temp[,6])-1)/4+1),6]
if(flag==1){
plot(temp1$position,type="l",lty=1,xlab=xname,ylab=yname,
xlim=range(c(temp1$position[,1],temp[,4])),
ylim=range(c(temp1$position[,2],temp[,5])))
lines(temp[,4],temp[,5],lty=2)
legend(locator(1),legend=c("Theoretical","Empirical"),
lty=c(1,2),cex=0.7)
}
if(flag==2){
plot(temp[,6],-temp1$value*100,axes=F,type="l",lty=1,
xlab="Positions taken in the 2-asset portfolio",
ylab="DRaR (%)",ylim=range(-c(0,temp1$value,temp[,3])*100))
lines(temp[,6],-temp[,3]*100,lty=2)
abline(v=v,lty=3)
axis(2)
axis(1,seq(0,2*pi,length=9),
c("LN","LL","NL","SL","SN","SS","NS","LS","LN"))
box()
legend(locator(1),legend=c("Gaussian","Empirical"),lty=c(1,2),cex=0.7)
}
```

```
if(flag==3){
plot(temp[,6],temp1$iv*100,axes=F,type="l",lty=1,
xlab="Positions taken in the 2-asset portfolio",
ylab="Volatility (%)",ylim=range(c(temp1$iv,temp[,7])*100))
lines(temp[,6],temp[,7]*100,lty=2)
axis(2)
axis(1,seq(0,2*pi,length=9),
c("LN","LL","NL","SL","SN","SS","NS","LS","LN"))
box()
legend(locator(1),bty="n",legend=c("MLE Gaussian ","EPMV"),
lty=c(1,2),cex=0.7)
}
if(flag==4){
angle_temp[-length(temp[,6]),6]
n_length(angle)
temp2_ifelse(abs(temp[,8])<1,temp[,8],NA)
temp3_temp2[is.na(temp2)==F]
plot(angle,rep(temp1$rho,n),axes=F,type="l",lty=3,
xlab="Positions taken in the 2-asset portfolio",
ylab="Correlation",xlim=range(temp[,6]),
ylim=range(c(temp3,temp1$rho)))
for(i in c(0:3)){
t_temp[(i*n/4+1):((i+1)*n/4),8]
temp4_ifelse(abs(t)<1,t,NA)
temp5_temp4[is.na(temp4)==F]
s_temp[(i*n/4+1):((i+1)*n/4),6]
temp4_ifelse(abs(t)<1,s,NA)
temp4_temp4[is.na(temp4)==F]
lines(temp4,temp5,lty=2)
}
```

```
abline(v=temp[c(1,46,91,136,181),6],lty=1)
axis(2)
axis(1,seq(0,2*pi,length=9),
c("LN","LL","NL","SL","SN","SS","NS","LS","LN"))
box()
legend(locator(1),bty="n",legend=c("MLE Gaussian","EPMC"),
lty=c(3,2),cex=0.7)
}
if(a==1){
par(mfcol=c(1,1),fin=c(8,8.6/6*2.03))
plot(temp[,6],temp[,1],type="l",lty=1,axes=F,
ylim=range(temp[,1:2]),
xlab="Positions taken in the 2-asset portfolio",
ylab="Portfolio Weighting")
lines(temp[,6],temp[,2],lty=2)
abline(v=v,lty=3)
axis(2)
axis(1,seq(0,2*pi,length=9),
c("LN","LL","NL","SL","SN","SS","NS","LS","LN"))
box()
legend(locator(1),legend=c("1st asset","2nd asset"),
lty=c(1,2),cex=0.7)
}
list(theo=temp1,emp=temp)
}

#this function plots the EPMV of the long and short positions
#of a portfolio
epmv_function(fxrate,col){
data_extract(fxrate,col)
```

```
p_c(1:length(data))/(length(data)+1)
data_sort(data)
result_(data-mean(data))/qnorm(p)*100
plot(p[p>0.6],result[p>0.6],type="l",lty=1,
xlab="100(p)% Tolerance Level",ylab="Volatility (%)",
ylim=range(c(result[p>0.6],result[p<0.4])))
lines(1-p[p<0.4],result[p<0.4],lty=2)
abline(h=sqrt(var(data))*100,lty=3)
legend(locator(1),bty="n",legend=c("EPMV (Long)","EPMV (Short)",
"MLE Gaussian"),lty=c(1,2,3),cex=0.7)
1
}
```

B.3 BLUE for Gaussian Type-II Censored Sample

```
#stresvol.src

#this function computes the SERs and stress volatilities of portfolios

stress_function(fxrate,col,n,p,flag){
alpha_diam(n,0)$positions
data_extract(fxrate,col)
select_c(1:round((1-p/100)*length(data[,1])))
temp_DJcov(length(data[,1]),select)
a_temp$a
b_solve(temp$b)
one_rep(1,length(select))
ca_rep(a,length(select))
```

```
ca_matrix(ca,ncol=length(select),byrow=T)
delta_b%*%(ca-t(ca))%*%b
d2_as.numeric((t(a)%*%b%*%a)*(t(one)%*%b%*%one)-(t(a)%*%b%*%one)^2)
delta_delta/d2
result_c(1:3)
for(i in c(1:length(alpha[,1]))){
print(i)
xdata_sort(data%*%alpha[i,])
x_xdata[select]
mu_-t(a)%*%delta%*%x
sigma_t(one)%*%delta%*%x
answer_tailev(mu,sigma,(1-p/100))
tildep_length(xdata[xdata<=(answer$exp/100)])/length(xdata)
stresvol_(answer$exp/100-mean(xdata))/qnorm(tildep)
if(flag==1){
qqnorm(xdata)
        abline(mu,sigma,lty=2)
        abline(mean(xdata),sqrt(var(xdata)),lty=3)
        legend(locator(1),legend=c("BLUE","MLE"),lty=c(2,3),cex=0.7)
        }
result_rbind(result,c(mu,sigma,stresvol))
}
result_result[2:length(result[,1]),]
result
}

#stres_stress(fxrate,col,n,p,0)
#flag = 1, plot the stress Gaussian parameters
#flag = 2, plot the SER
#flag = 3, plot the stress and PM volatility
```

```
stressplot_function(stres,fxrate,p,col,flag){
angle_seq(0,2*pi,length=length(stres[,1]))
if(flag==1){
par(mfcol=c(1,1))
par(pty="m")
par(mar=c(5,4,2,4))
plot(angle,stres[,2],type="l",lty=1,axes=F,
ylab="Standard deviation",xlab="")
axis(2)
axis(1,seq(0,2*pi,length=9),
c("LN","LL","NL","SL","SN","SS","NS","LS","LN"))
box()
mtext(side=1,line=3,"Asset allocation in portfolio")
par(new=TRUE)
plot(angle,stres[,1],type="l",lty=2,axes=F,ylab="",xlab="")
axis(side=4)
mtext(side=4,line=3,"Mean")
legend(locator(1),bty="n",legend=c("Standard deviation","Mean"),
lty=c(1,2),cex=0.7)
        }
if(flag==2){
pea_pea(fxrate,p,col,2,length(stres[,1])-1,0)
par(mar=c(5,4,4,2)+0.1)
temp1_pea$theo
temp_pea$emp
stresrisk_-(stres[,1]+qnorm(1-p/100)*stres[,2])
plot(temp[,6],temp1$value*100,axes=F,type="l",lty=1,
xlab="Positions taken in the 2-asset portfolio",
ylab="DRaR (%)",
ylim=100*range(c(temp1$value,temp[,3],stresrisk)))
```

```
lines(temp[,6],temp[,3]*100,lty=2)
lines(temp[,6],stresrisk*100,lty=3)
axis(2)
axis(1,seq(0,2*pi,length=9),
c("LN","LL","NL","SL","SN","SS","NS","LS","LN"))
box()
legend(locator(1),bty="n",legend=c("MLE Gaussian","Empirical",
"Stress Gaussian"),lty=c(1,2,3),cex=0.7)
}
if(flag==3){
peap_pea(fxrate,p,col,2,length(stres[,1])-1,0)
par(mar=c(5,4,2,4))
plot(angle,stres[,3]*100,axes=F,type="l",lty=1,
ylab="Volatility (%)",
xlab="Asset allocation in portfolio",
ylim=100*range(c(stres[,3],peap$emp[,7])))
lines(angle,peap$emp[,7]*100,lty=2)
axis(2)
axis(1,seq(0,2*pi,length=9),
c("LN","LL","NL","SL","SN","SS","NS","LS","LN"))
box()
legend(locator(1),bty="n",legend=c("Stress volatility",
"PM volatility"),lty=c(1,2),cex=0.7)
        }
1
}
```

B.4 Variance-Covariance Matrix for Gaussian Order Statistics

```
#David-Johnson Approximation for the mean, variance-covariance
#matrix of the standard normal order statistics os sample size n

#this approximates the mean by DJ, and approximates the matrix
#by the uniform correlation multiplies by the variances
#approximated by DJ. select is the selected order statistics
DJcov_function(n,select){
temp_Gi(n)
alpha_temp$g0+temp$p*(1-temp$p)/(n+2)*(temp$g2/2+1/(n+2)*
((1-2*temp$p)*temp$g3/3+temp$p*(1-temp$p)*
temp$g4/8)+1/(n+2)^2*((2*temp$p-1)*temp$g3/3+((1-2*temp$p)^2-
temp$p*(1-temp$p))*temp$g4/4+temp$p*(1-temp$p)*(1-2*temp$p)*
temp$g5/6+(temp$p*(1-temp$p))^2*temp$g6/48))
beta_temp$p*(1-temp$p)/(n+2)*temp$g1^2
+temp$p*(1-temp$p)/(n+2)^2*(2*(1-2*temp$p)*temp$g2*temp$g1+
temp$p*(1-temp$p)*(temp$g1*temp$g3+temp$g2^2/2))
+temp$p*(1-temp$p)/(n+2)^3*(-2*(1-2*temp$p)*temp$g1*temp$g2+
((1-2*temp$p)^2-temp$p*(1-temp$p))*(2*temp$g1*temp$g3+
3/2*temp$g2^2)+temp$p*(1-temp$p)*(1-2*temp$p)*
(5*temp$g1*temp$g4/3+3*temp$g3*temp$g2)+temp$p^2*(1-temp$p)^2*
(temp$g5*temp$g1+2*temp$g4*temp$g2+5/3*temp$g3^2)/4)
u_matrix(rep(1,(length(select))^2),ncol=length(select))
for(i in c(1:length(select)))
u[i,]_select[i]/(n+1-select[i])*beta[select[i]]
for(j in c(1:length(select)))
u[,j]_u[,j]*(n+1-select[j])/select[j]*beta[select[j]]
u_sqrt(u)
```

```
for(i in c(1:(length(select)-1)))
u[(i+1):length(u[,i]),i]_u[i,(i+1):length(u[,i])]
list(a=alpha[select],b=u)
}

#Compute the first six Gaussian derivatives evaluated at E(U(i,n))
Gi_function(n){
p_c(1:n)/(n+1)
G0_qnorm(p)
G1_1/dnorm(G0)
G2_G0/dnorm(G0)^2
G3_(1+2*G0^2)/dnorm(G0)^3
G4_G0*(7+6*G0^2)/dnorm(G0)^4
G5_(7+46*G0^2+24*G0^4)/dnorm(G0)^5
G6_G0*(127+326*G0^2+120*G0^4)/dnorm(G0)^6
list(p=p,g0=G0,g1=G1,g2=G2,g3=G3,g4=G4,g5=G5,g6=G6)
}

#Compute the mean, variace-covariance matrix
DJorder_function(n){
temp_Gi(n)
alpha_temp$g0+temp$p*(1-temp$p)/(n+2)*(temp$g2/2+1/(n+2)*
((1-2*temp$p)*temp$g3/3+temp$p*(1-temp$p)*temp$g4/8)+
1/(n+2)^2*((2*temp$p-1)*temp$g3/3+((1-2*temp$p)^2-temp$p*
(1-temp$p))*temp$g4/4+temp$p*(1-temp$p)*(1-2*temp$p)*
temp$g5/6+(temp$p*(1-temp$p))^2*temp$g6/48))
result_c(1:n)
for(i in c(1:(floor((n+1)/2)))){
print(i)
betaij_temp$p[i]*(1-temp$p[i:(n+1-i)])/(n+2)*temp$g1[i]*
```

```
temp$g1[i:(n+1-i)]
+temp$p[i]*(1-temp$p[i:(n+1-i)])/(n+2)^2*((1-2*temp$p[i])*
temp$g2[i]*temp$g1[i:(n+1-i)]+(1-2*temp$p[i:(n+1-i)])*
temp$g1[i]*temp$g2[i:(n+1-i)]+temp$p[i]*(1-temp$p[i])*
temp$g1[i:(n+1-i)]*temp$g3[i]/2+temp$p[i:(n+1-i)]*
(1-temp$p[i:(n+1-i)])*temp$g1[i]*temp$g3[i:(n+1-i)]/2+
temp$p[i]*(1-temp$p[i:(n+1-i)])*temp$g2[i]*
temp$g2[i:(n+1-i)]/2)
+temp$p[i]*(1-temp$p[i:(n+1-i)])/(n+2)^3*(-(1-2*temp$p[i])*
temp$g1[i:(n+1-i)]*temp$g2[i]-(1-2*temp$p[i:(n+1-i)])*
temp$g1[i]*temp$g2[i:(n+1-i)]+((1-2*temp$p[i])^2-temp$p[i]*
(1-temp$p[i]))*temp$g1[i:(n+1-i)]*temp$g3[i]+
((1-2*temp$p[i:(n+1-i)])^2-temp$p[i:(n+1-i)]*
(1-temp$p[i:(n+1-i)]))*temp$g1[i]*temp$g3[i:(n+1-i)]+
(3*(1-2*temp$p[i])*(1-2*temp$p[i:(n+1-i)])/2+
temp$p[i:(n+1-i)]*(1-temp$p[i])/2-2*temp$p[i]*
(1-temp$p[i:(n+1-i)]))*temp$g2[i]*temp$g2[i:(n+1-i)]+
5*temp$p[i]*(1-temp$p[i])*(1-2*temp$p[i])*temp$g1[i:(n+1-i)]*
temp$g4[i]/6+5*temp$p[i:(n+1-i)]*(1-temp$p[i:(n+1-i)])*
(1-2*temp$p[i:(n+1-i)])*temp$g1[i]*temp$g4[i:(n+1-i)]/6+
(temp$p[i]*(1-temp$p[i:(n+1-i)])*(1-2*temp$p[i])+temp$p[i]*
(1-temp$p[i])*(1-2*temp$p[i:(n+1-i)])/2)*temp$g3[i]*
temp$g2[i:(n+1-i)]+(temp$p[i]*(1-temp$p[i:(n+1-i)])*
(1-2*temp$p[i:(n+1-i)])+temp$p[i:(n+1-i)]*
(1-temp$p[i:(n+1-i)])*(1-2*temp$p[i])/2)*temp$g3[i:(n+1-i)]*
temp$g2[i]+temp$p[i]^2*(1-temp$p[i])^2*temp$g5[i]*
temp$g1[i:(n+1-i)]/8+temp$p[i:(n+1-i)]^2*
(1-temp$p[i:(n+1-i)])^2*temp$g5[i:(n+1-i)]*
temp$g1[i]/8+temp$p[i]^2*(1-temp$p[i])*(1-temp$p[i:(n+1-i)])*
temp$g4[i]*temp$g2[i:(n+1-i)]/4+temp$p[i]*temp$p[i:(n+1-i)]*
```

```
(1-temp$p[i:(n+1-i)])^2*temp$g4[i:(n+1-i)]*temp$g2[i]/4+
(2*temp$p[i]^2*(1-temp$p[i:(n+1-i)])^2+3*temp$p[i]*
temp$p[i:(n+1-i)]*(1-temp$p[i])*(1-temp$p[i:(n+1-i)]))*
temp$g3[i]*temp$g3[i:(n+1-i)]/12)
result_rbind(result,c(rep(NA,i-1),betaij,rep(NA,i-1)))
}
result_result[2:length(result[,1]),]
kiss_matrix(rep(1,n*length(result[,1])),ncol=n)
for(i in c(1:n))
kiss[,i]_result[,i]/sqrt(result[min(i,n+1-i),min(i,n+1-i)])
for(j in c(1:length(result[,1])))
kiss[j,]_kiss[j,]/sqrt(result[j,j])
list(a=alpha,b=result,r=kiss)
}

DJdiff_function(n){
temp_DJorder(n)
u_matrix(rep(1,n*length(temp$r[,1])),ncol=n)
x_c(1:n)
for(i in c(1:length(temp$r[,1])))
u[i,]_i/(n+1-i)
for(j in x)
u[,j]_u[,j]*(n+1-j)/j
u_sqrt(u)
for(i in c(1:(length(temp$r[,1])-1)))
u[(i+1):length(temp$r[,1]),i]_u[i,(i+1):length(temp$r[,1])]
diff_(temp$r-u)/u
list(max=max(diff[is.na(diff)!=1]),min=min(diff[is.na(diff)!=1]))
}
```

```
DJconv_function(k){
n_c(2:k)*100
result_c(1:2)
for(i in c(1:length(n))){
temp_DJdiff(n[i])
result_rbind(result,c(temp$min,temp$max))
}
result_result[2:length(result[,1]),]
result
}

concov_function(result,r,s){
for(i in c(1:(length(result[,1])-1)))
result[(i+1):length(result[,i]),i]_result[i,(i+1):length(result[,i])]
for(i in c(n:(n-length(result[,1])+2)))
result[(n-i+2):length(result[,i]),i]_result[(n-i+1),(i-1):
(n-length(result[,i])+1)]
result1_result[,(length(result[,1])+1):length(result[1,])]
result1_matrix(result1,ncol=length(result[,1]),byrow=T)
if((floor(n/2)*2==n)){
result2_result[,1:length(result[,1])]
result2_result2[length(result2):1]
result2_matrix(result2,ncol=length(result[,1]),byrow=T)
}
else{
result2_result[1:(length(result[,1])-1),1:(length(result[,1])-1)]
result2_result2[length(result2):1]
result2_matrix(result2,ncol=length(result[,1])-1,byrow=T)
}
result_rbind(result,cbind(result1,result2))
```

```
result[r:s,r:s]
}

#this function generates results for the estreme order statistics
DJextreme_function(n){
result_c(1:2)
for(i in c(1:n)*100){
print(i)
result_rbind(result,c(i,DJorder(i)[i]))
}
result_result[2:length(result[,1]),]
result
}
```

B.5 Assessment of Bivariate Gaussian Normality

```
#preass.src
#this file contains functions used in the section preliminary
#assessment

#this functions plots two series of prices (flag=1) or returns
#(flag!=1) parallel in time
#x is the two-column
parplot_function(x,flag){
if(flag==1){
x_ifelse(x==0,NA,x)
xname_dimnames(x)[[2]][1]
        yname_dimnames(x)[[2]][2]
time_seq(0,9.5,length=length(x[,1]))
par(mar=c(5,5,2,5))
```

```
plot(time,x[,1],type="l",lty=1,axes=F,ylab="",xlab="")
axis(2)
axis(1,c(0:9),c(85:94))
par(new=TRUE)
plot(time,x[,2],type="l",lty=2,axes=F,ylab="",xlab="")
axis(side=4)
mtext(side=2,line=3,xname)
mtext(side=1,line=3,"Year")
mtext(side=4,line=3,yname)
box()
legend(locator(1),bty="n",legend=c(xname,yname),lty=c(1,2),cex=0.7)
}
else{
xname_dimnames(x)[[2]][1]
        yname_dimnames(x)[[2]][2]
plot(x,ylab=yname,xlab=xname)
}
x
}

#this function plots the normalized scattergram (flag=1) or
#the histograms for the radius and angle (flag=1)
normalize_function(x,flag){
xname_dimnames(x)[[2]][1]
        yname_dimnames(x)[[2]][2]
m_apply(x,2,mean)
v_var(x)
v_solve(v)
temp_eigen(v)
diag_t(temp$vectors)%*%v%*%temp$vectors
```

```
diag_sqrt(diag)
g_diag%*%t(temp$vectors)
result_t(t(x)-m)%*%t(g)
if(flag==1){
par(mfrow=c(1,2))
xr_range(x[,1])
yr_range(x[,2])
r_c(min(xr[1],yr[1]),max(xr[2],yr[2]))
par(pty="s")
plot(x,ylab=yname,xlab=xname,xlim=r,ylim=r)
mtext("Original",side=3,line=1.5)
xr_range(result[,1])
yr_range(result[,2])
r_c(min(xr[1],yr[1]),max(xr[2],yr[2]))
plot(result,ylab=yname,xlab=xname,xlim=r,ylim=r)
mtext("Normalized",side=3,line=1.5)
}
else{
radii_sqrt(result[,1]^2+result[,2]^2)
angle_ifelse(result[,1]>0,ifelse(result[,2]>0,
atan(result[,2]/result[,1]),
2*pi-atan(abs(result[,2])/result[,1])),
ifelse(result[,2]>0,pi-atan(result[,2]/abs(result[,1])),
pi+atan(result[,2]/result[,1])))
b_seq(0,2*pi,length=37)
temp_hist(angle,breaks=b,plot=F)
cum_0
for(i in c(1:(length(b)-1))){
cum_c(cum,sum(temp$counts[1:i])/length(angle))
}
```

```
par(mfcol=c(1,2))
par(mar=c(5,4,2,4))
hist(angle,breaks=b,plot=TRUE,col=2,axes=F,xlab="Angle",
ylab="Frequency")
axis(2)
axis(1,seq(0,2*pi,length=5),c("0","pi/2","pi","3pi/2","2pi"))
par(new=TRUE)
plot(b,cum,type="l",lty=1,xlab="",ylab="",axes=F)
axis(side=4)
box()
par(mar=c(5,4,2,2))
br_seq(0,7.5,length=61)
hist(radii,breaks=br,plot=TRUE,axes=F,col=2,xlab="Radius",
ylab="Frequency")
axis(2)
axis(1,seq(0,7.5,length=7))
r_seq(0,7.5,length=1000)
par(new=TRUE)
plot(r,dchisq(r^2,2)*2*r,type="l",lty=1,axes=F,ylab="",xlab="")
box()
}
result
}
```

B.6 Bivariate Ellipsoids

```
#bivarnorm.src
#
#This is to calculate the p% confidence "ellipsoid"
#This is to compare on the same graph the 100(p)% normal
```

```
#and the empirical ellipsoid
#flag =1, plot ellipses, =0 no plot
bivar_function(fxrate,p,col,flag){
data_extract(fxrate,col)
x1_data[,1]
y1_data[,2]
xname_dimnames(data)[[2]][1]
yname_dimnames(data)[[2]][2]
x_x1-mean(x1)
y_y1-mean(y1)
mu_c(mean(x1),mean(y1))
result1_c(1:2)
result2_c(1:2)
temp_var(cbind(x,y))
temp1_solve(temp)
k_qchisq(p/100,2)
pie_seq(0,pi,length=181)
pie_pie[-181]
alpha_cbind(cos(pie),sin(pie))
kiss_alpha%*%temp1*alpha
kiss1_kiss[,1]+kiss[,2]
kis_alpha%*%temp*alpha
kis1_kis[,1]+kis[,2]
r1_sqrt(k/kiss1)
f1_pnorm(c(r1,-r1),mean=0,sd=sqrt(kis1))
f1_matrix(f1,ncol=2)
r_c(1:2)
for(i in c(1:length(alpha[,1]))){
print(i)
new_cbind(x,y)%*%alpha[i,]
```

```
r_rbind(r,quantile(new,f1[i,]))
}
r_r[2:length(r[,1]),]
result2_t(t(rbind(r[,1]*alpha,r[,2]*alpha))+mu)
result1_t(t(rbind(r1*alpha,-r1*alpha))+mu)
result1_rbind(result1,result1[1,])
result2_rbind(result2,result2[1,])
what_cbind(x,y)%*%temp1
what_what[,1]*x+what[,2]*y
what_what[what<k]
if(flag[1]==1){
par(pty="s")
xr_range(c(result1[,1]*100,result2[,1]*100))
yr_range(c(result1[,2]*100,result2[,2]*100))
plot(result1*100,type="l",lty=1,ylab=paste(yname," (%)"),
xlab=paste(xname," (%)"),
xlim=c(min(xr[1],yr[1]),max(xr[2],yr[2])),
ylim=c(min(xr[1],yr[1]),max(xr[2],yr[2])))
lines(result2[,1]*100,result2[,2]*100,lty=2)
if(flag[2]==1)
        mtext(paste("Comparison between Bivariate Normal &
Empirical Density Contour for",xname,"and",yname,
"at",p,"%"),side=3,line=1.5)
legend(locator(1),bty="n",legend=c("Gaussian","Empirical"),
lty=c(1,2),cex=0.5)
}
list(p=length(what)/length(x),theo=result1,emp=result2)
}

#this function produces the graph of ellipses in Chapter 2
```

```
eliplot_function(fxrate,p,col){
par(mfcol=c(1,2))
temp_bivar(fxrate,p[1],col,c(1,0))
mtext(paste(p[1],"% Ellipsoids"),side=3,line=1.5)
temp1_bivar(fxrate,p[2],col,c(1,0))
mtext(paste(p[2],"% Ellipsoids"),side=3,line=1.5)
1
}
```

B.7 Generating $\mathcal{W}$

```
#diam.src

#This function generates and draws the portfolio weightings (flag=1)
#n = number of points in a quadrant
diam_function(n,flag){
temp_seq(0,1,length=n+1)
temp_temp[-(n+1)]
dia_rbind(cbind((1-temp),temp),cbind(-temp,(1-temp)),
cbind((-1+temp),-temp),cbind(temp,(-1+temp)))
dia_rbind(dia,dia[1,])
angle_atan(dia[,2]/dia[,1])
angle[(n+1):(3*n)]_angle[(n+1):(3*n)]+pi
angle[(3*n+1):(4*n+1)]_angle[(3*n+1):(4*n+1)]+2*pi
if(flag==1){
par(pty="s")
plot(dia[,1],dia[,2],axes=F,type="l",lty=1,
xlab="1st asset's holding",ylab="2nd asset's holding")
axis(1,seq(-1,1,length=3),c("-1","0","1"))
axis(2,seq(-1,1,length=3),c("-1","0","1"))
```

```
box()
}
list(positions=dia,angle=angle)
}
```

Bibliography

[1] Barry C. Arnold & N. Balakrishnan. *Relations, Bounds and Approximations for Order Statistics.* Springer-Verlag, 1989.

[2] G.L. Tietjen & D.K. Kahaner & R.J. Beckman. Variances and covariances of the normal order statistics for sample sizes 2 to 50. Technical report, 1977. Selected Tables in Mathematical Statistics **5**, 1-73.

[3] N. Balakrishnan & A. Cifford Cohen. *Order Statistics and Inference, Estimation Methods.* Academic Press, Inc., 1991.

[4] H.A. David. *Order Statistics.* John Wiley & Sons, Inc., 1970.

[5] James J. Filliben. The probability plot correlation coefficient test. Technical report, National Bureau of Standards Statistical Engineering Laboratory, U.S. Dept. of Commerce, 1975. Technometrics **17**, No.1, 111-117.

[6] A.E Sarhan & B.G. Greenberg. Estimation of location and scale parameters by order statistics from singly and doubly censored samples. Technical report, 1956. Part I. Ann. Math. Statist. **27**, 427-51.

[7] T.M. Guldimann. *RiskMetrics^{TM}-Technical Document.* J.P. Morgan & Co., 2nd edition, November 1994. RiskMetrics^{TM} publications and datasets are accessible either in the World Wide Web via Mosaic and other equivalent browsers (URL-*http://www.jpmorgan.com*), or via ftp (*ftp.jpmorgan.com*).

[8] H.L. Hartner. Expected values of normal order statistics. Technical report, 1961. Biometrika 48, 151-165, Correction 48, 476.

[9] F.N. David & N.L. Johnson. Statistical treatment of censored data. i. fundamental formulae. Technical report, University College, London, 1954. Biometrika 41, 228-240.

[10] M.P. Vyas & P.J. Kempthorne. Risk measurement in global financial markets with asynchronous, partially missing price data. Technical report, International Financial Service Research Center, MIT, 1994. IFSRC Discussion Paper No 281-94.

[11] E. H. Lloyd. Least-squares estimation of location and scale parameters using order statistics. Technical report, Imperial College London, 1952. Biometrika 39, 88-95.

[12] E. Parzen. Nonparametric statistical data modelling. Technical report, 1979. Journal of American Statistical Association 74, 105-121.

[13] M. Csörgo & P. Revesz. *Strong Approximations in Probability and Satatistics.* Academic Press, Inc., 1981.

[14] J.G. Saw. A note on the error after a number of terms of the david-johnson series for the expected values of normal order statistics. Technical report, University College London, 1960. Biometrika **47**, 79-86.

[15] M.S. Bazaraa & H.D. Sherali & C.M. Shetty. *Nonlinear Programming Theory and Algorithms.* John Wiley & Sons, Inc., 1979.

[16] D. Teichroew. Tables of expected values of ordered statistics and products of ordered statistics for sample size twenty and less from a normal population. Technical report, 1956. Ann. Math. Statist. **27**, 410-26.

[17] L.H.C. Tippett. On the extreme individuals and the range of samples taken from a normal population. Technical report, 1925. Biometrika 17, 364-387.

[18] M.P. Vyas. Specification of gaussian return processes in the presence of missing or asynchronous data. Master's thesis, Massachusetts Institute of Technology, 1992.

[19] P.J. Kempthorne & A. Samarov & R.E. Welsch. Exploratory statistical analysis of currency and equity market volatility. Technical report, International Financial Services Center, M.I.T., 1992.

[20] S.S. Shapiro & M.B. Wilk. An analysis of variance test for normality. Technical report, General Electric Co. and Bell Telephone Laboratories, Inc., 1965. Biometrika **52**, 591-611.

[21] Richard A. Becker & John M. Chambers & Allan R. Wilks. *The New S Language, A Programming Environment for Data Analysis and Graphics.* Wadsworth & Brooks/Cole, 1988.